Investigation of competition and release mechanism of colicin Ib in *Salmonella enterica* serovar Typhimurium

Lubov Nedialkova

München 2014

Aus dem Max von Pettenkofer-Institut

für Hygiene und Medizinische Mikrobiologie

Lehrstuhl: Bakteriologie

der Ludwig-Maximilians-Universität München

Vormals Direktor: Prof. Dr. Dr. Jürgen Heesemann

Komm. Leitung: Prof. Dr. Rainer Haas

Thema der Dissertation

Investigation of competition and release mechanism of colicin Ib in *Salmonella enterica* serovar Typhimurium

Dissertation
zum Erwerb des Doktorgrades der Naturwissenschaften
an der Medizinischen Fakultät
der Ludwig-Maximilians-Universität München

vorgelegt von

Lubov Petkova Nedialkova

aus Zelenchukskaia/Russland

München, 2014

Mit Genehmigung der Medizinischen Fakultät
der Universität München

Betreuerin: Prof. Dr. Bärbel Stecher

Zweitgutachter: Prof. Dr. Axel Imhof

Mitbetreuung durch den
promovierten Mitarbeiter: ---

Dekan: Prof. Dr. med. Dr. h.c. M. Reiser, FACR, FRCR

Tag der mündlichen Prüfung: 16.12.2014

Eidesstattliche Erklärung

Ich, Lubov Nedialkova, erkläre hiermit an Eides statt, dass ich die vorliegende Dissertation mit dem Thema:

"Investigation of competition and release mechanism of colicin Ib in S*almonella enterica* serovar Typhimurium"

selbständig verfasst, mich außer der angegebenen keiner weiteren Hilfsmittel bedient und alle Erkenntnisse, die aus dem Schrifttum ganz oder annähernd übernommen sind, als solche kenntlich gemacht und nach ihrer Herkunft unter Bezeichnung der Fundstelle einzeln nachgewiesen habe.

Ich erkläre des Weiteren, dass die hier vorgelegte Dissertation nicht in gleicher oder in ähnlicher Form bei einer anderen Stelle zur Erlangung eines akademischen Grades eingereicht wurde.

München, den ………

_____

Table of contents

List of abbreviations

ANOVA	One-way analysis of variance
APS	Ammonium persulfate
ATP	Adenosine triphosphate
BSA	Bovine serum albumin fraction
cAMP	Cyclic adenosine monophosphate
cfu	Colony forming units
ColIa	Colicin Ia
ColIb	Colicin Ib
CRP	cAMP receptor protein
DMSO	Dimethyl *S*-oxide
DNA	Deoxyribonucleic acid
DTPA	Diethylenetriamine pentaacetic acid
DTT	Dithiothreitol
E. coli	*Escherichia coli*
EDTA	Ethylenediaminetetraacetic acid
EGTA	Ethylene glycol tetraacetic acid
EHEC	Enterohaemorrhagic *E. coli*
FACS	Fluorescence-activated cell sorting
Fe(III)	Ferric iron
GFP	Green fluorescent protein
H&E	Hematoxylin and eosin
HGT	Horizontal gene transfer
IBD	Inflammatory bowel disease
IgA	Immunoglobulin A
IL	Interleukin
INF-γ	Interferon-gamma
iNOS.	Inducible nitric oxide synthase
IPTG	β –D-thiogalactopyranoside
LB	Luria-Bertani
LCM	Low-complexity microbiota

Lcn-2	Lipocalin-2
MLNs	Mesenteric lymph nodes
NLRs	Pattern recognition NOD-like receptor
O.C.T.	Optimal cutting temperature
o.n.	Overnight
OD_{600}	Optical density of 600 nm
OMV	Outer membrane vesicles
ORFs	Open reading frame
PBS	Phosphate buffered saline
PCR	Polymerase chain reaction
pmf	Proton motive force
PMN	Polymorphonuclear neutrophil
PMSF	Phenylmethylsulfonyl fluoride
rlu	Relative luminescence units
RNA	Ribonucleic acid
RNS	Reactive nitrogen species
ROS	Reactive oxygen species
RT	Room temperature
S. Tm	*Salmonella enterica* serovar Typhimurium
SAR	Signal-anchor-release
SCV	*Salmonella*-containing vacuole
SDS	Sodium dodecyl sulfate
SPI	*Salmonella* pathogenicity island
ss	Single-stranded
StD	Standard diviation
STEC	Shiga-toxin producing *E. coli*
T3SS	Type III secretion systems
TEMED	Tetramethylethylenediamine
TLR	Pattern recognition Toll-like receptor
TMAO	Trimethylamine *N*-oxide
Vc	Culture volume

List of publications

Work described in this thesis has been published previously:

Nedialkova, L. P.*, Denzler, R.*, Koeppel, M. B., Diehl, M., Ring, D., Wille, T., Gerlach, R. G. & Stecher, B. (2014). Inflammation fuels colicin Ib-dependent competition of *Salmonella* serovar Typhimurium and *E. coli* in enterobacterial blooms. *PLoS Pathogens* 10, e1003844

* = Authors contributed equally to this work

Summary

Intestinal inflammation triggered by enteric pathogens or as result of inflammatory bowel diseases leads to shifts of the healthy microbiota and expansion of *Enterobacteriaceae* ("inflammation-inflicted blooms"). We investigated the role of colicins in competition of the human pathogenic *Salmonella enterica* serovar Typhimurium strain SL1344 (*S*. Tm) and commensal *Escherichia coli* (*E. coli*) in inflammation-induced blooms, employing a mouse model for *S*. Tm colitis, as well as bacterial gene reporters and a variety of bacterial mutants. Members of the *Enterobacteriaceae* family produce narrow-spectrum protein toxins, termed colicins, such as colicin Ib (ColIb) produced by *S*. Tm. Upon inflammation, *S*. Tm displayed a colicin-dependent competitive advantage over colicin-sensitive *E. coli* strains. In contrast, an avirulent *S*. Tm strain, which cannot trigger inflammation, failed to outgrow the sensitive competitor. Expression of ColIb (*cib*) is induced by iron limitation and the SOS response. Furthermore, iron limitation triggers expression of the outer membrane receptor CirA (*cirA*) involved in the iron uptake and exploited by ColIb for bacterial killing. *In vivo* studies of a mouse model for *S*. Tm colitis demonstrated that both, *cib* and *cirA* are induced in inflammation-inflicted blooms. Moreover, we showed that low iron concentrations lead to increased ColIb-sensitivity of *E. coli*. This explained why a colicin Ib-dependent benefit for *S*. Tm was only observed in the inflamed gut. In summary inflammation-induced *Enterobacteriaceae* blooms were defined as a new ecological niche favoring colicin-dependent bacterial competition due to the increased colicin expression and, importantly, elevated colicin-sensitivity.

Furthermore the mechanism of colicin Ib release was investigated. In contrast to group A colicins, it remains unknown how ColIb and other members of group B colicins are released. It was observed that ColIb is released only upon induction of the SOS response in *S*. Tm with the antibiotic mitomycin C. Mitomycin C induces DNA damage and is a trigger of the SOS response and lytic cycle of temperate phages residing in the bacterial chromosome. Activation of the lytic mode leads to production of phage lysis proteins triggering cell lysis and release of infectious phages. We hypothesized that ColIb might be released in the context of phage-mediated lysis in *S*. Tm. *S*. Tm harbors four temperate phages: Gifsy-1, Gifsy-2, SopEΦ and ST64B. We demonstrated that prophage-deficient *S*. Tm releases significantly less ColIb, which correlated with reduced lysis in response to SOS-stress. Moreover, different prophages had distinct effects on this process. ST64B-lysis contributed most to the release of ColIb. Further, we showed that ColIb-dependent competition of *S*. Tm against *E. coli in vitro* is strongly enhanced by phage-mediated lysis. Finally, we demonstrated that phage transduction enables the release of ColIb by a prophage-deficient *E. coli* strain, confirming that ColIb release is mediated by phage-dependent lysis. Taken together, our results suggest that group B colicins are released as result of phage-mediated lysis.

In conclusion, a novel role of prophages was identified: prophage-encoded lysis functions are an important mechanism leading to release of group B colicins in *S*. Tm. Thereby, prophages can enhance colicin-dependent bacterial fitness in competition against sensitive bacteria.

Zusammenfassung

Entzündungen des Verdauungstraktes, die entweder durch darmpathogene Krankheitserreger oder durch chronisch-entzündliche Darmerkrankungen verursacht werden, führen zu Veränderungen der gesunden Darmmikrobiota und zu einem Überhandnehmen von Enterobacteriazeen was als Entzündungs-vermitteltes „Blooming" bezeichnet wird. In diesem Zusammenhang haben wir die Rolle von Colicinen für die Fitness des Erregers *Salmonella enterica* serovar Typhimurium (*S*. Tm) in Kompetition mit kommensalen *E. coli* Stämmen untersucht. Hierzu wurde ein *S*. Tm Kolitis-Mausmodel, bakterielle Genreporter und verschiedene Bakterienmutanten verwendet. Bakterien der Familie der Enterobacteriazeen produzieren Bakteriozine, so genannte Colicine, welche Aktivität gegen nah verwandte Arten besitzen. Die Synthese von Colicin Ib (ColIb) verschafft *S*. Tm SL1344 einen kompetitiven Vorteil gegenüber Colicin-sensitiven *E. coli* Stämmen. Im Gegensatz dazu war ein avirulenter *S*. Tm Stamm, welcher keine Darmentzündung verursachen kann, nicht in der Lage einen Wachstumsvorteil gegenüber einem Colicin-sensitiven Konkurrenten zu erlangen. Die Expression von ColIb (*cib*) wird bei Eisenmangel sowie bei der sogenannten SOS Antwort induziert. Zudem wird auch der ColIb Rezeptor CirA (*cirA*), welcher in der äußeren Bakterienmembran lokalisiert ist, vermehrt unter Eisenmangel gebildet. *In vivo* Studien im *S*. Tm Kolitis-Mausmodel zeigten, dass die Expression beider Proteine, ColIb und CirA, in Entzündungs-vermittelten „Blooms" induziert wird. Überdies konnten wir feststellen, dass eine geringe Eisenkonzentration die Sensitivität von *E. coli* gegenüber ColIb erhöht. Diese Beobachtung erklärt, warum *S*. Tm nur unter Entzündungsbedingungen von ColIb profitiert. Zusammenfassend kann festgehalten werden, dass „Blooms" von Arten der Familie von Enterobacteriazeen in Folge einer Darmentzündung eine neue ökologische Nische für Colicin-abhängige Kompetition zwischen den Bakterien darstellen.

Zudem war auch die Untersuchung des Mechanismus der Colicin Ib Freisetzung Gegenstand dieser Arbeit. Im Gegensatz zu Gruppen A Colicinen war bisher unklar, wie ColIb und andere Mitglieder der Gruppe B Colicine aus den Bakterien freigesetzt werden. Es wurde beobachtet, dass die Freisetzung von ColIb nach einer Induktion der bakteriellen SOS-Antwort mit dem Antibiotikum Mitomycin C erfolgte. Als ein potentes SOS-Antwort-induzierendes Agens, schädigt Mytomycin C die DNA und löst den lytischen Zyklus von Prophagen aus. Die Induktion des lytischen Zyklus führt zur Produktion von Phagen-kodierten Lysisproteinen, die die Lyse der Bakterienzelle veranlassen was zur Freisetzung von infektiösen Phagen führt. Wir vermuteten, dass zwischen der Freisetzung von ColIb und der Phagen-induzierten Lyse von *S*. Tm ein Zusammenhang besteht. *S*. Tm SL1344 beinhaltet vier lysogene Phagen: Gifsy-1, Gifsy-2,

SopEΦ und ST64B. Wir konnten zeigen, dass ein Phagen-kurierter *S*. Tm Stamm (enthält keine funktionale Prophagen) deutlich weniger ColIb freisetzt was im Zuge einer SOS-Antwort mit einer deutlich verringerten Zell-Lyse korrelierte. Außerdem wirkten sich verschiedene Prophagen unterschiedlich auf die ColIb Freisetzung aus, wobei die durch ST64B induzierte Zelllyse am meisten zur ColIb Freisetzung beitrug. Überdies konnten wir in *in vitro* Studien zeigen, dass der ColIb-abhängige Wachstumsvorteil von *S*. Tm gegenüber E. coli positiv von einer durch Prophagen-induzierten Lyse beeinflusst wird. Zudem ermöglichte die Phagen-Transduktion in einen Prophagen-defizienten *E. coli* Stamm die Freisetzung von ColIb, was die Rolle von Phagen für die ColIb Freisetzung unterstreicht. Zusammenfassend konnten wir zeigen, dass Colicine der Gruppe B durch eine durch Phagen-induzierte Zelllyse freigesetzt werden können. Mit der Freisetzung von Colicinen der Gruppe B und dem damit verbundenen Fitnessvorteil gegenüber sensitiven Bakterien, lässt diese Studie Prophagen in *S*. Tm eine neue Rolle zukommen.

1 Introduction

1.1 The intestinal microbiota – general functions and its central role in protection against infections

The mammalian gastrointestinal tract harbors more than 10^{12} microorganisms increasing in numbers and diversity from the stomach to the distal intestine (Hooper & Macpherson, 2010). A healthy microbiota is predominantly composed of species from of the phyla Bacteroidetes and Firmicutes (Turnbaugh *et al.*, 2008; Turnbaugh, 2009). The intestinal bacterial community retains highly complex metabolic activities and can almost be viewed as a distinct organism maintaining a symbiotic relationship with its host (Gill, 2006). The host provides a nutrient rich environment with constant temperature, whereas the gut microbiota acts as a supplier of essential vitamins and enhances host digestion by processing complex polysaccharides. Along with these long-known contributions, the intestinal bacteria influence multiple processes of the host-organism, including organ development, immunity, cell proliferation, bone mass, adiposity and even behavior (Sommer & Backhed, 2013). Another crucial assignment of the gut microbiota is prevention of pathogen colonization, termed colonization resistance (Stecher & Hardt, 2011). This protective effect is achieved via modulation of the host immune system by the microbiota, as well as through a direct antagonism of invading pathogens and substrate competition.

The healthy microbiota modulates intestinal defense mechanisms including expression of various chemokines and antimicrobial compounds, as well as secretion of immunoglobulin A (IgA) (Chung *et al.*, 2012). Resident intestinal bacteria are constantly sensed by the pattern recognition Toll-like (TLRs) and NOD-like (NLRs) receptors (Geuking *et al.*, 2014). Ligation of these receptors with bacterial molecules leads to expression of different cytokines (e.g. IL22 and pro-IL-1β) and antimicrobial peptides, such as RegIIIγ (Cash *et al.*, 2006).

Direct inhibition of pathogen growth by the beneficial microbiota includes consumption of available nutrients such as various dietary and mucosal glycans (Ferreyra *et al.*, 2014). Furthermore, commensal bacteria release inhibitory molecules (e.g. bacteriocins) and various metabolites (e.g. short chain fatty acids, such as acetate and butyrate) suppressing either pathogen growth or expression of crucial virulence factors (Fukuda *et al.*, 2011; Gantois *et al.*, 2006; Riley & Gordon, 1999).

Further research will improve our understanding of the fine-tuned host-microbiota interactions leading to colonization resistance. Presently, it is established that disturbance of the intestinal microbiota caused by diet alteration or antibiotic treatment enhances pathogen invasion (Barthel *et al.*, 2003; Buffie *et al.*, 2012; Zumbrun *et al.*, 2013). Strategies of intestinal pathogens to bypass colonization resistance include: (*i*) initiation of gut inflammation, (*ii*) expression of exploitative competition factors required for survival upon inflammation and (*iii*) release of antibacterial compounds e.g. bacteriocins to kill resident commensal bacteria (interference competition) (Winter *et al.*, 2013a). The current work investigates the effect of a bacteriocin produced by enteric pathogen *Salmonella enterica* serovar Typhimurium (*S*. Tm) while "blooming" in the inflamed gut.

1.2 How do pathogens overcome colonization resistance?

1.2.1 Pathogens can benefit from disruption of the microbiota by antibiotics

Antibiotic administration leads to an alteration of microbiota composition (Dethlefsen & Relman, 2011). Furthermore, it can lead to subclinical inflammation causing disruption of the intestinal barrier (Spees *et al.*, 2013; Wlodarska *et al.*, 2011). In addition to the decreased numbers of commensals, antibiotic treatment can favor growth of otherwise low-numbered, facultative anaerobes (i.e., Bacilli and Proteobacteria) (Hill *et al.*, 2010). The latter include *Enterobacteriaceae* (class Gammaproteobacteria) (Ayres *et al.*, 2012; Lawley *et al.*, 2009). Reduced intestinal bacterial diversity upon antibiotic treatment fosters growth of intestinal pathogens (e.g. *Clostridium difficile* and *S*. Tm), as well as systemic spread of intestinal pathobionts such as *E. coli* (Lawley *et al.*, 2009; Sekirov *et al.*, 2008). Both the Gram-positive *C. difficile* and the Gram-negative *S*. Tm expand in the antibiotic-treated gut, utilizing the same nutrient source: host mucus-derived sialic acid. In the healthy intestine this monosaccharide is consumed by intrinsic commensal bacteria, which are eradicated as a result of antibiotic administration. Growing on the accessible sialic acid, *C. difficile* and *S*. Tm can reach numbers sufficient for development of pathogen-inflicted intestinal inflammation (Ng *et al.*, 2013).

1.2.2 Pathogen-induced inflammation re-engineers the gut ecosystem, disrupts colonization resistance and induces enterobacterial blooms

Pathogens belonging to the *Enterobacteriaceae* family (e.g. *Citrobacter rodentium* and *S*. Tm) trigger intestinal inflammation. This is characterized by neutrophil transmigration in the gut lumen, secretion of

numerous antimicrobials, as well as generation of various anaerobic electron acceptors. These environmental alterations tip the microbial balance in favor of the pathogen, along with other members of the *Enterobacteriaceae* family (Garrett *et al.*, 2010; Lupp *et al.*, 2007; Stecher *et al.*, 2007a). This is referred to as "Enterobacterial blooms" (Stecher *et al.*, 2013b). The inflammatory milieu generated upon pathogen infection or in the context of inflammatory bowel disease (IBD) supports growth of facultative anaerobes such as *E. coli* and *Enterococcus spp.*, on the account of obligate anaerobic bacteria (Lupp *et al.*, 2007; Mondot *et al.*, 2011). In the healthy intestine, obligate anaerobes of the phyla Bacteroidetes and Firmicutes metabolize carbohydrates and amino acids by fermentation (Faber & Baumler, 2014). Upon inflammation, secretion of interferon-gamma (INF-γ) leads to induction of epithelial oxidases and the inducible nitric oxide synthase (iNOS). Their activity leads to the generation of antimicrobial reactive oxygen species (ROS) and reactive nitrogen species (RNS), respectively (Harper *et al.*, 2005; Kuwano *et al.*, 2006; Nathan, 2006). Furthermore, neutrophils delivered at the site of inflammation, likewise produce ROS (e.g. superoxide (O_2^-)) and RNS (Nathan, 2006; Winter *et al.*, 2010). These antimicrobials are involved in the generation of oxidized anaerobic electron acceptors, such as tetrathionate, nitrate (NO_3^-), trimethylamine *N*-oxide (TMAO) and dimethyl *S*-oxide (DMSO) (Winter *et al.*, 2013a). In contrast to the obligate anaerobes, *Enterobacteriaceae* species (e.g. *E. coli, S.* Tm and *Yersinia enterocolitica*) produce respiratory reductases, which reduce the anaerobic electron acceptors. Anaerobic respiration confers a selective advantage over the obligate anaerobes by facilitating the utilization of various substrates as energy and nutrients source (e.g. ethanolamine) (Faber & Baumler, 2014; Winter *et al.*, 2010; Winter *et al.*, 2013b). Ethanolamine, an end product of bacterial fermentation, is used as a nitrogen and carbon source by various enteric pathogens, including *S.* Tm, enterohaemorrhagic *E. coli* (EHEC) and *C. difficile* (Bertin *et al.*, 2011; Pitts *et al.*, 2012; Thiennimitr *et al.*, 2011).

Another characteristic of the environmental conditions in the inflamed intestine is iron limitation (Loetscher *et al.*, 2012; Raffatellu, 2009). Furthermore, apoptotic neutrophils and epithelial cells in the inflamed intestine release antimicrobial proteins, which sequester metal ions (e.g. iron and zinc) that are essential for bacterial growth. Iron is an essential component of many bacterial enzymes involved (Braun & Hantke, 2011). Bacteria can sequester environmental ferric iron (Fe(III)) by producing small molecule chelators, termed siderophores. Specific outer membrane receptors of Gram-negative bacteria (e.g. CirA, FhuA, FecA) bind and translocate siderophore-Fe(III) complexes across the outer membrane and periplasm. The energy-dependent translocation is implemented via TonB along with inner membrane proteins ExbB and ExbD (Braun & Hantke, 2011; Miethke, 2013). Upon infection, increased biosynthesis of the hormone hepcidin in the liver results in reduction of both intestinal iron uptake and iron release by macrophages. Intestinal iron is further restricted by the iron-binding protein lactoferrin and siderophore-

binding Lipocalin-2 (Lcn-2) released at inflammatory sites (Chu *et al.*, 2010). *S*. Tm and some other members of *Enterobacteriaceae* can circumvent Lcn-2 activity by expressing a modified siderophore, salmochelin, which is not bound by Lcn-2 (Deriu *et al.*, 2013; Raffatellu, 2009). Likewise, *S*. Tm is resistant against other antimicrobial proteins, such as zinc-binding protein calprotectin and C-type lectin RegIIIβ (Liu *et al.*, 2012; Stelter *et al.*, 2011). Thus, differential killing of the microbiota and pathogens by inflammatory immune response may contribute to the observed microbiota shift in the inflamed gut.

1.3 *Salmonella* Typhimurium - a model human pathogen to study microbiota-pathogen interaction in the gut

1.3.1 *Salmonella* Typhimurium pathogenesis

Infections with nontyphoidal *Salmonellae* (e.g. *S*. Tm) generally lead to a self-limiting diarrhea, but can be particularly dangerous for immunocompromised individuals by causing bacteremia (Gordon *et al.*, 2008). Once *S*. Tm bacterium reaches the small intestine, the pathogen is directed by chemotactic flagella-mediated motility towards the gut epithelium, penetrating the mucus layer (**Figure 1.1A**) (Stecher *et al.*, 2004). *S*. Tm adheres to the epithelium by employing various fimbriae and non-fimbrial adhesins (Fabrega & Vila, 2013; Kaiser *et al.*, 2012). Tissue invasion of *S*. Tm requires expression of numerous effector proteins encoded within the five *Salmonella* pathogenicity islands (SPIs) (Fabrega & Vila, 2013; Kaiser *et al.*, 2012). The type III secretion systems (T3SS-1) encoded by SPI-1 represents a needle-like structure, which injects at least 14 different effector proteins into the epithelial cells (Kaiser *et al.*, 2012). Effector proteins of T3SS-1 cause actin rearrangement and formation of membrane ruffles leading to pathogen engulfment by the cell. Furthermore, some effector proteins induce expression of pro-inflammatory cytokines, e.g. interleukin-1 (IL-1) and interleukin-8 (IL-8). This is termed the "classical" pathway for initiation of inflammation. In addition to the T3SS-1 mediated invasion mechanism, *S*. Tm is internalized by pathogen-sampling dendritic cells (Stecher & Hardt, 2011). Once inside the cells, pathogens are safely encapsulated in a *Salmonella*-containing vacuole (SCV) (Fabrega & Vila, 2013). Residing in the SCVs, *S*. Tm induces the SPI-2 encoded T3SS-2, which injects effector proteins that trigger the "alternative" pathway, which causes tissue-wide inflammation (Kaiser *et al.*, 2012; Stecher & Hardt, 2011). Moreover, effector proteins secreted by T3SS-2 support intracellular survival, proliferation and dissemination of *S*. Tm to systemic sites (the mesenteric lymph nodes (MLNs), the spleen, and the liver) (Kaiser *et al.*, 2012).

Besides T3SS-1 and T3SS-2, numerous proteins encoded by SPI3 - SPI5 and virulence plasmid pSLT contribute to the pathogenesis (Fabrega & Vila, 2013). Induction and amplification of the initial pro-

inflammatory signals by *S*. Tm results in: granulocyte migration towards the intestinal lumen, T-cell activation, mucosal edema, epithelial damage, reduced numbers of mucus-loaded goblet cells and mucin secretion (**Figure 1.1B,C**) (Fabrega & Vila, 2013; Kaiser *et al.*, 2012).
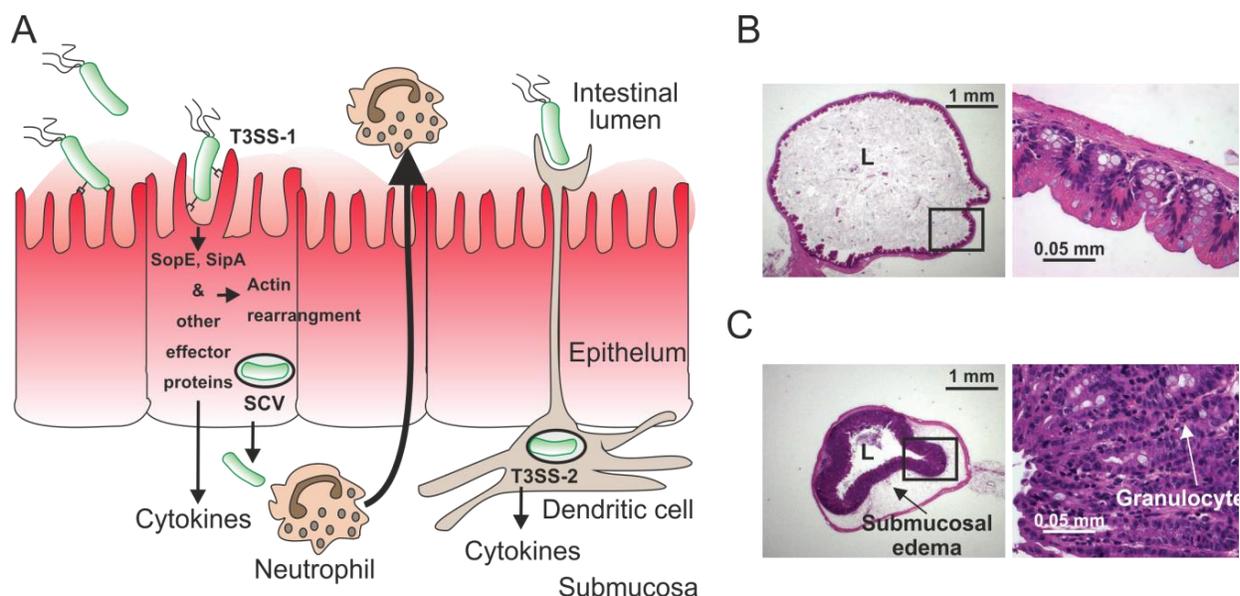
Figure 1.1. *Salmonella* **Typhimurium pathogenesis.** *S*. Tm moves towards the gut epithelium, where it adheres to epithelial cells, followed by activation of the T3SS-1 and injection of various effector proteins into the cell. Effector proteins of T3SS-1 cause expression of pro-inflammatory cytokines, as well as actin rearrangement and formation of membrane ruffles leading to pathogen engulfment followed by *S*. Tm encapsulation in a SCV (classical pathway for initiation of inflammation). Encapsulated inside a pathogen-sampling dendritic cell, *S*. Tm activates the T3SS-2. Effector proteins of T3SS-2 cause tissue-wide inflammation (alternative pathway for initiation of inflammation) (**A**). Hematoxylin and eosin (H&E)–stained cecal sections of healthy (**B**) and *S*. Tm-infected mice (**C**). *S*. Tm infection leads to granulocyte infiltration, mucosal edema and epithelial damage (**C**). An enlarged section (square) is shown in the right panel. Adapted from (Stecher *et al.*, 2007a).

1.3.2 Mechanisms of *Salmonella* Typhimurium overgrowth in the inflamed gut

Blooming in the inflamed intestine *S*. Tm employs various competitive strategies, which ensure not simply just survival, but lead to even further displacement of the resident commensal microbiota (**Figure 1.2**).

Intestinal sulfate-reducing bacteria release toxic H_2S, which is oxidized by the cecal mucosa to thiosulfate (Levitt *et al.*, 1999). Nitric oxide (NO) radicals and ROS, release by the inflamed mucosa as part of the

inflammatory response, lead to oxidation of thiosulfate to the anaerobic electron acceptor tetrathionate. Unable to use tetrathionate, commensal bacteria rely entirely on energetically less efficient fermentative metabolism and are ultimately outcompeted by the pathogen, which can utilize tetrathionate for anaerobic respiration (Winter *et al.*, 2010). Switch from tetrathionate to even more energetically efficient nitrate-respiration, further promotes growth of some epidemic *S*. Tm strains harboring the T3SS-1 effector protein SopE. SopE further enhances production of iNOS in the intestinal mucosa, while suppressing expression of tetrathionate utilization genes. iNOS mediates production of NO_3^-, by generating more NO and ROS, which can be used by the pathogen as terminal electron acceptor (Lopez *et al.*, 2012).

S. Tm-triggered expression of inflammatory pro-cytokines (e.g. IL-22 / IL-17) leads to secretion of numerous antimicrobials (e.g. Lcn-2) by intestinal epithelial cells and infiltrating neutrophils. Lcn-2 binds siderophores (e.g. enterochelin) and thereby inhibits bacterial iron-uptake. Unlike many commensal bacteria, *S*. Tm maintains a sustainable iron supply by expressing a Lcn-2-resistant glycosylated enterochelin derivative, termed salmochelin, encoded on the *iroBCDEN* gene cluster (Raffatellu, 2009). Likewise, *S*. Tm avoids action of zinc-binding protein calprotectin by production of ZnuABC transporter, which enables acquisition of this essential micronutrient even under zinc-limiting conditions (Liu *et al.*, 2012). In addition, intestinal secretory cells (Paneth cells) release various antimicrobial peptides including, α-defensins and C-type lectins RegIIIγ and RegIIIβ (Vaishnava *et al.*, 2008). RegIIIβ kills competing commensal bacteria, but is relatively harmless for the inflammation-eliciting pathogen *S*. Tm due to alterations in its peptidoglycan structure and lipopolysaccharide composition (Stecher & Hardt, 2011; Stelter *et al.*, 2011).
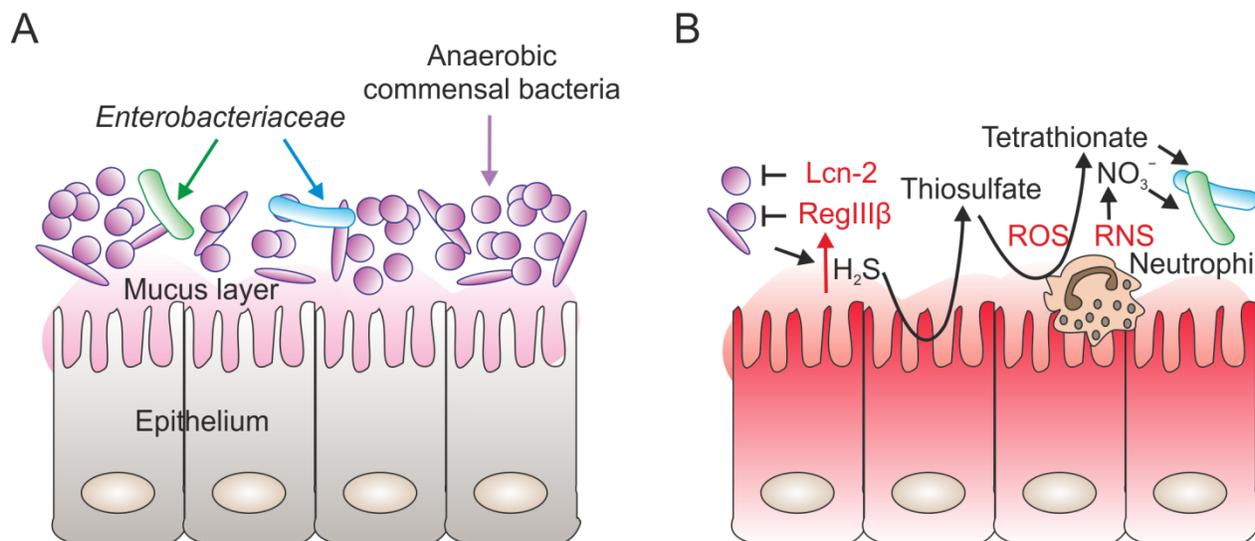
Figure 1.2. Mechanisms of *Salmonella* Typhimurium overgrowth in the inflamed gut. Under homeostatic conditions, *Enterobacteriaceae* (blue, green) are reduced in numbers as they are overgrown by the obligate anaerobic microbiota (violet-blue) (**A**). *S*. Tm-triggered inflammation results in transmigration of neutrophils into the gut lumen, release of reactive oxygen and nitrogen species (ROS, RNS), production of anaerobic electron acceptors (tetrathionate and NO_3^-), utilized by *Enterobacteriaceae*. Release of antimicrobials (e.g. RegIIIβ and iron-depleting Lcn-2) inhibits growth of resident obligate anaerobic microbiota (**B**).

1.3.3 *Salmonella* Typhimurium-triggered inflammation leads to enterobacterial blooms and horizontal gene transfer

S. Tm-elicited inflammation leads to parallel blooms of commensal and pathogenic Proteobacteria (Lopez *et al.*, 2012; Stecher *et al.*, 2007a). It was shown that expansion of *Enterobacteriaceae* promotes horizontal gene transfer (HGT) by conjugation (Stecher *et al.*, 2012). In contrast to stepwise evolution via mutations, HGT can provide rapid evolution and acquisition of entire fitness and virulence genes. This transmission of new traits can occur by transformation, phage-mediated transduction and conjugation-mediated plasmid exchange. Conditions in the intestine are expected to favor the latter two mechanisms. Plasmid transfer via the conjugative pilus requires direct cell-cell contact (Frost *et al.*, 2005; Scott, 2002). Therefore, high densities of metabolically active bacteria in the gut form the ideal environment for a successful conjugation. Indeed, *S*. Tm-elicited inflammation resulted in an extremely efficient transfer of conjugative pCol1B9_SL1344 plasmid (further termed P2) into parallel "blooming" *E. coli* (Stecher *et al.*, 2012). This was attributed mostly to the high titers of donor and recipient strains upon pathogen-fostered gut inflammation. In the absence of inflammation, overgrowth of obligate anaerobic members of the gut

microbiota lead to a decrease in *Enterobacteriaceae* and thereby interfered with the conjugation Upon inflammation P2 conferred a competitive-advantage to the *S*. Tm over ColIb-sensitive *E. coli* (Stecher *et al.*, 2012). This suggested that ColIb could be an important fitness factor for pathogen growth in the inflamed intestine.

1.4 Colicin biology: bacterial warfare

1.4.1 Colicins: types and functions

Colicins are relatively large proteins (40 to 80 kDa) belonging to a group bacterial peptide toxins, termed bacteriocins. Colicins, as their name suggests, are bacteriocins produced by *E. coli* and some related *Enterobacteriaceae* species (Cascales *et al.*, 2007). Twenty-four percent and 59% of intestinal *E. coli* isolates of human and mice, respectively produce colicins. These numbers imply that colicinogeny is somewhat important in natural bacterial communities (Gordon *et al.*, 1998; Gordon & O'Brien, 2006). Colicins are classified into two groups (A and B), based on their uptake mode: Tol- or TonB-mediated colicin uptake, respectively (**Figure 1.3**). Colicins exert their lethal activity to closely related species by pore-formation or enzymatic activity. Pore-forming colicins (e.g. ColIb) form channels in the inner membrane of the victim, which leads to membrane depolarization, leakage of intracellular ions and ultimately cell death (Weaver *et al.*, 1981). Enzymatic colicins mainly target deoxyribonucleic acid (DNA) or ribonucleic acid (RNA), with the exception of colicin M, which interferes with peptidoglycan biosynthesis in the periplasm (Cascales *et al.*, 2007). Colicins are harmless for the producing bacteria due to the expression of cognate colicin immunity proteins, which either form heterodimers with the nuclease colicins in the cell cytosol, or insert into the inner membrane and block pore-forming colicins.
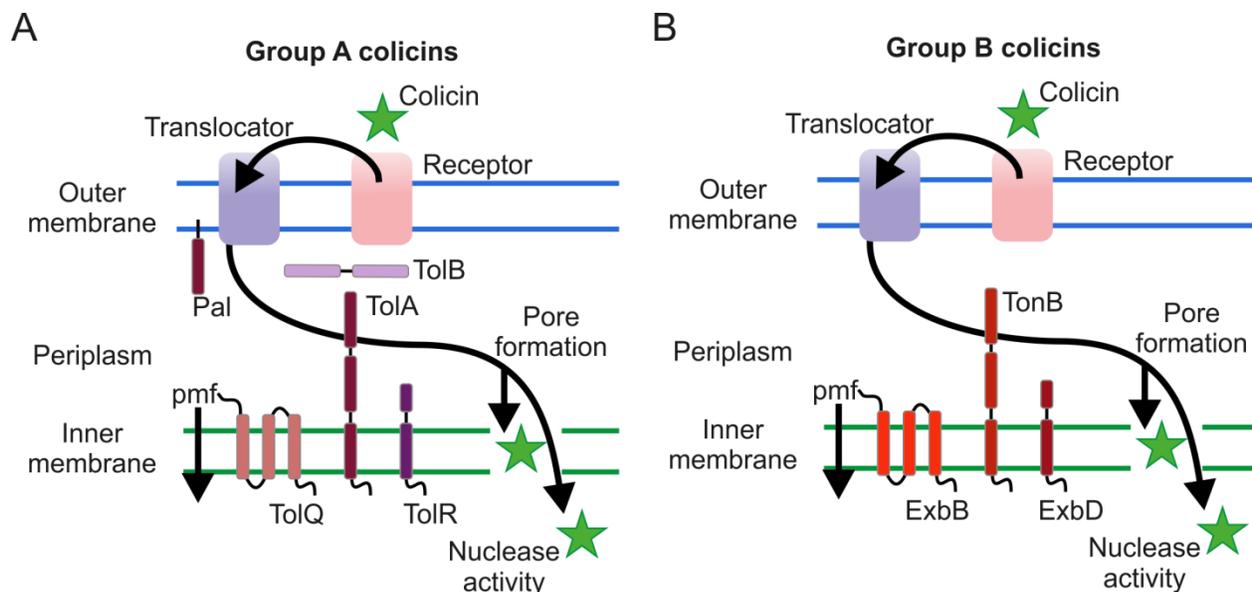
Figure 1.3. Mechanisms of colicin uptake. Group A and group B colicins bind an outer membrane receptor and are further translocated through the outer membrane and periplasm by an outer membrane translocator. The energy-dependent translocation of group A colicins involves proteins TolA, TolB, TolQ, TolR (**A**). Group B colicins require the protein TonB assisted by ExbB and ExbD (**B**). Following translocation colicins are either inserted into the inner membrane forming a voltage-gated ion channel, or are further directed into the cytoplasm targeting nucleic acids. Adapted from (Kleanthous, 2010).

Colicins are organized into three domains, each governing a specific function: receptor-binding (R), translocation (T) and killing activity (A). The central R-domain and amino-terminal T-domain exploit outer membrane receptors and porins (e.g. OmpF, OmpW), as colicin receptors and translocators. Colicin-receptors are normally involved in uptake of essential bacterial compounds; e.g. vitamin B12 (BtuB), siderophores (CirA, FyuA) and ferrichrome (FhuA) (Cascales *et al.*, 2007). Following binding of a translocator protein, the colicin T-domain interacts with host proteins located in the periplasm and inner membrane, directing colicin translocation. The T-domain of group A colicins recruits Tol proteins (TolA, TolB, TolQ, TolR), which are generally involved in outer membrane stabilization during cell division (Gerding *et al.*, 2007; Kleanthous, 2010). The uptake mechanism of group B colicins has been investigated in detail for the ColIb homologue - colcin Ia (ColIa) (Mankovich *et al.*, 1984). The ColIa R-domain binds to the outer membrane receptor CirA, while the T-domain engages a second CirA as ColIa translocator. ColIa translocation is carried out via TonB (Kleanthous, 2010). TonB assisted by ExbB and ExbD proteins (as well as Tol-system), employs inner membrane proton motive force (pmf) for the

9

energy-dependent translocation of their natural ligands and colicins. Following translocation, the third colicin domain, carboxy-terminal A-domain, is either inserted into the inner membrane forming a voltage-gated ion channel (pore-forming colicins), or is directed further towards the cytoplasm (nucleases) (Cascales *et al.*, 2007).

1.4.2 Genetic control of colicin expression

Colicins are associated with two types of plasmids which exhibit differential genetic organization. The majority of group A colicins are encoded by small (6-10 kb) high-copy plasmids, reaching up to 30 copies per bacterial cell. Group B colicins (e.g. ColIb) are mostly encoded on larger (~ 40 kb), single-copy conjugative plasmids.

The operon of group A nuclease-type colicins includes three genes, the gene encoding colicin activity (*cxa*), followed by immunity protein (*cxi*) and a lysis protein gene (*cxl*) (**Figure 1.4**) (Cascales *et al.*, 2007). The *cxi* genes of pore-forming colicins of both A and B groups are encoded on the opposite DNA strand (with respect to the *cxa* gene) and in some cases can be completely absent. Generally, transcription of the colicin operon is regulated by a strong negatively controlled common promoter *P*, conferring 1000-fold increase of colicin expression upon induction (Zgur-Bertok, 2012), and transcriptional terminators *T1* and *T2*. Furthermore, the *cxi* is regulated by its own constitutive promoter *Pim* ensuring constant expression of the immunity protein, thereby protecting the producer cell against colicin activity. The transcriptional terminator *T1*, upstream of the lysis gene of group A colicins, blocks lysis gene expression. Lysis protein activity is lethal for the colicinogenic strain; therefore tight regulation of the lysis gene is necessary to concede intracellular accumulation of the colicin before the cell death. Expression of colicin operons is controlled by LexA protein, which is the major repressor of SOS response system (Zgur-Bertok, 2012).

The SOS response is a global cellular response to DNA damage leading to induction of multiple genes involved in DNA repair (Little, 1991). Therefore, the SOS response is triggered by many environmental factors including: acidic pH, antimicrobial molecules (e.g. hydrogen peroxide and nitric oxide), antibiotics (e.g. mitomycin C, ciprofloxacin) and UV light. The key players of the SOS response are LexA, the transcriptional repressor and RecA, its activator. LexA homodimers rapidly bind consensus DNA sequences in the promoter region of SOS-regulated genes, known as "LexA (SOS) boxes", thereby blocking access of the RNA polymerase (Butala *et al.*, 2008; Shinagawa, 1996). During replication, damaged DNA blocks the replication fork, which results in accumulation of single-stranded DNA

(ssDNA). RecA proteins bind to ssDNA and assisted by adenosine triphosphate (ATP) form RecA–ssDNA active filaments (RecA*). RecA* is a co-protease assisting self-cleavage of free LexA dimers, which is followed by swift degradation of the cleaved proteins. As a result, LexA levels decrease, which leads to dissociation of the LexA repressor from the consensus DNA and expression of the SOS-controlled genes. LexA dissociation rates vary between different SOS boxes leading to distinct timing of gene expression (Butala *et al.*, 2011). A large group of colicin promoters contains two overlapping SOS boxes leading to co-operative repression by two LexA proteins (Gillor *et al.*, 2008). This tight repression of the colicin operon, including the lysis gene, gives the cell time to repair the DNA defects and prevents colicin release (Zgur-Bertok, 2012).
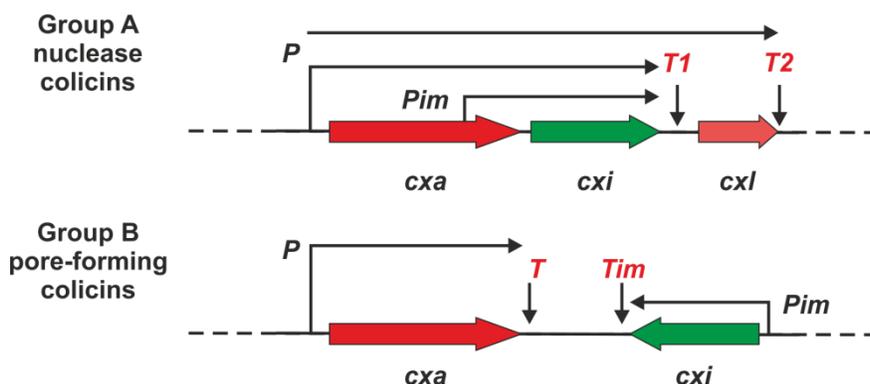
Figure 1.4. Organization of colicin operons. The operon of group A nuclease-type colicins is controlled by the common promoter *P*, followed by genes encoding colicin activity protein (*cxa*) (red arrow) and colicin immunity protein (*cxi*) (green arrow). The latter is additionally controlled by the promoter *Pim*. The last gene of the operon of group A nuclease-type colicins encodes a lysis protein (*cxl*) (light pink arrow). Transcriptional terminators *T1* and *T2* are located before and after the *cxl*, respectively. The *cxa* of group B colicins is followed by the transcriptional terminator *T*, while the *cxi* is located on the opposite DNA strand and is regulated by its own promoter (*Pim*) and terminator (*Tim*). Adapted from (Cascales *et al.*, 2007).

Of note, ColIa and ColIb operons are an exception from the double-LexA repression, as they contain only one SOS box (Gillor *et al.*, 2008; Mankovich *et al.*, 1986). Furthermore, expression of some colicins is blocked by additional repressors. Some pore-forming colicins (e.g. colicin K and E1) are controlled by the global transcriptional repressor IscR, which is liberated upon nutrient depletion (Butala *et al.*, 2012). Additionally the cAMP receptor protein (CRP) is shown to regulate colicin expression and

downregulation of colicin lysis gene expression is mediated by RNA-binding protein CsrA. This suggests that colicin expression is regulated by a complex transcriptional and post-transcriptional mechanism (Zgur-Bertok, 2012).

1.4.3 Colicin ecology

Although, approximately a third of natural *Enterobacteriaceae* communities are colicinogenic (Riley & Gordon, 1999), this number differs according to the habitat of the strain (e.g. only 9% colicinogenic *E. coli* soil isolates against 30% faecal isolates). This variability is associated with the high metabolic costs of colicin production, as well as lethality of colicin release. The high cost paid by the producer is an important factor influencing the outcome of the competition against colicin-sensitive rivals. The interplay between colicin producers and colicin-sensitive strains is further complicated upon introduction of a colicin resistant strain, which acquires resistance upon alteration of the colicin uptake machinery by mutation. This is a less costly trait compared to colicin production, however it confers a fitness disadvantage against colicin-sensitive competitors. The interplay between producer, sensitive and resistant strains is compared to the game of Rock, Paper, Scissors, whereby the producer is outcompeting the sensitive strain, but being outnumbered by the resistant bacteria, which in turn is outgrown by the sensitive strain (**Figure 1.5**). The dynamic equilibrium established *in vivo* between these three competitors is proposed to support bacterial diversity (Kirkup & Riley, 2004; Riley & Wertz, 2002)
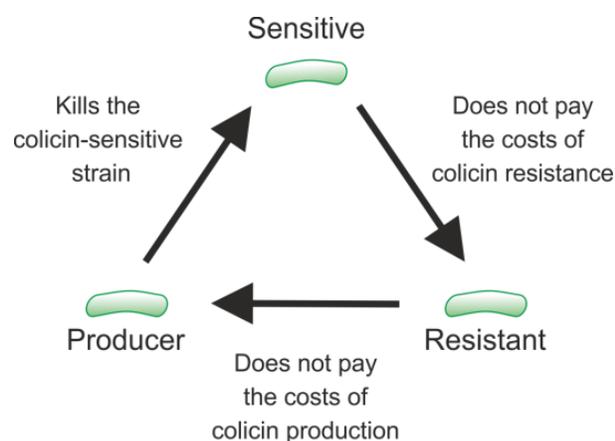
Figure 1.5. The Rock, Paper, Scissors interplay. The colicin-producing strain kills the colicin-sensitive strain. The sensitive strain, which is not paying the costs of resistance, outcompetes the resistant strain. The latter is resistant to the colicin and it is not burdened by colicin production, which allows it to outgrow the colicin-producing strain. Adapted from (Hibbing *et al.*, 2010)

Furthermore, it was shown that a colicinogenic strain invading an environment with randomly distributed nutrients at low numbers, loses against the resistant strain, which grows faster due to the absence of production costs (Chao & Levin, 1981). In contrast, competition in a more structured environment (e.g. the mammalian intestine) is expected to support the colicin producer, which is killing the neighboring or invasive colicin-sensitive bacteria, thereby directly liberating niche space and nutrients (Chao & Levin, 1981; Majeed *et al.*, 2011).

Of note, under physiological conditions, only a small fraction of the producer's population expresses the colicin (Mulec *et al.*, 2003). The rest of the population benefits from the colicin and nutrients released by the lysing producer (Butala *et al.*, 2012). This is referred to as "division of labor", which is enabled by heterogeneous activation of colicin expression due to the impact of stochastic factors, as well as the binding affinity of LexA (Kamensek *et al.*, 2010; Mrak *et al.*, 2007).

1.4.4 The enigma of group B colicins release

Release of group A colicins is mediated by cognate colicin lysis proteins (Cascales *et al.*, 2007). Lysis proteins of group A colicins are small lipoproteins, which display sequence homology with exception of their N-terminal signal sequence. They kill bacteria in two steps: (*i*) damage the inner membrane and direct translocation of colicin into the periplasm and, (*ii*) cause membrane perturbation and activate the outer membrane phospholipase OmpLA (Chen *et al.*, 2011). OmpLA governs accumulation of lysophospholipids which leads to outer membrane permeabilization and release of colicins along with other periplasmic and cytoplasmic proteins (Baty *et al.*, 1987).

Hitherto, the release mechanism of group B colicins remains unclear (Cascales *et al.*, 2007). Group B colicin operons do not encode the *cxl* gene and no signal sequence directing these proteins towards the inner membrane for secretion has been identified. In the course of the current work, the mechanism of ColIb release in relation to the intracellular protein leakage upon prophage-mediated cell lysis was investigated.

1.5 Prophages

1.5.1 General introduction

Bacterial viruses – bacteriophages - are the most abundant biological form on Earth with an estimated number of $> 10^{30}$ phages in the biosphere (Brussow & Hendrix, 2002). The mammalian gut, which is densely populated by bacteria, represents an environment enriched in phages, with viruses (represented mainly by bacteriophages) reaching 10^9 per gram of human feces (Kim *et al.*, 2011). Phages, particularly lysogenic phages are able to integrate into the bacterial host genome (prophages) and confer benefit to the host bacteria in multiple ways. Prophages block superinfection by lytic phages and they enhance bacterial fitness upon host-pathogen interactions (Brussow *et al.*, 2004). Moreover, phages participate in HGT through either general transduction, or lysogenic conversion. The latter, drives transfer of extra genes, called "morons", encoded within the prophage genome. These extra genes encode various bacterial fitness factors. Morons influence propagation of prophages by enhancing survival and dissemination of the lysogen, thereby increasing chances for vertical prophage transfer to the next generation of host cells (by bacterial divisions). Many morons are organized into autonomous genetic elements flanked by their own promoter and terminator. Thereby, expression of these genes is independent of the prophage life cycle and can be coordinated according to the needs of the host bacterium. Moron-encoded virulence factors are linked to biofilm formation, sporulation, as well as regulation, expression and release of bacterial toxins (e.g. phage-encoded botulinum neurotoxins of *Clostridium botulinum* and Shiga toxin (Stx) of Shiga-toxin producing *E. coli* (STEC)) (Brussow *et al.*, 2004).

1.5.2 Phage life cycle

At the first step of the infection phages bind bacterial outer membrane components (e.g. proteins, oligosaccharides or lipopolysaccharides). Next, prophage DNA is "injected" into the bacterial cytoplasm through the phage tail followed by rapid circularization of the injected DNA to avoid degradation by the exonucleases of the host. The internalized prophage redirects host metabolism to serve the phage multiplication process, including: (*i*) phage genome replication, (*ii*) phage protein production, (*iii*) assembly of infectious particles and (*iv*) phage release. These events describe the phage lytic cycle, which is abolished upon integration of the phage genome into the bacterial chromosome (**Figure 1.6**). Thereby, the prophage is replicated and inherited alongside with the bacterial genome upon cell division (Guttman, 2005). This dormant existence, termed lysogeny, can be terminated by various conditions jeopardizing the host bacterial cell (e.g. nutritional stress, oxidative stress, UV radiation, antibiotic treatment, heat shock,

quorum sensing signals), upon which DNA-integrated prophages engage into the lytic cycle to abandon the "sinking ship" (Guttman, 2005).
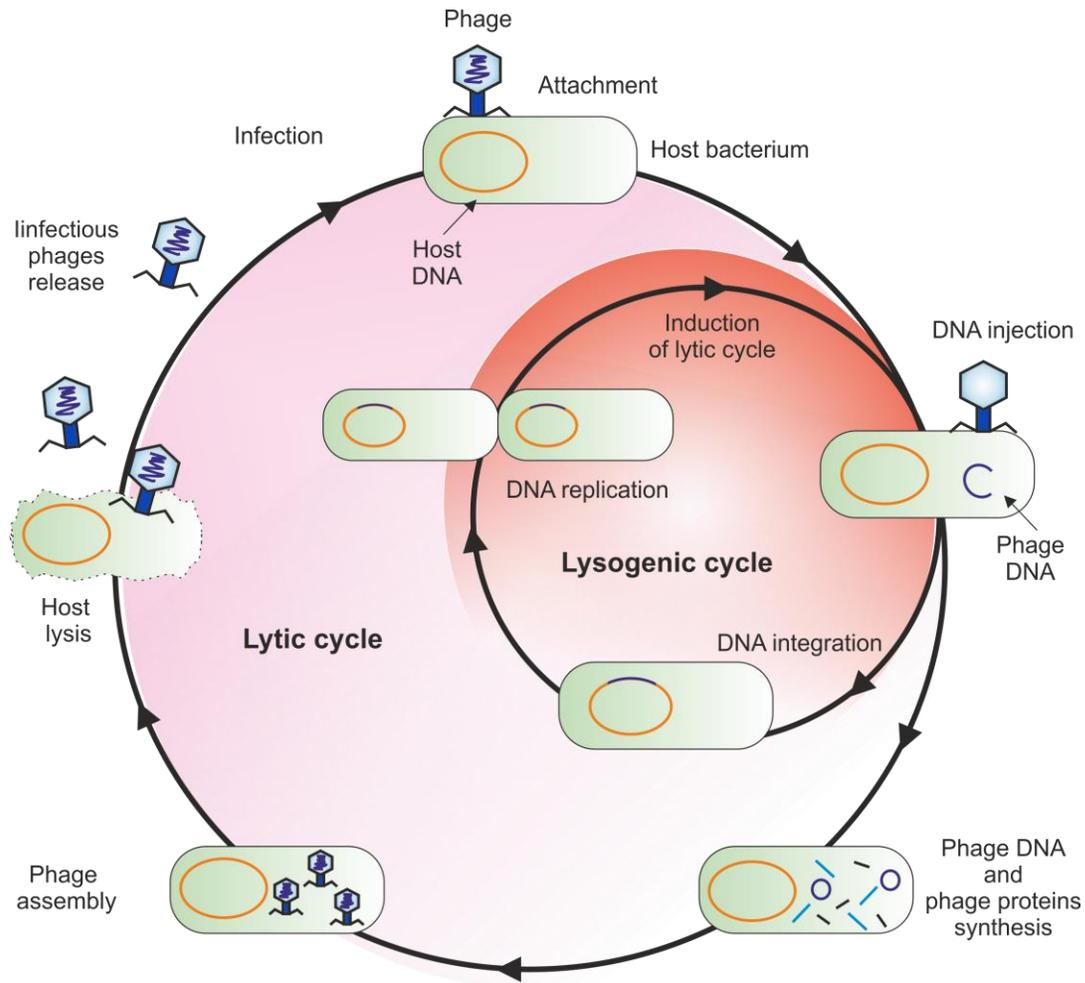
Figure 1.6. Life cycle of a temperate lambdoid phage. Upon attachment to the host, the phage injects its DNA into bacterial cytoplasm. Lysogenic development of the phage takes place upon DNA integration into the host chromosome. The prophage is transferred to each new bacterium upon proliferation of the lysogenic strain. The switch from lysogenic to lytic mode takes place upon conditions threatening the host bacterial cell (SOS-response). The lytic cycle includes synthesis of phage DNA and proteins and, assembly of infectious particles, which is followed by lysis and release of phages. Adapted from (Campbell, 2003).

A complex interplay between prophage promoters and terminators directs decision in favor of either the lytic or the lysogenic infection. Widely studied lambdoid prophages possess two early promoters, *pL* and *pR,* which initiate transcription of the prophage genes in opposite directions (**Figure 1.7**) (Court *et al.*, 2007; N.J. Dimmock, 2001). Following expression of the *N* gene, located directly downstream of *pL*, the bacterial RNA polymerase is arrested at the terminator *tL1*. Likewise, only the *cro* gene is expressed following transcription initiation from the *pR* promoter. Transcription of the *pR*-downstream located replication genes (*O*, *P* and *ren*) and the antiterminator protein encoding *Q* gene is halted by the terminator *tR1*. The N protein is an antiterminator which, in association with the RNA polymerase and Nut host proteins, induces expression of genes downstream of *tL1* and *tR1*. The latter includes the genes *cII* and *cIII* required for establishment of lysogeny. CII initiates transcription from three promoters *pI*, *pRE* and *pAQ*, controlling expression of *int*, *cI* genes and an antisense RNA of the *Q* gene, respectively. The CI repressor is critical for establishment and maintenance of lysogeny. CI homodimer binds both, *pL* and *pR*, repressing expression of all prophage genes, except of its own one by auto-activation of the *pRM* promoter, which is situated upstream of the *cI* gene. Upon superinfection of a lysogen, CII, CIII and CI produced by the resident prophage direct the newly incoming prophage towards lysogenic mode. RecA* (**Section 1.4.2**), the central protein activated in the course of the SOS response acts as co-protease of CI leading to cleavage of the CI monomers and de-repression of prophage genes (e.g. *cro, Q, int* and *xis*) (Cohen *et al.*, 1981). The Cro protein is a week repressor, which binds the operators *OL* and *OR*, thereby inhibiting expression of the lysogenic mode proteins, CIII and CII. Furthermore, the Q antiterminator directs expression of prophage morphogenesis and cell lysis genes located downstream of *pR'* promoter, which in absence of Q protein is inhibited by the terminator *tR'* (Court *et al.*, 2007).
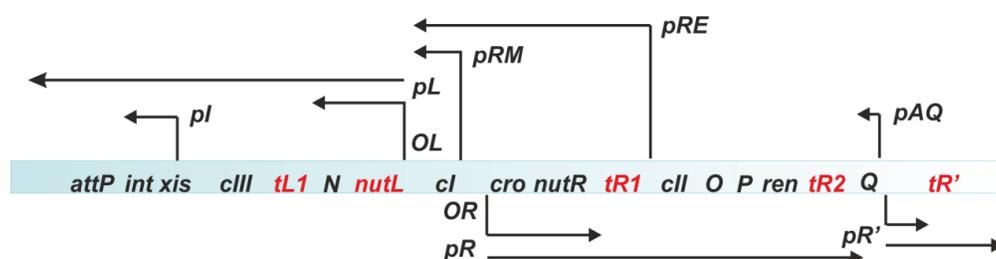
Figure 1.7. Regulation of a temperate lamdoid phage. Transcription of phage early genes initiated at the *pL* and *pR* promoters (arrows indicate direction of transcription) is arrested at the terminators *tL1* and *tR1* (red color). Antiterminator N induces expression of genes located downstream of *tL1* and *tR1* including *cIII* and *cII*, respectively. CII induces transcription from *pI*, *pRE* and *pAQ* promoters. The antiterminator Q activates expression of phage late genes located downstream of the *pR'* promoter, which in absence of Q protein is inhibited by the terminator *tR'*. Cro repressor binds operators *OL* and *OR* blocking transcription from *pL* and *pR*. Adapted from (Court *et al.*, 2007).

1.5.3. Function of phage lysis proteins and mechanism of action

Up to five prophage proteins are engaged in the lysis of the host bacterium. The lysis genes of lambdoid prophages are generally organized in a "cassette" located downstream of the prophage late promoter *pR'* (**Figure 1.8A**) (Young, 2013). In the "canonical λ prophage holin-endolysin" lysis model (Young, 2014), the lysis cassette starts with gene *S* encoding a small membrane protein holin, followed by *R* gene encoding the muralytic enzyme (endolysin). Late gene expression results in production of holins, which are uniformly integrated in the host's inner membrane (**Figure 1.8B**). Concomitantly, active R endolysins accumulate in the cytoplasm. Upon reaching a critical concentration, multiple holins aggregate in a small number of clusters, designated as "rafts". Raft-formation is thought to cause local membrane depolarization that directs assembly of one to three micron-scale holes. The holes are large enough (340 nm-1 μm) to allow transition of the R endolysin into the periplasm of Gram-negative bacteria, where endolysins destroy the peptidoglycan network (Young, 2013).
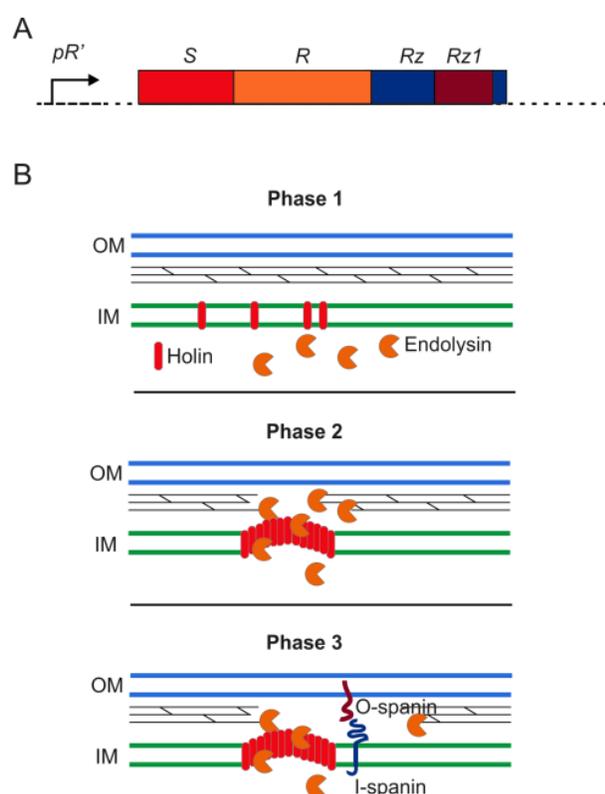
Figure 1.7. Lambda prophage lysis model. The lysis genes of lambdoid prophage *S*, *R*, *Rz* and *Rz1*, encoding S-holin, R-endolysin, i-spanin and o-spanin, respectively, are organized in a "cassette" located downstream of the prophage late promoter *pR'* (**A**). Adapted from (Young, 2013). Initially, holins integrate into the inner membrane, while the endolysins accumulate in the cytoplasm (Phase 1). Upon reaching a critical concentration, multiple holins form a micron-scale hole, which allows the endolysins to enter the periplasm and destroy the peptidoglycan network (Phase 2). Finally, i-spanins and o-spanins (anchored in the inner and outer membrane, respectively) form heterodimers, which lead to disruption of the outer membrane (Phase 3) (**B**). Adapted from Young *et al.* (2014).

Apart from the described model, prophages such as Stx-encoding phages H-19B and 933W follow the pinholin-SAR (for <u>s</u>ignal-<u>a</u>nchor-<u>r</u>elease) endolysin lysis pathway (Neely & Friedman, 1998; Young, 2013). Phage-encoded SAR endolysins are translocated into the periplasm by the host's *sec* secretion system. Inactive SAR endolysins accumulate, membrane-tethered in the inner membrane. Pinholins are small holins engaged in activation of SAR endolysin (Young, 2014). Pinholins accumulate in the inner membrane forming multiple small (~2 nm) heptameric channels. These channels, too small to assist SAR endolysin transport, cause the collapse of the pmf leading to release and activation of the muralytic SAR enzymes. Both holin and pinholin proteins are inactivated by proteins called antiholins. The latter possess a positively charged N-terminal domain, which activates holins and pinholins upon collapse of pmf. Together, holins, pinholins and antiholins time lysis of the cell. Two additional lysis proteins encoded by the genes *rz* and *rz1* finalize the cell lysis. Rz, also known as i-spanin, is an integral membrane protein, while Rz1 (o-spanin) is a lipoprotein. Spanins form heterodimers anchored in the inner and outer membrane, respectively. Upon peptidoglycan degradation, i- and o-heterodimers aggregate and trigger outer membrane disruption, possibly by causing membrane fusion. Some phages express a single u-spanin conducting function of Rz and Rz1 (Young, 2013). Furthermore, some ssDNA and ssRNA phages encode only one small lysis protein. Although the exact mechanism of these lysis proteins is still unknown, it is suggested that they arrest the peptidoglycan synthesis in actively growing bacteria, causing cell burst (Young *et al.*, 2000).

1.5.4 *Salmonella* Typhimurium SL1344 prophages: Gifsy-1, Gifsy-2, SopEΦ and ST64B

S. Tm strains harbor a set of prophages encoding multiple virulence factors. *S.* Tm SL1344 along with LT2, and ATCC14028 is lysogenic for the lambda-like prophages Gifsy-1 and Gifsy-2 (**Figure 1.9**) (Figueroa-Bossi & Bossi, 1999). Both prophages enhance the establishment of the pathogen and its systemic spread in mice, while Gifsy-2 has more profound impact compared to Gifsy-1. The Gifsy-2 prophage encodes [Cu, Zn] superoxide dismutase SodCI, which converts superoxide radicals to hydrogen peroxide, thereby protecting *S.* Tm against the ROS (Figueroa-Bossi *et al.*, 2001). Gifsy-1 encodes other virulence factors, such as the T3SS-2 effector protein SseI and the effector GipA, both supporting intracellular survival of the pathogen (Fabrega & Vila, 2013; Miao & Miller, 2000; Stanley *et al.*, 2000). Furthermore, *S.* Tm SL1344 strains harbor a member of P2 family of prophages - SopEΦ (Mirold *et al.*, 1999). This prophage is found in several epidemic *S.* Tm strains and encodes the effector protein SopE. Exported by T3SS-1, SopE is an important virulence factor, which not only supports nitrate respiration in

the inflamed intestine (Section 3.2), but also acts as a cellular invasion factor and triggers release of pro-inflammatory cytokines (Muller *et al.*, 2009). A fourth prophage encoded within the *S*. Tm SL1344 genome is a lambda-like prophage ST64B (Figueroa-Bossi & Bossi, 2004; Mmolawa *et al.*, 2003). A reversible frameshift mutation in the ST64B genome leads to expression of tailless prophages, which are noninfectious (Figueroa-Bossi & Bossi, 2004). ST64B supports survival of the *S*. Tm lysogen in the blood, suggesting that it might contribute to the systemic spread of the pathogen (Herrero-Fresno *et al.*, 2014). Nevertheless, it is possible that ST64B encodes proteins, which as other less characterized prophage-encoded effector proteins (e.g. GogB of Gifsy-1), enhance *S*. Tm SL1344 growth in specific hosts or at distinct ecological niches inhabited by the pathogen (e.g. the outer environment) (Brussow *et al.*, 2004).
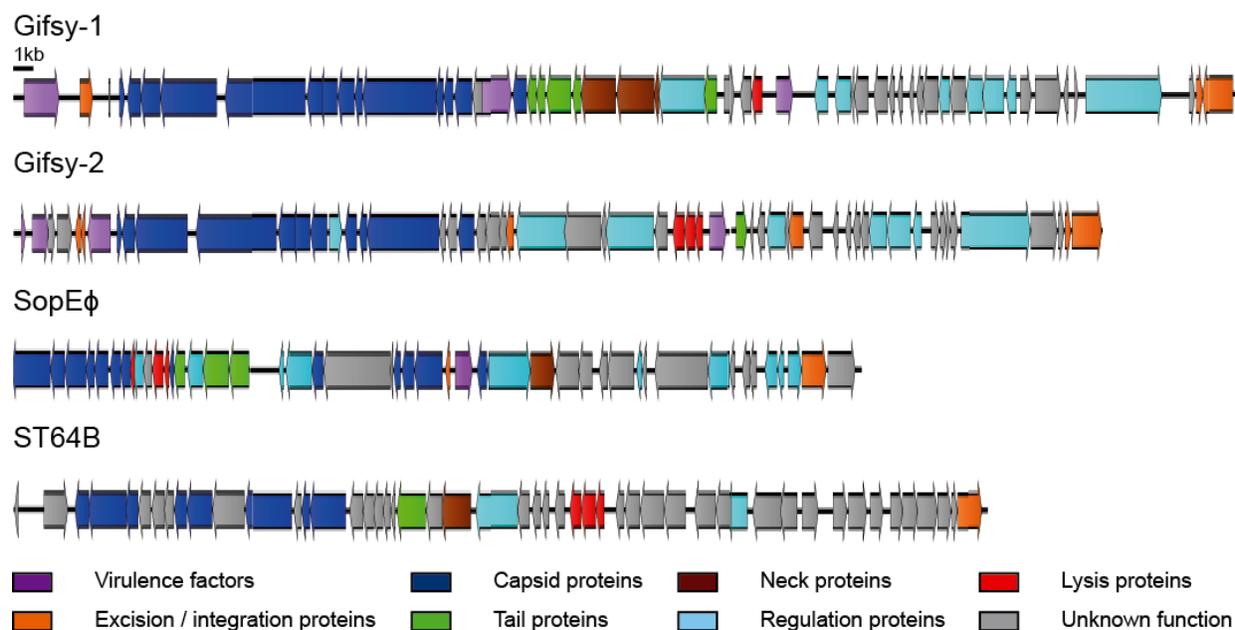
Figure 1.9 Prophages of *S*. Tm SL1344. Arrows indicate direction of transcription of open reading frames (ORF) located within the genome of phages Gifsy-1, Gifsy-2, SopEΦ and ST64B. The color code defines genes encoding virulence factors (violet), proteins involved in excision and integration of the phage genome (orange), capsid proteins (dark blue), tail proteins (green), neck proteins (brown), regulation proteins (light blue) and lysis proteins (red). Genes encoding proteins with unknown functions are marked in grey.

2 Objectives

1) *S*. Tm-elicited inflammation leads to parallel blooms of commensal and pathogenic *Enterobacteriaceae*, which compete for the available nutrients in the intestine (Lupp *et al.*, 2007; Stecher *et al.*, 2007a). Members of *Enterobacteriaceae* family employ protein toxins termed colicins to kill colicin-sensitive competitors belonging to the same family (Cascales *et al.*, 2007). One third of the natural *E. coli* population can produce colicins (Riley & Gordon, 1999), suggesting that colicin production should be a beneficial trait for colonizing the mammalian intestine. However, experimental results using *in vivo* infection models yielded contradictory results (Ikari *et al.*, 1969; Kirkup & Riley, 2004). It was observed that ColIb-producing *S*. Tm outgrows ColIb-sensitive *E. coli* upon inflammation, suggesting that production of ColIb could be an important fitness trait supporting growth of the pathogen in the inflamed intestine (Stecher *et al.*, 2012).

The first part of this PhD-thesis aimed to determine how *S*. Tm-elicited inflammation influences ColIb-dependent competition between *S*. Tm and *E. coli* investigating two main questions: does intestinal inflammation affect production of ColIb by *S*. Tm and is ColIb-sensitivity of *E. coli* enhanced upon inflammation. To answer these questions, a mouse model for *S*. Tm colitis, as well as bacterial gene reporters and a variety of bacterial mutants shall be employed.

2) In contrast to group A colicins, which are released by the activity of a colicin lysis protein, the release mechanism of group B pore-forming colicins (e.g. ColIb), lacking the lysis protein, is not known. In the course of the current work, it was observed that ColIb can be detected in the culture supernatant only upon supplementation of mitomycin C. A DNA damaging antibiotic, mitomycin C is known to activate prophages, a process which leads to cell lysis and release of cytoplasmic protein content (Guttman, 2005).

Therefore, in the second part of this PhD-thesis, the release mechanism of ColIb was investigated in the context of phage-mediated lysis. The influence of four prophages encoded within the genome of *S*. Tm SL1344 (Gifsy-1, Gifsy-2, SopEΦ and ST64B) was evaluated with respect to the release of ColIb and ColIb-dependent competition of *S. Tm* against *E. coli in vitro*.

3 Materials and Methods

3.1 Materials

3.1.1 Oligonucleotides, plasmids and strains

Table 1. Oligonucleotides

Designation	Sequence	Application
K12Δ*cirA*_rev	GCAGTATTTACTGAAGTGAAAGTCCGCCCGGTTC GCCGGGCATCTTCTCAtgtgtaggctggagctgcttc	LPN2
K12Δ*cirA*_fwd	TGTTCCGGCTTTCTGGGATGATCACCTGCATAAA AAATAAGTCCACCGCGatatgaatatcctccttagtt	LPN2
cirA - up	TTCCGGCTTTCTGGGATGATCAC	LPN2
cirA - down	GCGTATTCAGCCGGGATATGATCAC	LPN2
cirA - d1	AGATCCGGGCTACCCACAATCTTAC	LPN2
*ΔoriTnikA*_rev-val	GAAGCCATTGGCACTTTCTC	LPN5
ΔoriTnikA val	AGTTCCTCATCGGTCATGTC	LPN5
ssaV-check_fwd	GGAGCTCTGGTTACGATT	LPN5
ssaV-check_rev	ATATTTCAGCCTCAGACG	LPN5
For_colicin_*Nhe*I	CCCGCTAGCATGTCTGACCCTGTACGTATT	pLPN14
Re_colicin_*Xho*I	CCCCTCGAGGATACCAATAAGTTTATTG	pLPN14
For_*cirA_Nhe*I	CCCGCTAGCATGCTGCCGTACGCAAGGGGA	pLPN13
Re_*cirA_Xho*I	CCCCTCGAGGAAGCGATAATCCACTGC	pLPN13
p*CirA-Bam*HI	CCCGGATCCCGCGGTGGACTTATTTGTATG	pLPN1
p*CirA-Xba*l	CCCTCTAGATTCCTCCCTTCCTTGCTAAGC	pLPN1
pColIb-*Xba*I	CCCTCTAGACGTCAGCAGGCTTTCTGA	pM1437
pColIb-*Bam*HI	CCCGGATCCTCGGTATCTCCTTCATCC	pM1437
Luc-for-*Bam*HI	CCCGGATCCTAAGAAGGAGATATACCATGG A	pLPN15, LPN16
Luc-rev-*Hind*III	CGAAAGCTTACAATTTGGACTTTCCGC	pLPN15, LPN16
Gifsy-1-for	CGCCACCCTTACAGTTCAAT	Gifsy-1 prophage

Designation	Sequence	Application
Gifsy-1-rev	AGCAGCTTTCGCGTGATTAT	Gifsy-1 prophage
Gifsy-2-for	GCGCTCGATCTGATGTGTTA	Gifsy-2 prophage
Gifsy-2-rev	ACTTTCGTGGTTACGCCATC	Gifsy-2 prophage
SopE-phi-for	GGTTTGGCTACGGTCTACCA	SopEΦ prophage
SopE-phi-rev	CTGGCGGACACGGTAATACT	SopEΦ prophage
ST64B-for	ACACGGGCTCTACTGGATTC	ST64B prophage
ST64B-rev	GCTGTTGCATAAATCGCAGA	ST64B prophage
*SB51-53*_for	TCCACTCACCCGATACCCGGGTAAACAGTCTCCC GGACAGGGGGAGGTCatatgaatatcctccttagtt	LPN9, LPN14, LPN24
*SB51-53*_rev	ACGAGGCATTTTCATGAAAGTCACTTGTCAAATT TCTATGTGATGGAATgtgtaggctggagctgcttc	LPN9, LPN14, LPN24
check_ST64_for	STGTTTGGCGGCCTTTTC	LPN9, LPN14, LPN24
check2_ST64_rev	AAGGCACCGATCACCAAA	LPN9, LPN14, LPN24,
check_ST64_1	CTGCTGAAATTGGGATTC	LPN9, LPN14, LPN24
check_pKD4_Kan_For	ATCTCCTGTCATCTCACC	LPN9, LPN14, LPN24, LPN25 ,LPN26
check_pKD4_Kan_Rev	CTTGACAAAAAGAACCGGG	LPN9, LPN14, LPN24, LPN25, LPN26
Lys_Sop_phi_For	CATTACGGCGTCAACCACGGCGCAGACCGTCCAG CTATGGGACTGAATtatatgaatatcctccttagtt	LPN11, LPN25
Lys_Sop_phi_Rev	CCGCCCAGGCGGCCTCGGTTTCATCCAGCACCGC GTTCAGATCGCCGTgtgtaggctggagctgcttc	LPN11, LPN25
Lys_SopE_Check_Fwd	GGCCCATTTTTACCGCAC	LPN11, LPN25, LPN26
Lys_SopE_Check_Rev	CTGACACGCAATAATCGT	LPN11, LPN25, LPN26
*strB*_For	GGGATAGGAGAAGTCGCT	LPN28
*strB*_Rev	TGCCTTCTATCTGCGATT	LPN28
*spvB*_For	GGCCAGTTTCAGGAGATA	LPN28
*spvB*_Rev	CCTTATCTGGCGATGTACT	LPN28
Stx2-Luc fusion Fw	TTATATCTGCGCCGGGTCTGGTGCTGATTACTTCA GCCAAAAGGAACACCTGTATATGgaagacgccaaaaacat aagaa	MBK6, MBK7

Designation	Sequence	Application
*Stx2*_Com fusion Rev	ATTAACAGAAGCTAATGCAAATAAAACCGCCATA AACATCTTCTTCATGCTTAACTCCTcgtgtaggctggagct gcttc	MBK6
Stx2 R/S Com fusion Rev	CAGGATTTCGTGTTATCCGTCCAGGTAAGCAAAC CTCATTTTTCAGCAAAATATTCTTCcgtgtaggctggagct gcttc	MBK7
Stx2 Operon Fw	GATCGGTATGTTGAGCGTGA	MBK6, MBK7, MBK13, MBK14, LPN21, LPN22
Stx2 Operon Rev	TGCTCAGTCTGACAGGCAAC	MBK6, MBK13, LPN21
R/S outside Rev	GAGATGCGCAGAAATGACAA	MBK7, MBK14, LPN22

Table 2. Plasmids

Plasmid	Lab-internal plasmid number	Genotype	Reference
pWKS29 and pWKS30	pWKS29 and pWKS30		(Wang & Kushner, 1991)
p2^{cm}	p2^{cm}	P2::*cat*	(Stecher *et al.*, 2012
pM979	pM979	Constitutive *gfp*mut2-reporter plasmid (ribosomal *rpsM* promoter)	(Stecher *et al.*, 2004)
pLB02	pLB02	Firefly-luciferase reporter plasmid	(Gunn *et al.*, 1995)
pC831-2	pC831-2	expression of the ColIb (*cib*) immunity protein gene *imm*	(Stecher *et al.*, 2012)
pLPN13	pLPN13	*cirA-6-x-his*	(Nedialkova *et al.*, 2014)
pLPN14	pLPN14	*cib-6-x-his*	(Nedialkova *et al.*, 2014)
p$^{cirA-luc}$	pLPN15	*cirA*-promoter firefly-luciferase reporter	(Nedialkova *et al.*, 2014)
p$^{cib-luc}$	pLPN16	*cib*-promoter firefly-luciferase reporter	(Nedialkova *et al.*, 2014)
pM1437	pM1437	*cib*-promoter gfp-reporter	(Nedialkova *et al.*, 2014)
pLPN1	pLPN1	*cirA*-promoter gfp-reporter	(Nedialkova *et al.*, 2014)
p$^{compl.\ cirA}$	pWRG693-1	*cirA* complementation vector	(Nedialkova *et al.*, 2014)
p$^{compl.\ cib}$	pWRG694	*cib* complementation vector	(Nedialkova *et al.*, 2014)

Table 3. Strains

S.Tm strains	Lab-internal strain number	Genotype	Reference
S. Tm[wt]	SB300	*S.* Tm strain SL1344	(Hoiseth & Stocker, 1981)
S. Tm[Δcib]	M990	P2 *cib imm*::*aphT*	(Stecher *et al.*, 2012)
S. Tm[wt amp]	SB300	*S.* Tm carrying plasmid pWKS30 (Wang & Kushner, 1991)	(Stecher *et al.*, 2012)
S. Tm[ΔoriT]	M1407	P2 Δ*oriT nikA*::*cat*	(Nedialkova *et al.*, 2014)
S. Tm[avir] p2[cm]	M996	*invG*; *sseD::aphT* P2::*cat*	(Stecher *et al.*, 2012)
S. Tm[ΔoriT Δcib]	MAD1	p2 Δ*oriT nikA*::*cat cib imm*::*aphT*	(Stecher *et al.*, 2012)
S. Tm[ΔP2 avir]	MBK15	*invG*; *sseD::aphT* cured of p ColIb plasmid (P2)	(Nedialkova *et al.*, 2014)
S. Tm[avir]	M557	*invG*; *sseD::aphT*	(Hapfelmeier *et al.*, 2005)
S. Tm[ΔoriT avir]	LPN5	*invG*; *sseD::aphT*(Hapfelmeier *et al.*, 2005); P2 Δ*oriT nikA*::*cat*	(Nedialkova *et al.*, 2014)
S. Tm[MA6118]	MA6118	*S.* Tm strain SL1344	(Figueroa-Bossi *et al.*, 2001)
S. Tm[ΔG1ΔG2]	MA6247	Δ*Gifsy-1* Δ*Gifsy-2*	(Figueroa-Bossi & Bossi, 1999)
S. Tm[ΔG1ΔG2ΔST]	MA7551	Δ*Gifsy-1* Δ*Gifsy-2 ST64B*::*aphT*	(Figueroa-Bossi & Bossi, 2004)
S. Tm[ΔPh]	MA7891	Δ*Gifsy-1* Δ*Gifsy-2 ST64B*::*aphT SopEΦ*::*cat*	(Alonso *et al.*, 2005)
S. Tm[ΔlysST]NT	LPN9	ST64B *(SL1344_1955-SL1344_1957)::aphT*	Unpublished
S. Tm[ΔlysSφCm]NT	LPN11	SopEΦ *(SL1344_2684- SL1344_2687)::cat*	Unpublished
S. Tm[ΔlysST]	LPN14	ST64B *(SL1344_1955-SL1344_1957)::aphT*	Unpublished
S. Tm[ΔG1ΔG2ΔlysST]	LPN24	Δ*Gifsy-1* Δ*Gifsy-2* ST64B *(SL1344_1955-SL1344_1957)::aphT*	Unpublished
S. Tm[ΔlysSφCm]	LPN15	SopEΦ *(SL1344_2684- SL1344_2687)::cat*	Unpublished
S. Tm[ΔG1ΔG2ΔlysSφC]	LPN17	Δ*Gifsy-1* Δ*Gifsy-2* SopEΦ *(SL1344_2684- SL1344_2687)::cat*	Unpublished
S. Tm[ΔlysSφ]	LPN19	SopEΦ Δ*(SL1344_2684- SL1344_2687)*	Unpublished
S. Tm[ΔG1ΔG2ΔlysSφ]	LPN20	Δ*Gifsy-1* Δ*Gifsy-2* SopEΦ Δ*(SL1344_2684- SL1344_2687)*	Unpublished

S.Tm strains	Lab-internal strain number	Genotype	Reference
S. Tm$^{\Delta G1 \Delta G2 \Delta lysS \phi K}_{NT}$	LPN25	Δ*Gifsy-1* Δ*Gifsy-2* SopEΦ *(SL1344_2684- SL1344_2687)::aphT*	Unpublished
S. Tm$^{\Delta G1 \Delta G2 \Delta lysS \phi K}$	LPN26	Δ*Gifsy-1* Δ*Gifsy-2* SopEΦ *(SL1344_2684- SL1344_2687)::aphT*	Unpublished
S. Tm$^{\Delta Ph}$ Sm^R	LPN27	MA7891 pRSF1010-SL1344	Unpublished
S. Tm$^{\Delta G1 \Delta G2 \Delta lysST}$ Sm^R	LPN28	Δ*Gifsy-1* Δ*Gifsy-2* ST64B *(SL1344_1955-SL1344_1957)::aphT* pRSF1010-SL1344	
S. Tm^{A36}	A36	*S*. Tm wild type isolate no prophage	(Mirold *et al.*, 1999)
S. Tm^{M4}	M4	*S*. Tm wild type isolate no prophage SopEΦ *sopE::aphT*	(Mirold *et al.*, 1999)
S. Tm^{A36} p2^{cm}	LPN12	*S*. Tm^{A36} P2::*cat*	Unpublished
S. Tm^{M4} p2^{cm}	LPN13	*S*. Tm^{M4} P2::*cat*	Unpublished
S. Tm^{wt} p2^{cm}	M995	SB300 *collB-HA::cat*	(Stecher *et al.*, 2012)
E. coli strains			
Ec DH5α			Invitrogen
Ec BL21 (DE3)			Stratagene
Ec ^{Nissle}			(Stecher *et al.*, 2012)
Ec^{8178}			(Stecher *et al.*, 2012)
Ec^{MG1655}		*E. coli* K-12 wild type strain MG1655, streptomycin-resistant	(Moller *et al.*, 2003)
Ec$^{MG1655 \Delta cirA}$	LPN2	*cirA*::*aphT*	(Nedialkova *et al.*, 2014)
Ec$^{MG1655 amp}$		*E. coli* K-12 wild type strain MG1655, streptomycin-resistant, carrying plasmid pWKS30 (Wang & Kushner, 1991)	Unpublished
C600W34		C600 *E. coli* K12 lysogen of 933W	(O'Brien *et al.*, 1984)
MBK6		C600 *E. coli* K12 lysogen of 933W *stx2A::luc aphT*	M. Koeppel
MBK7		C600 *E. coli* K12 lysogen of 933W *(stx2A R S)::luc aphT*	M. Koeppel
Ec^{Stx}	MBK13	Ec^{MG1655} lysogen of 933W *stx2A::luc aph*	M. Koeppel
Ec$^{Stx\Delta SR}$	MBK14	Ec^{MG1655} lysogen of 933W *(stx2A R S)::luc aphT*	M. Koeppel
Ec^{Stx} p2^{cm}	LPN21	MBK13 P2::*cat*	Unpublished
Ec$^{Stx\Delta SR}$ p2^{cm}	LPN22	MBK14 P2::*cat*	Unpublished
Ec^{MG1655} p2^{cm}	LPN23	Ec^{MG1655} P2::*cat*	Unpublished

3.1.2 Chemicals and consumables

Table 4. Chemicals and consumables

Item	Supplier
$(MgCO_3)_4Mg(OH)_2$ x $5H_2O$	Sigma-Aldrich Chemie (Munich)
Acrylamide 30%	Serva (Heidelberg)
Cell sieve 40 µm	Milian
LumiNunc™ F96 MicroWell™ Plates, white, sterile, F-bottom	Thermo Fisher Scientific Biosciences (St. Leon-Rot)
TC-Plates 96-well, flat-bottom	Thermo Fisher Scientific Biosciences (St. Leon-Rot)
Agar bacto™	Becton, Dickinson and Company (BD) (Heidelberg)
Albumin factor V	Roth (Karlsruhe)
Aminolink kit	Thermo Fisher Scientific Biosciences (St. Leon-Rot)
Antimicrobial susceptibility test discs	Oxoid, Thermo Fisher Scientific Biosciences (St. Leon-Rot)
Ammonium persulfate (APS)	Roth (Karlsruhe)
Boric acid	Roth (Karlsruhe)
Bovine serum albumin fraction (BSA), PAA	GE Healthcare (Munich)
Bromphenolblue	Roth (Karlsruhe)
$CaCl_2$	Merck Chemicals (Schwalbach)
Colistinsulfate	Roth (Karlsruhe)
Chloroform	Roth (Karlsruhe
Cryotubes	Thermo Fisher Scientific Biosciences (St. Leon-Rot)
D(-) luciferin	Sigma-Aldrich Chemie (Munich)
ddH_2O (Ampuwa)	Fresenius Kabi (Bad Homburg)
D-glucose	Roth (Karlsruhe)
$DiBaC_4$	Invitrogen, Thermo Fisher Scientific Biosciences (St. Leon-Rot)
Diethylenetriamine Pentaacetic Acid (DTPA)	Sigma-Aldrich Chemie (Munich)
dNTP Set	Thermo Fisher Scientific Biosciences (St. Leon-Rot)
DreamTaq PCR Master Mix (2 x)	Thermo Fisher Scientific Biosciences (St. Leon-Rot)
Dithiothreitol (DTT)	Roth (Karlsruhe)
ECL detection system	GE Healthcare (Munich)
Ethylenediaminetetraacetic acid (EDTA)	Roth (Karlsruhe)
Ethylene glycol tetraacetic acid (EGTA)	Roth (Karlsruhe)
Electroporation cuvette (1 mm)	Eppendorf (Wesseling-Berzdorf)
Ethanol ROTIPURAN® ≥99,5 %, p.a	Roth (Karlsruhe
Restriction enzymes	Thermo Fisher Scientific Biosciences (St. Leon-Rot)
$FeCl_3$	Sigma-Aldrich Chemie (Munich)
GeneRuler 1kb DNA ladder	Thermo Fisher Scientific Biosciences (St. Leon-Rot)
Glycerol	Roth (Karlsruhe)
Glycine	MP Biomedicals
Glycylglycin	Roth (Karlsruhe)
High-fidelity PCR enzyme	Thermo Fisher Scientific Biosciences (St. Leon-Rot)
Histidine	Roth (Karlsruhe)
HisTrap column (5 ml)	GE Healthcare (Munich)

Item	Supplier
HiTrap desalting column (5 ml)	GE Healthcare (Munich)
Immobilion Western Chemoluminescent HRP substrat	Merck Chemicals (Schwalbach)
K_2HPO_4	Roth (Karlsruhe)
KCl	Fluka, Sigma-Aldrich Chemie (Munich)
KH_2PO_4	Roth (Karlsruhe)
L-(+)-Arabinose	Sigma-Aldrich Chemie (Munich)
Li_3-Coenzym A	Sigma-Aldrich Chemie (Munich)
Lysozyme from chicken egg white	Sigma-Aldrich Chemie (Munich)
MacConkey agar	Oxoid, Thermo Fisher Scientific Biosciences (St. Leon-Rot)
MacConkey agar	Roth (Karlsruhe)
Mg-ATP	Sigma-Aldrich Chemie (Munich)
$MgSO_4$	Roth (Karlsruhe)
Methanol ROTIPURAN® ≥99,5 %, p.a	Roth (Karlsruhe)
Milk powder	Roth (Karlsruhe)
Mitomycin C	Roth (Karlsruhe)
Na_2HPO_4 unhydrated	Roth (Karlsruhe)
Na_2HPO_4 x $2H_2O$	Roth (Karlsruhe)
NaCl	Roth (Karlsruhe)
NH_4Cl	Sigma-Aldrich Chemie (Munich)
Nitrocellulose membrane	GE Healthcare (Munich)
Nonidet P-40	ICN Biomedicals
Benzonase nuclease (Novagen)	Merck Chemicals (Schwalbach)
NucleoSpin Gel and PCR clean-up kit	Macherey-Nagel (Düren)
NucleoSpin Plasmid kit	Macherey-Nagel (Düren)
Tissue-Tek Optimal Cutting Temperature (O.C.T.) compound	Sakura Finetek, (Torrance)
Page ruler prestained protein ladder	Thermo Fisher Scientific Biosciences (St. Leon-Rot)
PD-10 desalting column	GE Healthcare (Munich)
Peptone	Oxoid, Thermo Fisher Scientific Biosciences (St. Leon-Rot)
Phenylmethylsulfonyl fluoride (PMSF),	Serva (Heidelberg)
Plasmid Plus Midi Kit	QIAGEN (Hilden)
Oligonucleotides	Metabion (Martinsried)
Protein assay reagent	Bio-Rad (Munich)
Sodium dodecyl sulfate (SDS)	Serva (Heidelberg)
Sodium Azide	Merck Chemicals (Schwalbach)
T4 DNA ligase	Thermo Fisher Scientific Biosciences (St. Leon-Rot)
Tergitol	Sigma-Aldrich Chemie (Munich)
Thiamine	Sigma-Aldrich Chemie (Munich)
Tetramethylethylenediamine (TEMED)	Biomol Feinchemikalien (Hamburg)
Tris	MP Biomedicals (Eschwege)
Triton X-100	Roth (Karlsruhe)
Tryptone	Roth (Karlsruhe)

Item	Supplier
Tween	Roth (Karlsruhe)
Urea	MP Biomedicals (Eschwege)
Yeast extract	MP Biomedicals (Eschwege)
Zebra Spin desalting columns (5 ml)	Thermo Fisher Scientific Biosciences (St. Leon-Rot)
β –D-thiogalactopyranoside (IPTG)	Roth (Karlsruhe)
Filter Millex 0.22 μm	Merck Chemicals (Schwalbach)

3.1.2.1 Antibodies and supplements

Table 5. Primary antibodies

Antibody	Origin	Supplier	Final concentration
α-ColIb-His	Rabbit	Pineda (Berlin)	1:500
α-CirA-His	Rabbit	Pineda (Berlin)	1:50
α - DnaK (*E. coli*)*	Mouse	Enzo Life Sciences (Lörrach)	1:1,000

*Also recognizes *S*. Tm DnaK due to the high identity.

Table 6. Secondary antibodies

Antibody	Origin	Supplier	Final concentration
α-rabbit-HRP	Goat	GE-Healthcare (Munich)	1:10,000
α -mouse-HRP	Goat	Sigma-Aldrich Chemie (Munich)	1:10,000

Table 7. Antibiotics

Antibiotic	Supplier	Final concentration
picillin	Roth (Karlsruhe)	100 μg/ml
Chloramphenicol	Roth (Karlsruhe)	30 μg/ml
Kanamycinsulfate	Roth (Karlsruhe)	30 μg/ml
Streptomycin	Roth (Karlsruhe)	50 μg/ml

3.1.3 Buffers and Media

Table 8. Luria-Bertani (LB) medium

Component	Per liter medium
NaCl	5 g
Yeast extract	5 g
Tryptone	10 g

All components were dissolved in dH_2O

Table 9. LB agar

Component	Per liter medium
NaCl	5 g
Yeast Extract	5 g
Tryptone	10 g
Agar	15 g

All components were dissolved in dH_2O.

Table 10. LB soft agar

Component	Per liter medium
NaCl	5 g
Yeast Extract	5 g
Tryptone	10 g
Agar	7 g

All components were dissolved in dH_2O

Table 11. M9 medium

Component	Final concentration
$Na_2HPO_4 2H_2O$	40 mM
KH_2PO_4	20 mM
NaCl	9 mM
NH_4Cl	2 g/l
D-glucose	2 g/l
$MgSO_4$	1 mM
$CaCl_2$	100 µM
Thiamine	10 mg/ml
Histidine	500 mg/l

All components were dissolved in ddH_2O (Ampuwa).

Table 12. Peptone-glycerol broth

Component	Per 0.5 l broth
Peptone	10 g
Glycerol	25 ml

All components were dissolved in dH_2O.

Table 13. Phosphate Buffered Saline (PBS) 10x

Component	Per liter buffer
NaCl	80 g
KCl	2 g
Na_2HPO_4 anhydrous	6.1 g
KH_2PO_4	2.4 g

All components were dissolved in dH_2O.

Table 14. Recombinant protein purification lysis buffer

Component	Final concentration
Na_2HPO_4	40 mM
NaCl	0.3 M
Imidazole	5 mM
PMSF	2 mM
Benzonase nuclease	(1:2,000)
*Urea	6 M

The pH was adjusted to 7.8 with 1 M NaOH or 1 M HCl and the buffer was sterile filtered (22 µm).
*Urea was added only to buffer applied for CirA-His purification.

Table 15. Recombinant protein purification loading buffer

Component	Final concentration
Na_2HPO_4	40 mM
NaCl	0.3 M
Imidazole	5 mM
*Urea	6 M

The pH was adjusted to 7.8 with 1 M NaOH or 1 M HCl and the buffer was sterile filtered (22 µm).
*Urea was added only to buffer applied for CirA-His purification.

Table 16. Recombinant protein purification elution buffer

Component	Final concentration
Na_2HPO_4	40 mM
NaCl	0.3 M
Imidazole	0.5 M
*Urea	6 M

The pH was adjusted to 7.8 with 1 M NaOH or 1 M HCl and the buffer was sterile filtered (22 µm).
*Urea was added only to buffer applied for CirA-His purification.

Table 17. Recombinant protein purification exchange buffer 1

Component	Final concentration
Na_2HPO_4	20 mM
NaCl	100 mM
*Urea	4 M

The pH was adjusted to 7.8 with 1 M NaOH or 1 M HCl and the buffer was sterile filtered (22 µm).
*Urea was added only to buffer applied for CirA-His purification.

Table 18. Recombinant protein purification exchange buffer 2

Component	Final concentration
Boric acid	50 mM
NaCl	300 mM
EDTA	2 mM

The pH was adjusted to 9.0 with 1 M NaOH or 1 M HCl and the buffer was sterile filtered (22 µm).

Table 19. 10% resolving gel

Component	Per 10 ml
dH_2O	4 ml
30% Acrylamide	3.32 ml
1.5 M Tris HCl pH 8.8	2.5 ml
20% SDS (in dH_2O)	0.05 ml
10% APS (in dH_2O)	0.1 ml
TMED	0.004 ml

All components were dissolved in dH_2O.

Table 20. 5% stacking gel

Component	Per 1 ml
dH$_2$O	0.68 ml
30% Acrylamide	0.17 ml
1.5 M Tris HCl pH 6.8	0.13 ml
20% SDS (in dH$_2$O)	0.005 ml
10% APS (in dH$_2$O)	0.01 ml
TMED	0.001 ml

All components were dissolved in dH$_2$O.

Table 21. Protein loading buffer 5 x

Component	Final concentration
1.5.M Tris	250 mM
DTT	500 mM
SDS	10%
Bromphenolblue	0.5%
Glycerol	50%
1.5 M Tris	250 mM

All components were dissolved in dH$_2$O.

Table 22. Running buffer

Component	Final concentration
Tris	25 mM
Glycine	250 mM
SDS	0.1%

All components were dissolved in dH$_2$O.

Table 23. Transfer buffer

Component	Final concentration
Tris	25 mM
Glycine	192 mM
Methanol	20%

All components were dissolved in dH$_2$O.

Table 24. Immunoblot lysis buffer

Component	Final concentration
Tris pH 7.5	50 mM
NaCl	150 mM
EDTA	5 mM
Nonidet P-40	0.25%
Lysozyme	100 mg/ml

All components were dissolved in dH_2O.

Table 25. Luciferase assay lysis buffer

Component	Final concentration
K_2HPO_4	100 mM
KH_2PO_4	100 mM
EDTA	2 mM
Triton X-100	1%
BSA (PAA)	5 mg/ml
DTT	1 mM
Lysozyme	5 mg/ml

All components were dissolved in ddH_2O (Ampuwa).

Table 26. Luciferase reagent

Component	Final concentration
Tricine	20 mM
$(MgCO_3)_4Mg(OH)_25H_2O$	1 mM
EDTA	0.1 M
D(-) Luciferin	470 μM
DTT	33 mM
Li_3-Coenzym A	270 μM
Mg-ATP	530 μM
Glycylglycin	125 μM
Tricine	5 mg/ml

All components were dissolved in ddH_2O (Ampuwa).

3.2 Methods

3.2.1 Bacterial growth

3.2.1.1 Generation of bacterial cryostocks

Bacteria streaked from -80° C cryostocks were grown overnight (o.n.) on LB agar with the appropriate antibiotics at 37° C. A single bacterial colony was inoculated in 3 ml LB medium (supplemented with the appropriate antibiotic(s)) and grown o.n. at 37° C on a wheel rotor. Further, o.n. culture was spun down at 4° C for 15 min and 4,500 rpm. The supernatant was removed and the bacterial pellet were resuspended in 1 ml peptone-glycerol broth (**Table 12**) and stored in cryotubes at -80° C.

3.2.1.2 Growth of bacterial strains for *in vitro* assays (Section 4.1)

Bacteria streaked from -80° C cryostocks were grown o.n. on LB agar with the appropriate antibiotics at 37° C. A single colony grown in a starter culture in LB or M9 media for 12 h and used for inoculation of subcultures (1:20), except for the *in vitro* co-cultures, where subcultures were inoculated to an optical density of 600 nm (OD_{600}) of 0.05, measured by using BioPhotometer (Eppendorf). The following supplements were used: mitomycin C (to a final concentration of 0.25 µg/ml), diethylenetriaminepentaacetic acid (DTPA) (to a final concentration of 100 µM), and $FeCl_3$ (to a final concentration of 1 µM, 10 µM, 0.1 mM or 1 mM). All cultures were grown at 37° C on a wheel rotor, except of *in vitro* co-cultures, where subcultures were grown in Erlenmeyer-flasks in a shaker at 200 rpm.

3.2.1.3 Growth of bacterial strains (Section 4.2)

Bacteria grown on LB agar without antibiotics from -80° C cryostocks and incubated o.n. at 37° C. Bacterial colonies were re-streaked once again on LB agar plates and grown o.n. at 37° C. Three individual colonies per strain were used for inoculation of 3 ml LB cultures, which were grown for 12 h at 37° C on a wheel rotor. These starter cultures were subsequently diluted and normalized to an OD_{600} of 0.0025 in 10 ml fresh LB (subculture I). After 3 h growth in Erlenmeyer flasks at 37° C and 180 rpm, subculture I was diluted and normalized to an OD_{600} of 0.0025 in 10 ml fresh LB supplemented with 0.5µg/ml mitomycin C (subculture II). For the control subculture II no supplements were used. Subculture II was incubated for 6 h at 37° C and 180 rpm. Bacterial density (OD_{600}) determined each hour.

For assays done in 96-well, plates the starter cultures were prepared as described and subsequently diluted and normalized to an OD_{600} of 0.025 in 3 ml fresh LB (subculture I). Following 2 hours growth at 37° C, on a wheel rotor, subculture I was diluted and normalized to an OD_{600} of 0.2 in fresh LB (supplemented or with 0.5 µg/ml mitomycin C) and 200 µl/well were transferred to a 96-well plate (subculture II). No supplements were used for the control subculture II. All conditions were done in 3-5 replicates. Subculture

34

II was incubated up to 4-5 h at 37° C and 180 rpm. Bacterial density was measured each hour using a FLUOstar Optima plate reader (BMG Labtech).

3.2.1.4 *In vitro* co-cultures (Section 4.2)

Bacteria were streaked out on MacConkey agar plate supplemented with selective antibiotic(s) from -80° C cryostocks and incubated o.n. at 37° C. Strains were re-streaked on LB agar plates without antibiotics and grown o.n. at 37° C. Three individual colonies per strain (*S*. Tm and *E. coli*) were used to inoculate 3 ml LB medium cultures, which were grown for 12 h at 37° C on a wheel rotor. These starter cultures were diluted and normalized to an OD_{600} of 0.025 in 3 ml fresh LB (subculture I). After 2 hours growth at 37° C on a wheel rotor subculture I was diluted and normalized to an OD_{600} of 0.4 and subsequently mixed (1:1). Thereafter, the strain mixture was added to fresh LB (1:1) with or without supplements (subculture II). The following supplements were added: mitomycin C (to a final concentration of 0.25 µg/ml) and DTPA (to a final concentration of 100 µM). For each setup 200 µl/well were transferred in 96-well plate and incubated for 6 h at 180 rpm at 37° C. At time point 0 h, 3 h and 6 h OD_{600} was determined using a FLUOstar Optima plate reader (BMG Labtech). At each of the selected time points, 100 µl from a replicate for each sample were taken for determination of the colony forming units (cfu). Cultures were 10-fold diluted up to 10^{-6} in PBS and plated on MacConkey agar plates without antibioticz and supplemented with 100 µg/ml ampicillin. Plates were incubated at 37° C and cfu were determined.

3.2.1.5 Bacterial live-dead staining and FACS

Bacteria were streaked out on LB agar plates from -80° C cryostocks and incubated o.n. at 37° C. Next, a single colony was inoculated in 3 ml LB medium and grown for 12 h at 37° C on a wheel rotor. This starter cultures were used for inoculation of subculture I in 3 ml LB medium (1:20), supplemented with 100 µM DTPA (subculture I). For the control subculture I no supplements were used. Following incubation of 1 to 4 hours (37° C, wheel rotor) subculture I was diluted and normalized to an OD_{600} of 0.01 in LB medium (subculture II) supplemented with ColIb-His in recombinant protein purification exchange buffer 2 (**Table 18**) to a final concentration of 7.5 ng/ml or colistin sulphate to a final concentration of 0.3 µg/ml. Next, 180 µl of each subculture II were transferred into a 96-well plate. Subculture II was incubated for 2 hours at 37° C. To detect dead bacteria, $DiBaC_4$ (Invitrogen) were added to a final concentration of 10 µg/ml and after 25 min incubation (room temperature (RT), in darkness) each sample was diluted in PBS (1:1) and analyzed by fluorescence-activated cell sorting (FACS) using BD FACSCanto[TM] II (BD Biosciences).

3.2.2 Generation of samples for immunoblot

3.2.2.1 Generation of samples for immunoblot (Section 4.1)

Bacteria were streaked out on LB agar plates from -80° C cryostocks and incubated o.n. at 37° C. Next, a single colony was used for inoculation of a starter culture in 3 ml M9 medium, grown for 12 at 37° C. The starter culture was used for inoculation (1:20) of 2 ml M9 medium supplemented with $FeCl_3$ to a final concentration of 1 µM, 10 µM, 0.1 mM or 1 mM. These subcultures were grown for 7 h. A starter culture of 3 ml LB was grown for 12 h and used for inoculation of 3ml LB. The following supplements were used: mitomycin C (to a final concentration of 0.25 µg/ml) and DTPA (to a final concentration of 100 µM). The subcultures were grown for 4 h. From each subculture, 250 µl (for an OD_{600} of 1) was taken, spun down at at 10, 000 rpm, for 10 min, 4° C. The supernatant was removed and the bacterial pellet was frozen in liquid nitrogen and thawn at RT for 15 min (freeze-thawing was repeated three times), resuspended in 100 µl immunoblot lysis buffer (**Table 24**) and incubated in thermomixer at 550 rpm, for 1 h, 23° C. Thereafter, the lysate was spun down 10, 000 rpm, for 10 min, 4° C. Total protein was quantified in the lysate using aprotein assay reagent (Bio-Rad). Next, the bacterial lysate was added to 1 x protein loading buffer (**Table 21**) and incubated for 10 min at 95° C. For the supernatant fractions 500 µl (for an OD_{600} of 1) of the subculture were spun down twice, supernatant was added to 5 x protein loading buffer and incubated for 10 min at 95° C.

3.2.2.2 Generation of samples for immunoblot (Section 4.2)

A 100 µl of subculture II grown in a 96-well plate (**Section 3.2.1.3**) was taken and spun down at 4° C for 10 min, at 10,000 rpm. Following this, the supernatant was transferred in a new tube, while bacterial pellets were resuspended in 100 µl 1 x protein loading buffer (**Table 21**) and incubated for 10 min at 95° C. The supernatant was spun down once more to eliminate all bacteria and 80 µl of the so obtained supernatant were added to 20 µl 5 x protein loading buffer (**Table 21**). Next, samples were incubated for 10 min at 95° C. Samples from cultures grown in Erlenmeyer flasks were processed in the same way, but instead 500 µl were taken from subculture II and resuspended in 250 µl 1x protein loading buffer for cell lysate fraction. For supernatant fraction 200 µl from the supernatant were added to 50 µl 5x protein loading buffer (**Table 21**).

3.2.3 Colicin-killing assay (Halo-assay)

3.2.3.1 Colicin-killing assay (Halo-assay) (Section 4.1)

Bacteria were streaked out on LB agar plates from -80° C cryostocks and incubated o.n. at 37° C. Next, a single colony was grown in 3 ml LB medium for 12 h, on a wheel rotor, at 37° C. Cultures were subsequently diluted and normalized to an OD_{600} of 0.025 and 2 µl were spotted on LB agar plates supplemented with mitomycin C to a final concentration of 0.25 µg/ml. Plates were incubated o.n. at 37° C and consequently overlaid with 6 ml LB soft agar (**Table 10**) mixed with 100 µl *E. coli* grown o.n. in 3 ml LB medium, at 37° C. Following this, plates were incubated o.n. at 37° C and inhibition zone (halo) size was measured.

3.2.3.2 Colicin-killing assay (Halo-assay) (Section 4.2)

Starter cultures (**Section 3.2.1.3**) were diluted and normalized to an OD_{600} of 0.025 and 2 µl for each strain were spotted on LB agar plates supplemented with mitomycin C to a final concentration of 0.5 µg/ml. Plates were incubated o.n. at 37° C and consequently overlaid with 6 ml LB soft agar (**Table 10**) mixed with 100 µl Ec[MG1655] grown o.n. in 3 ml LB medium, at 37° C. Next, the plates were incubated o.n. at 37° C and inhibition zone (halo) size was measured using Adobe Photoshop CS5 ruler tool on an image of the plate taken with ChemiDoc MP System (Bio-Rad), Image Lab software.

3.2.3.3 Colicin-killing assay using colicin released in the bacterial culture supernatant

At the final point of the bacterial growth (**Section 3.2.1.3**) 0.6-1.0 ml from subculture II (in case of 96-well plate assay, triplicates for each sample were pooled together) were spun down at 10,000 rpm for 10 min, 4° C. Following this, the supernatant was sterile filtered (0.22 µm filters). LB agar plates were overlaid with 6 ml LB soft agar (**Table 10**) mixed with 100 µl Ec[MG1655] grown o.n. in 3 ml LB medium, at 37° C. Antimicrobial susceptibility test discs (Oxoid) were laid on each plate and 6µl sterile spent supernatant was spotted on each disc. Plates were incubated o.n. at 37° C and inhibition zone (halo) size was measured using Adobe Photoshop CS5 Ruler tool on an image of the plate taken with ChemiDoc MP System (Bio-Rad), Image Lab software.

3.2.4 Luciferase assay

3.2.4.1 Luciferase assay for samples obtained *in vitro* (Section 4.1)

Luciferase assays were performed as described (Gerlach *et al.*, 2007). Briefly, a starter cultures of 3 ml LB (supplemented with 100 µg/ml ampicillin) grown for 12 h was used for inoculation of 3 ml LB (1:20) (containing 100 µg/ml ampicillin and respective supplements), which were cultured for 4 h. From each of these subcultures, 250 µl (of an OD_{600} of 1) was spun down at 14,000 rpm for 5min, 4° C. The supernatant

was removed and the bacterial pellet was frozen at -80° C for 1 h. Next, the pellet was thawn and resuspended in 500 µl luciferase assay lysis buffer (**Table 25**) and incubated for 15 min, at RT while vortexing every 3 minutes. Bacterial lysates (25 µl) were transferred in 96-well plates (white) and 50 µl luciferase reagent was added to each well. Luminescence was measured using a FLUOstar Optima plate reader (BMG Labtech).

3.2.4.2 Luciferase assay for samples from cecum content (Section 4.1)

To determine the luciferase activity in bacteria extracted from cecum content, the cecum content was harvested from infected mice and stored on ice until further use (1-2 h). The cecum content was resuspended in 500 µl PBS (0.1% tergitol) and homogenized in a tissue-lyser (Qiagen; 5 min; 50 Hz). Further, the content was filtered through a 40 µm cell-sieve (Milian). Samples were taken to determine the cfu/ml of the reporter strain by plating on MacConkey agar with the respective antibiotics. A defined volume (*i.e.* 900 µl) was spun down at 14,000 rpm for 2 min, 4° C. The supernatant was removed and the pellet was frozen on dry ice and stored at -80 C. The samples were then thawn and processed as described above. Only values above detection limit (control cecum content) were considered. The relative luminescence units (rlu) per cfu luciferase-reporter strain were calculated.

3.2.4.3 Luciferase assay (Section 4.2)

In order to measure luciferase activity in bacterial lysates, 100 µl of each sample from subculture II (**Section 3.2.1.3**) was spun down at 10,000 rpm for 5 min, 4° C. The supernatant was transferred to a new tube to be further used for extracellular luciferase activity evaluation. Pelleted bacteria were frozen at -80° C for >1 hour. Frozen bacteria were thawn to RT and resuspended in 500 µl luciferase assay lysis buffer (**Table 25**). Samples were left to lyse for 15 min at RT, vortexing shortly each 3 min. luciferase activity was measured as described (**Section 3.2.5.2**). In order to quantify extracellular luciferase activity, the supernatant of each sample was spun down one more time and 25 µl from the newly obtained supernatant were measured as described for the bacterial lysates.

3.2.5 Molecular biology methods

All methods were developed based on the protocols described by Sambrook *et. al.* (Sambrook *et al.*, 1989).

3.2.5.1 PCR on bacterial lysates

Polymerase chain reaction (PCR) on bacterial lysates was carried out in order to verify correct construction of bacterial mutants. A single bacteria colony was inoculated in 3 ml LB medium (supplemented with selective antibiotic(s)) and grown o.n. at 37° C on a wheel rotor. 5 µl of the o.n. culture was added to 95 µl ddH$_2$O, incubated at 95° C, for 10 min and placed on ice immediately after incubation. One 20 µl PCR reaction contained 1 µl of 10 µM forward primer, 1 µl of 10 µM reverse primer, 3 µl ddH$_2$O, 5 µl bacterial lysate and 10 µl of 2 x DreamTaq PCR Master Mix using standard PCR protocol, applying a primer-specific annealing temperature.

3.2.5.2 Gel extraction

DNA extraction from 1% agarose gel was done using NucleoSpin Gel and PCR Clean-up kit.

3.2.5.3 DNA ligation

Extracted from 1% agarose gel vector and insert DNA were mixed in a 1:3 ratio and ligated using T4 DNA ligase following protocol provided by the supplier adjusted to final reaction volume of 18 µl.

3.2.5.4 Plasmid extraction

Plasmid extraction was done using NucleoSpin Plasmid kit according to the manufacturer's instruction. In case of Large-scale preparation was performed using Plasmid Plus kit.

3.2.5.5 Preparation of electro-competent bacteria

A single bacterial colony was inoculated in 3-10 ml LB medium and grown o.n. at 37° C on a wheel rotor. Further, o.n. culture was used to inoculate (1:20) 10-100 ml LB medium, incubated at 37° C and 180 rpm. At an OD$_{600}$ of 0.5-0.8, the culture was chilled on ice for 30 min and subsequently spun down at 4° C, 15 min and 4,500 rpm. The supernatant was removed and pelleted cells were washed three times in 1x culture volume (Vc) of sterile ice-cold dH$_2$O, one time in ½ Vc dH$_2$O and one time in 1/10 Vc sterile ice cold 10% glycerol, respectively. After each step bacteria were spun down at 4° C, 15 min and 4,500 rpm. Finally, bacteria were resuspended in 1/50 Vc ice-cold 10% glycerol, distributed into 80 µl aliquots, which were shock-frozen in liquid nitrogen and stored at -80° C.

3.2.5.6 Electro-transformation of DNA

A frozen stock of electro-competent cells was thawn on ice and 1-10 µl of the plasmid or linear DNA was added. Bacteria were incubated for 10 min on ice, subsequently transferred into an ice-cold 1 mm electroporation cuvette and pulsed at 1800 V/cm, 5 ms using Gene Pulser Xcell (Bio-Rad). Following this, 900 µl LB medium was added and bacteria were incubated for 1 h in a thermomixer at 37° C, 850 rpm. Afterwards, bacteria were spun down at RT for 2 min, 10,000 rpm and 900 µl from the supernatant were removed. The bacterial pellet was resuspended in the remaining liquid and plated on LB agar plates supplemented with the appropriate antibiotic(s).

3.2.5.7 P22-transduction

Preparation of P22–lysates: A single colony of the donor strain was inoculated in 3 ml LB medium supplemented with 5 mM $CaCl_2$ and grown o.n. at 37° C on a wheel rotor. Further, 500 µl of the o.n. culture were added to 10 µl P22-lysate (kindly provided by Prof. Dr. M. Hensel) and incubated for 15 min at 37° C. Next, the mixture was used to inoculate 5 ml LB culture, which was incubated o.n. at 37° C on a wheel rotor. On the next day 50 µl chloroform were added to the o.n. culture followed by an incubation for 30 min at 37° C. Next, the culture was spun down at 4° C, for 10 min at 4,500 rpm and the supernatant was filtered through (0.45 µm) and 20 µl chloroform were added to the 1.5 ml filtrate. Filtered lysate was stored at 4° C for further use. Sterility of the lysate was verified by plating 50 µl on LB agar followed by an o.n. incubation at 37° C.

P22-transduction: A single colony of the recipient strain was inoculated in 3 ml LB medium supplemented with 5 mM $CaCl_2$ and grown o.n. at 37° C on a wheel rotor. Next, 100 µl of the o.n. culture were added to 10 µl P22-lysate of the donor strain and incubated for 15 min at 37° C. Subsequently, the bacteria-phage mixture was added to 900 µl LB medium supplemented with 10mM EGTA and incubated in a thermomixer at 37° C and 850 rpm. After 1 h incubation, the bacterial culture was spun down at RT for 2 min at 10,000 rpm and 900 µl of the supernatant were removed. Pelleted bacteria were resuspended in the remaining liquid and plated on 10 mM EGTA LB agar plates supplemented with the appropriate antibiotic(s).

3.2.5.8 Conjugation

A single colony of the donor and the recipient strain were inoculated in 3 ml LB medium cultures, respectively, supplemented with the appropriate antibiotics and grown at 37° C o.n. on a wheel rotor. Next, 1 ml of each o.n. culture was spun down at RT for 1 min, 8,000 rpm, supernatant was removed and bacteria were washed with 1 ml LB medium and subsequently spun down for 1 min at 8,000 rpm. The

washing step was repeated three more times. Following this, bacterial pellets of donor and recipient were pooled together and resuspended in 100 µl LB medium. The mixture was spread on an LB agar plate and bacteria were grown o.n. at 37° C. On the next day bacteria were washed from the plate with 2 ml LB medium. Bacteria were plated on MacConkey agar (supplemented with selective antibiotics for the conjugated recipient strain) at different dilutions and grown at 37° C to obtain single colonies.

3.2.5.9 Generation of deletion mutants by lambda Red recombination

Lambda Red recombination described by Datsenko and Wagner (Datsenko & Wanner, 2000) was applied for introduction of an antibiotic-resistance cassettes into *S*. Typhimurium and *E. coli* genomes, in frame gene deletions and generation of luciferase-reporter strain. Oligonucleotides, used for amplification of the cassettes from template plasmids pKD3, pKD4 and pWRG, were designed to be homologous to circa 50 bp upstream from the start codon of the targeted gene(s) and 50 bp downstream from the stop codon of the gene(s), respectively. To verify correct insertion of the antibiotic resistance cassette, control oligonucleotides were designed to bind 20 bp upstream and downstream of the PCR fragment. For PCR, the following reaction components (**Table. 27**) and program (**Table. 28**) were applied.

Table 27. Lambda Red PCR reaction components

Reagent	Per 50 µl reaction mixture
ddH$_2$O	29.75 µl
High-fidelity buffer	5 µl
7.5 mM MgCl$_2$ (5x)	
2.5 mM dNTPs	4 µl
10 µM Forward primer	5 µl
10 µM Reverse primer	5 µl
Template plasmid	1 µl
(pKD3/4) (50ng/µl)	
High-fidelity PCR	0.25 µl
polymerase (5 U/µl)	

Table 28. Lambda Red PCR program

Step	Temperature [°C]	Time
1	95	5 min
2	95	45 sec
3	58	45 sec
4	72	2-3 min
5	95	45 sec
6	68	45 sec
7	72	2-3 min
8	72	10 min
9	8	hold

Steps 2 to 4 were repeated for 3 cycles; steps 5 to 7 for 27 cycles.

In order to purify and concentrate the amplified DNA, 1/10 volumes 3 M NaAc (ddH$_2$O solution) and 2 volumes ethanol p.a. were added to 250 µl PCR product. The mixture was mixed gently and DNA was precipitaed at 4° C, 30 min at 14,000 rpm. The supernatant was removed and the pellet was washed with 500 µl 70% ethanol and spun down at 4° C, 15 min at 14,000 rpm. The supernatant was immediately removed and the precipitated DNA was dried for 30 min at RT. DNA was subsequently resuspended in

20-30 µl ddH$_2$O. Nucleic acid concentration of purified DNA was spectrophotometrically assessed using NanoDrop Spectrophotometer ND-1000 (PEQLAB Biotechnology).

The bacterial strain to be mutagenised was transformed with pKD46 (Datsenko & Wanner, 2000) (**Section 3.2.5.6**). Transformed bacteria were grown at 30° C. In order to prepare electro-competent bacteria of the pKD46 carrying strain, 3 ml LB medium supplemented with 100 µg/ml ampicillin were inoculated and grown o.n. at 30° C at 180 rpm. On the next day, the o.n. culture was diluted (1:20) in LB medium supplemented with 10 mM L-(+)-arabinose and 100 µg/ml ampicillin and grown for 3 h at 30° C, 180 rpm until OD$_{600}$ of 0.5-0.6 was reached. Further, to harvest the cells, 4 ml of the arabinose-induced culture was spun down at 4° C, for 2 min and 10,000 rpm. The supernatant was removed and pelleted bacteria were washed with 1 ml ice cold sterile dH$_2$O. Washing was repeated for three times. Finally, bacteria were resuspended in 80 µl dH$_2$O and were electroporated with 6-10 µl of the purified 1 µg/ml PCR product (**Section 3.2.5.5**).

3.2.5.10 Elimination of antibiotic resistance genes using the Flp-recombinase

The mutant strain, containing FRT-flanked antibiotic-resistance cassette, were transformed with 1 µg pCP20 (**Section 3.2.5.5**). After electroporation bacteria were immediately recovered in 1 ml pre-warmed to LB medium (30° C). Following 1 h incubation in a thermomixer at 30° C, 850 rpm, bacterial culture was spun down at RT for 2 min, 10,000 rpm and 900 µl of the supernatant were removed. The bacterial pellet were resuspended in the liquid left and plated on LB agar plate supplemented with 100 µg/ml ampicillin, followed by o.n. incubation at 30° C to maintain pCP20. On the next day, 20 colonies were picked, streaked on LB agar plates and incubated o.n. at 42° C to induce the Flp-mediated recombination. Next, antibiotic sensitive colonies were identified by double plaiting. In order to cure the strain from the temperature-sensitive pCP20 selected clones were re-streaked twice on LB plates and incubated each time at 37° C.

3.2.6 Construction of plasmids and bacterial strains

Bacterial plasmids and strains generated in this study are listed in **Table 2** and **Table 3**, respectivly.

3.2.6.1 Identification of regulator binding sites

For annotation of transcription factor binding sites (Fur and LexA regulon), all known transcription factor binding sites of each family one were taken from RegulonDB (version 8.0) (Salgado *et al.*, 2013) and a binding motif was created using MEME (Bailey & Gribskov, 1998). The nucleotide sequences of the *cib*

(*S.* Tm SL1344; EMBL accession no. FQ312003) and *cirA* promoter regions (*E. coli* MG1655 genome accession no. NC_000913.2) were searched for the computed MEME binding site motifs using MAST (Bailey & Gribskov, 1998).

3.2.6.2 Annotation of prophage genomes in *S.* Tm[MA6118] (*S.* Tm SL1344)

Sequences of Gifsy-1(accession no. NC_010392.1) and Gifsy-2 (accession no. NC_010393), (McClelland *et al.*, 2001)*,* SopEΦ (accession no. AY319521.1) (Pelludat *et al.*, 2003) and ST64B (accession no. AY055382.1) (Mmolawa *et al.*, 2003) prophages were aligned to *S.* Tm SL1344 genome (accession no. FQ312003), using Mauve Genome Alignment software (Darling *et al.*, 2004). Open reading frames (ORFs) for each prophage were localized within *S.* Tm SL1344 genome and annotated with the corresponding systematic ID for *S.* Tm SL1344 (Kroger *et al.*, 2012) (Figure 1.9 and Table 29). These annotations were used for construction of deletions within the SopEΦ (**Figure 3.1A,B**; **Table 30**) and ST64B (**Figure 3.1C,D**; **Table 31**) prophages (**Section 3.2.7.2**).

Table 29. Systematic IDs of prophages

Prophage	Systematic ID of ORFs in *S.* Tm SL1344
Gifsy-1	SL1344_2546-SL1344_2600
Gifsy-2	SL1344_0942-SL1344_0996
SopEΦ	SL1344_2665-SL1344_2710
ST64B	SL1344_1927-SL1344_1976
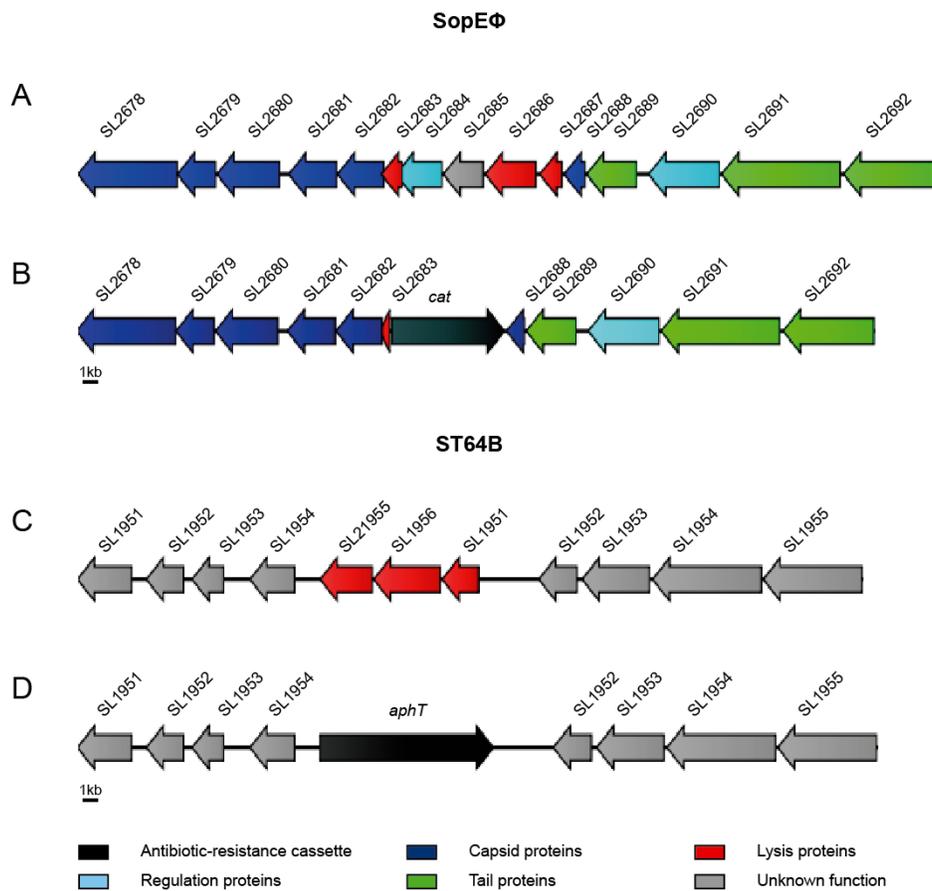
Figure 3.1. Construction of deletions within the SopEΦ and ST64B prophages. Arrows indicate direction of transcription of open reading frames (ORF). SopEΦ genes encoding lysis proteins (red) (*SL1344_2684-SL1344_2687*) (**A**) were substituted with chloramphenicol-resistance (*cat*) cassette (black and dark green), 134 bp of the (3') end of *SL1344_2683* gene remain intact in the new construct. (**B**). ST64B genes encoding lysis proteins (red) (*SL1344_1955-SL1344_1957*) (**C**) were substituted with kanamycin-resistance (*aphT*) cassette (black) (**D**). The color code defines genes encoding capsid proteins (dark blue), tail proteins (green) and regulation proteins (light blue). Genes encoding proteins with unknown function are marked in grey.

Table 30. Genes of SopEΦ reported to encode lysis proteins

S. Tm SL1344 ORF (FQ312003) (Kroger *et al.*, 2012).	GenBank product	EMBL product	Corresponding ORF (AY319521.1) (Pelludat *et al.*, 2003)	GenBank product
SL1344_2683	Hypothetical protein	Hypothetical conserved bacteriophage protein (thought to be involved in host lysis)	*orf*26	Similar to gpR (tail completion)
			*orf*25	Similar to lysis protein LysB
SL1344_2684	Lysis-like protein	Hypothetical regulatory protein	*orf*25	Similar to lysis protein LysB
SL1344_2685	Not annotated	Predicted bacteriophage protein	Not annotated	Not annotated
SL1344_2686	Not annotated	Hypothetical lysozyme	*orf*24	Similar to gp17 lysozyme
SL1344_2687	Phage-holin-like protein	Possible secretion protein	*orf*23	Possible secretion protein
SL1344_2688	Phage tail-like protein	Hypothetical bacteriophage tail protein	*orf*22	Similar to gpX

Deletion of SopEΦ lysis genes were generated by deletion of *orf*23-*orf*25 reported to be involved in cell lysis (Pelludat *et al.*, 2003). The same study assigned *orf*22 as a lysis-related gene. However, this was not confirmed by annotation of the GeneBank database and *orf*22 was left intact. Alignment of annotated SopEΦ lysis between two different studies (Pelludat *et al.*, 2003), (Kroger *et al.*, 2012) identified a disagreement: in the latter study (Kroger *et al.*, 2012) a new ORF (*SL1344_2683)* was annotated as a lysis-related gene (**Figure 3.1A**). *SL1344_2683* (204 bp) was not considered during the deletion of the SopEΦ lysis genes, which was done based on the earlier annotations (Pelludat *et al.*, 2003). Nevertheless, *orf*25 is overlapping 70 bp of the (5') end of *SL1344_2683*. Therefore, this sequence is missing in the strains with deleted SopEΦ lysis genes, with the consequence that presumably no functional product of *SL1344_2683* is expressed. However, there is no available structural information on *SL1344_2683* encoded protein, to confirm that.

Table 31. Genes of ST64B reported to encode lysis proteins

S. Tm SL1344 ORF (FQ312003) (Kroger *et al.*, 2012).	GenBank product	EMBL product	Corresponding ORF (AY319521.1) (Pelludat *et al.*, 2003)	GenBank product
SL1344_1955	Hypothetical protein	Hypothetical bacteriophage endopeptidase	*sb*53	Lysis protein
SL1344_1956	Not annotated	Hypothetical bacteriophage encoded lysozyme	*sb*52	Lytic enzyme (putative glycohydrolase)
SL1344_1957	Hypothetical protein	Hypothetical bacteriophage holin	*sb*51	Lysis protein (holin)

In order to create a ST64B lysis-genes deficient mutant, *sb53-sb53* reported to be involved in cell lysis were deleted (**Figure 3.1C**) (Mmolawa *et al.*, 2003). Of note, *sb51* does not align completely to *SL1344_1957*. In contrast *sb53, sb52* align to the *SL1344_1955, SL1344_1956* with 100% similarity.

3.2.6.3 Construction of plasmids

Generation of pLPN13 and pLPN14: Correct insertion was verified by PCR using oligonucleotides *ΔoriTnikA*rev_val/*ΔoriTnikA*_val (**Table 1**). For the generation of c-terminal CirA-His-tag fusion, the open reading frame of *cirA* was amplified from *E. coli* Nissle genomic DNA by PCR, using Fow_*cirA_Nhe*I and Re_*cirA_Xho*I oligonucleotides (**Table 1**) and cloned into pET-24c (Novagen) via *Nhe*I *and Xho*I to yield pLPN13. For the generation of c-terminal ColIb-His-tag fusion, the ColIb gene *cib* was amplified from *S.* Tm^{wt} genomic DNA by PCR, using oligonucleotides Fow_*colicin_Nhe*I and Re_*colicin_Xho*I (**Table 1**) and cloned into pET-24c via *Nhe*I and *Xho*I to yield pLPN14.

Generation of pLPN1: To generate pLPN1, the *cirA* promoter was amplified from *E. coli* Nissle using oligonucleotides *pcirA-Bam*HI/*pcirA-Xba*I (**Table 1**) and inserted in *Bam*HI and *Xba*I digested pM979 (Stecher *et al.*, 2004).

Generation of pM1437: For generation of pM1437, the *cib* promoter from *E. coli*[8178] was amplified using oligonucleotides pColIb-*Xba*I, pColIb-*Bam*HI (**Table 1**) and inserted in pM968 (Stecher *et al.*, 2004) via restriction with *Xba*I and *Bam*HI. The *cib* promoter sequence of *E. coli*[8178] is identical to the one of *S.* Tm^{wt} (SB300).

Generation of pLPN15 and pLPN16: To generate pLPN15 and pLPN16, the firefly-luciferase gene *luc* from pLB02 (Gunn *et al.*, 1995) was amplified with oligonucleotides Luc-for-*Bam*HI and Luc-rev-*Hind*III (**Table 1**) and inserted into the *Bam*HI/*Hind*III digested plasmids pLPN1 or pM1437, respectively.

Construction of *cirA* and *colIb* complementation plasmids: Oligonucleotides pWSK29-Gbs-for and pWSK29-Gbs-rev (**Table 1**) were used in a PCR with pWSK29 (Wang & Kushner, 1991) as a template to amplify the low-copy-number plasmid (**Table 1**). Oligonucleotides CirA-pWSK29-Gbs-for and CirA-pWSK29-Gbs-rev were used in a PCR with chromosomal DNA of Ec^MG1655 as a template to amplify *cirA* including its natural promoter. Oligonucleotides Cib-Imm-pWSK29-Gbs-for and Cib-Imm-pWSK29-Gbs-rev were used in a PCR with *S.* Tm^wt (SB300) plasmid pCol1B9_SL1344 as a template to amplify the *cib/imm* locus including both natural promoters. The pWSK29 PCR fragment was combined with the *cirA* or *cib/imm* fragment in a Gibson assembly reaction (Gibson *et al.*, 2009). Four microliters of the Gibson assembly mix were transformed into chemically competent *E. coli* Mach1 T1 cells (Life Technologies). Constructs were verified using colony PCR, restriction analysis and sequencing. The complementatiom plasmids were generated by Thorsten Wille (Robert Koch-Institut, Wernigerode Branch, Junior Research Group 3, Wernigerode, Germany).

3.2.6.4 Construction of mutant strains

Construction of Ec^MG1655 ^ΔcirA (LPN2): Ec^MG1655 ^ΔcirA (LPN2) was constructed using the lambda Red recombinase system as described (**Section 3.2.5.9**) using pKD4 as template for the kanamycin-resistance gene including the FRT-sites (Datsenko & Wanner, 2000). Briefly, Ec^MG1655 was transformed with the plasmid pKD46. The kanamycin resistance cassette from plasmid pKD4 was amplified by PCR using oligonucleotides K12*ΔcirA*_Fwd*/*K12*ΔcirA*_Re and transferred in Ec^MG1655 pKD46. Correct recombination was verified by PCR using oligonucleotides *cirA*-up*/cirA*-down and *cirA*-up*/cirA*-d1 (**Table. 1**).

Construction of *S.* Tm^avir Δ*oriT* (LPN5): *S.* Tm^avir Δ*oriT* (LPN5) was generated by P22-transduction of the Δ*oriTnikA::cat* allele from M1407 into M557 (Hapfelmeier *et al.*, 2005). Correct insertion was verified by PCR using oligonucleotides *ΔoriTnikA*rev_val*/ΔoriTnikA*_val d1 (**Table 1**).

Confirmation of prophage deletions in *S.* Tm^MA6118 and derivatives: For all strains included in the ColIb release study (**Section 4.2**) presence and absence of respective prophages (Gifsy-1, Gifsy-2, SopEΦ and ST64B) was verified by PCR using oligonucleotides Gifsy-1-for/Gifsy-1-rev, Gifsy-2-for/Gifsy-2-rev, SopE-phi-for/SopE-phi-rev and ST64B-for/ST64B-re (**Table 1**), respectively.

Construction of *S.* Tm^ΔlysST_NT (LPN9): In order to delete ST64B lysis genes (*SL1344_1955-SL1344_1957*) lambda Red recombinase system was used (Datsenko & Wanner, 2000). The kanamycin-resistance cassette was amplified by PCR from pKD4 using oligonucleotides SB51-53_for/SB51-53_rev

and subsequently transformed in *S*. Tm^{MA6118} carrying pKD46. Correct recombination in *S*. Tm$^{\Delta lysST}_{NT}$ (LPN9) was verified by PCR using oligonucleotides check_ST64_for/check_pKD4_Kan_For, check_pKD4_Kan_Re/check_ST64_rev and check_ST64_for/ check_ST64_1 (**Table 1**).

Construction of *S*. Tm$^{\Delta lysS\phi C}_{NT}$ (LPN11): In order to replace SopEΦ lysis genes (*SL1344_2684-SL1344_2687*) lambda Red recombinase system was used (Datsenko & Wanner, 2000). Oligonucleotides Lys_Sop_phi_For/Lys_Sop_phi_Rev were used to amplify chloramphenicol-resistance cassette from plasmid pKD3. Further, purified PCR product was transformed in *S*. Tm^{MA6118} carrying pKD46. Correct recombination in *S*. Tm$^{\Delta lysS\phi C}_{NT}$ (LPN11) was verified by PCR using oligonucleotides Lys_SopE_Check_Fwd / Lys_SopE_Check_Rev (**Table 1**).

Construction of *S*. Tm$^{\Delta lysST}$ (LPN14) and *S*. Tm$^{\Delta G1\Delta G2\Delta lysST}$ (LPN24): P22-transduction of the *(SL1344_1955-SL1344_1957)::aphT* allele from Tm$^{\Delta lysST}_{NT}$ into *S*. Tm^{MA6118} and *S*. Tm$^{\Delta G1\Delta G2}$ was used for generation of *S*. Tm$^{\Delta lysST}$ (LPN14) and *S*. Tm$^{\Delta G1\Delta G2\Delta lysST}$ (LPN24), respectively. Correct insertion of the allele was verified by PCR using oligonucleotides check_ST64_for/check_pKD4_Kan_For, check_pKD4_Kan_Re/check_ST64_rev and check_ST64_for/ check_ST64_1 (**Table 1**).

Construction of *S*. Tm$^{\Delta lysS\phi C}$ (LPN15) and *S*. Tm$^{\Delta G1\Delta G2\Delta lysS\phi C}$ (LPN17): P22-transduction of the *(SL1344_2684- SL1344_2687)::cat* allele of *S*. Tm$^{\Delta lysS\phi C}_{NT}$ into *S*. Tm^{MA6118} and *S*. Tm$^{\Delta G1\Delta G2}$ (MA6247) was done in order to generate *S*. Tm$^{\Delta lysS\phi C}$ (LPN15) and *S*. Tm$^{\Delta G1\Delta G2\Delta lysS\phi C}$ (LPN17), respectively. Correct instertion of the allele was verified by PCR using oligonucleotides Lys_SopE_Check_Fwd/Lys_SopE_Check_Rev (**Table 1**).

Construction of *S*. Tm$^{\Delta lysS\phi}$ (LPN19) and *S*. Tm$^{\Delta G1\Delta G2\Delta lysS\phi}$ (LPN20): pCP20 was transformed in LPN15 and LPN17 in order to eliminate the chloramphenicol-resistance gene (**Section 3.2.6.10**). Deletion of the antibiotic-resistance gene in *S*. Tm$^{\Delta lysS\phi}$ (LPN19) and *S*. Tm$^{\Delta G1\Delta G2\Delta lysS\phi}$ (LPN20), respectively, was confirmed by PCR using oligonucleotides Lys_SopE_Check_Fwd/Lys_SopE_Check_Rev (**Table 1**).

Construction of *S*. Tm$^{\Delta G1\Delta G2\Delta lysS\phi K}_{NT}$ (LPN25): In order to engineer *S*. Tm$^{\Delta G1\Delta G2\Delta lysS\phi K}_{NT}$ (LPN25), oligonucleotides Lys_Sop_phi_For/Lys_Sop_phi_Rev were used to amplify pKD4 kanamycin-resistance cassette. The purified PCR product was transformed in *S*. Tm$^{\Delta G1\Delta G2}$ carrying pKD46. Correct recombination was verified by PCR using oligonucleotides Lys_SopE_Check_Fwd/check_pKD4_Kan_For and Lys_SopE_Check_Rev/check_pKD4_Kan_rev (**Table 1**).

Construction of *S.* Tm$^{\Delta G1\Delta G2\Delta lysS\phi K}$ (LPN26): To generate *S.* Tm$^{\Delta G1\Delta G2\Delta lysS\phi K}$ (LPN26), the P22-transduction of the (*SL1344_2684- SL1344_2687)::aphT* allele of *S.* Tm$^{\Delta G1\Delta G2\Delta lysS\phi K}_{NT}$ into *S.* Tm$^{\Delta G1\Delta G2}$ was done. Correct insertion was confirmed by PCR using oligonucleotides Lys_SopE_Check_Fwd/ Lys_SopE_Check_Rev (**Table 1**).

Construction of *S.* Tm^{A36} p2^{cm} (LPN12) and *S.* Tm^{A36} p2^{cm} (LPN13): Plasmid pCol1B9_SL1344 carrying chloramphenicol resistance (Stecher *et al.*, 2012) was conjugated from M995 into *S.* Tm^{A36} and *S.* Tm^{M4} (Mirold *et al.*, 1999) to construct *S.* Tm^{A36} p2^{cm} (LPN12) and *S.* Tm^{A36} p2^{cm} (LPN13), respectively (Section Conjugation). Single colonies were selected on chloramphenicol-supplemented LB agar plates. Functional transfer of p2^{cm} was confirmed by testing ColIb expression by a colicin-killing assay.

Construction of MBK6 and MBK7: C600W34 (kindly provided by Prof. Dr. Dr. Jürgen Heesemann) is a C600 *E. coli* K12 strain lysogenized with Shiga toxin 2 phage 933W (originally isolated from EHEC strain O157:H7 EDL933) (O'Brien *et al.*, 1984). Lambda Red recombination was used to replace s*tx2A* gene (Shiga toxin 2 subunit A) of the 933W phage with the firefly luciferase gene (*luc*) and a kanamycin-resistance cassette (*aphT*) flanked by FRT-sites to create MBK6. The same method was applied to replace the s*tx2A* gene and the two lysis genes (*S* and *R*) located downstream in order to construct MBK7. Shortly, C600W34 was transformed with the temperature sensitive plasmid pKD46 containing the lambda Red recombinase system (Datsenko & Wanner, 2000). The luciferase reporter gene and the kanamycin-resistance cassette were amplified from plasmid p3121 (Gerlach *et al.*, 2007) by PCR using oligonucleotides "*Stx2-luc* fusion Fw/*Stx2*_Com fusion Rev" for replacement of *stx2A* gene and *"Stx2-luc* fusion Fw*/Stx2 R/S* Com fusion Rev" for s*tx2A*, *S* and *R* gene replacement. Correct recombination was verified by PCR using "*Stx2* operon Fw*/Stx2* Operon Rev" oligonucleotides for MBK6 and "*Stx2* Operon Fw*/R/S* outside Rev" for MBK7 (**Table 1**).

Construction of MBK13 and MBK14: MBK13 was created via lysogenization of Ec^{MG1655} with the luciferase-reporter phage from MBK6. Likewise, MBK14 was created via lysogenization of Ec^{MG1655} with the reporter phage from MBK7. To generate the phage lysate, MBK6 (MBK7) was grown in 3 ml LB medium o.n. at 37° C, on a wheel rotor. This starter culture was used for inoculation (1:20) of 5 ml LB medium and grown until log-phase culture (OD$_{600}$ of 0.5). The prophage was induced by addition of 0.5 µg/ml mitomycin C to the culture and subsequent incubation o.n. at 37° C, on a wheel rotor. On the next day, 100 µl chloroform was added to the culture and incubated for 10 min at RT, while vortexing. Further, the lysate was spun down (4° C, 10 min at 6,000 rpm), the supernatant was filtered (0.45 µm filter) and 100 µl chloroform was added to the filtrate for short term storage at 4° C. For the phage transduction 100 µl of a 1:1,000 dilution of an o.n. culture of Ec^{MG1655} (grown in 3 ml LB medium) was mixed with 500 µl

49

phage lysates (low titer), 100 µl 0.1 M CaCl$_2$ and LB medium was added to final volume of 2 ml. This culture was then grown at 37° C o.n. on a wheel rotor. Finally, the o.n. culture was diluted and plated onto LB-agar plates supplemented with kanamycin. Single grown colonies were isolated and checked for lysogeny by PCR using the oligonucleotides "*Stx2* Operon Fw*/Stx2* Operon Rev" for MBK13 and "*Stx2* Operon Fw*/R/S* outside Rev" for MBK14 (**Table 1**).

Construction of Ec^{Stx} p2^{cm} (LPN21), Ec$^{Stx\Delta SR}$ p2^{cm} (LPN22), Ec p2^{cm} (LPN23): p2^{cm} from donor strain M995 (Stecher *et al.*, 2012) was conjugated into MBK13, MBK14 and Ec^{MG1655}, to construct Ec^{Stx} p2^{cm} (LPN21), Ec$^{Stx\Delta SR}$ p2^{cm} (LPN22) and Ec p2^{cm} (LPN23), respectively. Acquisition of p2^{cm} was confirmed by testing ColIb expression via a colicin-killing assay.

Construction of *S*. Tm$^{\Delta Ph\ smR}$ (LPN27) and *S*. Tm$^{\Delta G1\Delta G2\Delta lysST\ smR}$ (LPN28): Presence of the streptomycin-resistance plasmid (pRSF1010-SL1344) and virulence plasmid (pSLT-SL1344) of *S*. Tm SL1344 were detected by PCR (using *strB*_for*/strB*_rev and *spvB*_for*/spvB*_rev oligonucleotides, respectively) for *S*. Tm^{MA6118}. pRSF1010-SL1344 was found to be absent in *S*. Tm$^{\Delta G1\Delta G2}$, *S*. Tm$^{\Delta G1\Delta G2\Delta ST}$ and *S*. Tm$^{\Delta Ph}$. Both plasmids were extracted from *S*. Tm^{MA6118} using Plasmid Plus kit, in order to construct streptomycin-resistant LPN27 (*S*.Tm$^{\Delta Ph\ smR}$) and LPN28 (*S*. Tm$^{\Delta G1\Delta G2\Delta lysST\ smR}$), the plasmids were trandsformed in *S*. Tm$^{\Delta Ph}$ and *S*. Tm$^{\Delta G1\Delta G2\Delta lysST}$, respectively. Successful transfer of pRSF1010-SL1344 transformation was confirmed by PCR using *strB*_for*/strB*_rev oligonucleotides (**Table 1**).

3.2.7 Biochemical methods

3.2.7.1 Generation and affinity purification of recombinant His-tagged proteins

For generation of ColIb-His, *E. coli* BL21 (DE3) transformed with pC831-2 (expression of the ColIb immunity protein gene *imm* (Stecher *et al.*, 2012)) and pLPN14 (Table.26) was used. For generation of CirA-His, *E. coli* BL21 (DE3) was used, transformed with pLPN13 (Table. 26). Bacterial cultures grown o.n. at 180 rpm, 37° C in LB medium containing antibiotics were used for inoculation of 1-2 L LB (dilution 1:20). At an OD_{600} between 0.6-0.8, this subculture was induced with 0.1 mM isopropyl β–D-thiogalactopyranoside (IPTG) and incubated at 180 rpm for 4 h, 37° C. Bacteria were harvested (at 4,500 rpm for 30 min, 4° C), resuspended in 40 ml 1x PBS and spun down at 4,500 rpm for 20 min, 4° C. The pellet was frozen at -20° C. Thereafter, the pellet was thawn and resuspended in 25 ml recombinant protein purification lysis buffer supplemented with 2 mM phenylmethylsulfonyl fluoride (PMSF) and benzonase nuclease (**Table 14**). Bacteria were lysed in the French Press (1,000 PSI). The lysate was spun down at the supernatant was filtered (0.22 µm). Further, the lysate was loaded on a 5 ml HisTrap column, and purified using the ÄKTA system (GE Healthcare, Munich) applying recombinant protein loading buffer (**Table 15**). ColIb-His was eluted with recombinant protein elution buffer (**Table 16**). The fractions containing the protein were desalted on a 5 ml HiTrap desalting column, using the ÄKTA system and recombinant protein purification exchange buffer 1 or 2 (**Table 17** and **Table 18**). The protein purification exchange buffer 2 was applied, as the recombinant protein was found to be unstable when stored for several months in recombinant protein purification exchange buffer 1 (**Table 17**). CirA-His was purified as outlined above for ColIb-His, but with following exceptions: the recombinant protein purification lysis(**Table 14**), loading(**Table 15**), elution (**Table 16**) and exchange buffer(**Table 17**), each contained 6 M urea and the protein purification exchange buffer 1 contained 4 M urea. Rabbit antisera against ColIb-His and CirA-His were raised using standard protocols (Pineda Antikörper-Service, Berlin, Germany). In order to do this, 6 mg/ml ColIb-His (in 20 mM Na_2HPO_4, 100 mM NaCl, pH 7.4) and 6 mg/ml CirA-His (in 20 mM Na_2HPO_4, 100 mM NaCl, 4 M Urea, pH 7.4) were used for rabbit immunization. Control and immune sera were received from bleedings at day 61, 90 and 135 post-immunisation.

3.2.7.2 Affinity purification of rabbit-antisera

Affinity purification of polyclonal rabbit α-ColIb-His antiserum was done using the Aminolink kit (Thermo Fisher Scientific) following the manufacturer's protocol with some minor modifications: PBS

was used as binding/wash buffer and 1 M glycine, pH 2.7 was used as elution buffer. ColIb-His (stored in 20 mM Na_2HPO_4, 100 mM NaCl, pH 7.4) was added to the binding buffer at 1:3 ratio. Next, desalting of the affinity-purified rabbit-α-ColIb-His antiserum was done using PD-10 desalting columns (GE Healthcare) with PBS used as exchange buffer. The Aminolink kit was likewise used for the affinity purification of polyclonal rabbit α-CirA-His antiserum. His-tagged CirA (20 mM Na_2HPO_4, 100 mM NaCl, 4M urea, pH 7.4) was dialyzed against PBS using 5 ml Zebra Spin (Thermo Fisher Scientific) desalting columns shortly before coupling. Coupling of the His-tagged to the chromatographic column was done with the Aminolink kit coupling buffer supplemented with 4 M urea. Next, desalting of the affinity-purified rabbit-α-CirA-His was done with the Zebra Spin desalting columns using PBS containing. Purified antisera were supplemented with sodium azide to 0.01% and stored at -80° C.

3.2.7.3 SDS-polyacrylamide gel electrophoresis (PAGE) and immunoblot

Proteins were separated by SDS gel electrophoresis (Laemmli, 1970). Acrylamide was used for the 10% resolving (**Table 19**) and the 5% stacking gel (**Table 20**). Proteins were transferred onto a nitrocellulose membrane at 300 mA for 2 h, using the transfer buffer (**Table 23**). The membrane was blocked in PBS (0.1% tween; 5% milk powder) and probed with either affinity-purified rabbit α-CirA-His, affinity-purified rabbit α-ColIb-His, or mouse monoclonal α-*E. coli* DnaK (**Table 5**). Goat-α-rabbit-HRP and goat-α-mouse-HRP were used as secondary antibodies (**Table 6**). Blots were developed with ECL detection system (GE Healthcare) or Immobilion Western Chemoluminescent HRP substrate (Merck Chemicals). The relative quantity of ColIb and DnaK was determined by densitometry using Image Lab software (Bio-Rad).

3.2.8 Animal experiments

3.2.8.1 Ethics statement

All animal experiments were approved by the Regierung von Oberbayern and the Kantonales Veterinäramt Zürich and performed according to local guidelines (Deutsches TschG; Schweizer Kantonale Tsch).

3.2.8.2 Infection experiments, determination of bacterial loads and histopathological analysis

All mice used in the study were on C57BL/6J background and bred at the Rodent Center, ETH Zürich and the Max-von-Pettenkofer Institute, LMU Munich under SPF conditions in individually ventilated cages. Low-complexity microbiota (LCM) mice were generated by associating germfree mice with members of the altered Schaedler Flora (Dewhirst *et al.*, 1999) as described previously (Stecher *et al.*, 2010). Conventional SPF C57BL/6J mice were purchased from Janvier, Le Genest-Saint-Isle. For infections, conventional and LCM mice were pretreated with streptomycin and infected by gavage with 5×10^7 cfu *S.* Tm or mixtures of *S.* Tm and *E. coli* as described (Stecher *et al.*, 2012). For *in vivo* luciferase-assays, LCM mice were pretreated with ampicillin (20 mg/animal 24 h prior to infection). Live bacterial loads in the cecal content were determined by plating on MacConkey-agar (Roth or Oxoid) with respective supplements (streptomycin 100 μg/ml; kanamycin 30 μg/ml; chloramphenicol 30 μg/ml; ampicillin 100 μg/ml and tetracycline 12.5 μg/ml). Histology of the cecum was done at necropsy. Cecum tissue was embedded in O.C.T. and flash frozen. Cryosections (5 μm) of the cecal tissue were H&E-stained and scored as described in detail in (Stecher *et al.*, 2007b). The parameters submucosal edema, polymorphonuclear neutrophils (PMNs) infiltration, loss of goblet cells and epithelial damage were scored according to the severity of inflammatory symptoms yielding a total score of 0–13 points. For infections, *E. coli* and *S.* Tm strains were grown as previously described (Hapfelmeier *et al.*, 2004). Briefly, cultures in LB supplemented with 0.3 M NaCl were inoculated with 2-3 bacterial colonies from plates. Bacteria were grown o.n. for 12 h and subcultures (1:20) for an additional 4 h. Bacteria were mixed (as indicated) washed in PBS and applied to the mice in a total volume of 50 μl by oral gavage.

3.2.9 Statistical analysis

Statistical analysis of data obtained from the *in vivo* experiments were performed using the exact Mann-Whitney U Test (Graphpad Prism Version 5.01). Statistical analysis of data obtained from the *in vitro* studies was analysed by one-way analysis of variance (ANOVA) and unpaired Student's *t*-test (Graphpad Prism Version 5.01). P-values less than 0.05 (2-tailed) were considered as statistically significant.

4 Results

4.1 ColIb-dependent competition of *Salmonella* Typhimurium and *E. coli*

4.1.1 ColIb affords *S.* Tm a growth advantage over colicin-sensitive *E. coli* strains in the inflamed, but not in the normal gut

It has been shown previously that production of ColIb grants significant competitive advantage to *S.* Tm over colicin-sensitive *E. coli* strains (Stecher *et al.*, 2012). Sensitivity to ColIb of two *E. coli* strains was tested *in vitro.* The probiotic *E. coli* Nissle (Ec^{Nissle}) strain showed intermediate susceptibility to ColIb by formation of a turbid inhibition zone (**Figure 4.1**). However, a K-12 strain *E. coli* MG1655 (in the following termed Ec^{MG1655}) displayed high sensitivity producing a clear inhibition zone in the vicinity of *S.* Tm (**Figure. 4.1**). Based on these results, Ec^{MG1655} was selected for further studies.
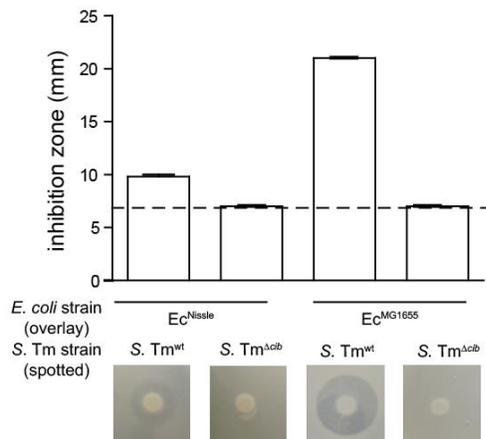
Figure 4.1. Halo-assay to determine phenotypes of ColIb susceptibility. ColIb susceptibility of Ec^{Nissle} and Ec^{MG1655} was tested. *S.* Tm^{wt} was spotted on LB agar plates containing mitomycin C and incubated o.n. to induce ColIb secretion. Ec^{Nissle} and Ec^{MG1655} were cultivated in LB medium o.n., mixed with soft agar and overlaid on the agar plates. The experiments were done in triplicates and the diameter of the ColIb inhibition zone (halo) was measured after 24 hours. The detection limit (dotted line) is the average size of the *S.* Tm^{wt} colony.

Co-infection experiments with *S.* Tm strains and Ec^{MG1655} in the streptomycin *Salmonella* mouse colitis model (Barthel *et al.*, 2003) were conducted to test whether ColIb confers a fitness benefit to *S.* Tm. Initially, gnotobiotic mice colonized with a LCM were confirmed to harbour no *Enterobacteriaceae*

species which can affect the outcome of the experiments, i.e. by producing other colicins. Streptomycin was administered to the LCM mice 24 h before infection. This was done in order to disturb the residual microbiota which can otherwise prevent development of enteric salmonellosis due to colonization resistance (Stecher *et al.*, 2007a). In regard to the high levels of intrinsic transfer of P2-plasmid from *S.* Tm to the co-colonizing *E. coli* strains in the gut (Stecher *et al.*, 2012), all *S.* Tm strains used in this study carried a mutation in the origin of transfer of P2 ($\Delta oriT$). Thereby, the P2 transconjugation was blocked. LCM mice (pre-treated with streptomycin) were co-infected with 1:1 mixtures of Ec^{MG1655} and either ColIb-producing (*S.* Tm$^{\Delta oriT}$) or ColIb-deficient strains (*S.* Tm$^{\Delta oriT\ \Delta cib}$). By day 4 post infection (p.i.) Ec^{MG1655} was remarkably outnumbered by *S.* Tm$^{\Delta oriT}$. In contrast, the ColIb-deficient pathogen (*S.* Tm$^{\Delta oriT\ \Delta cib}$) was unable to surpass its comptetitor (**Figure 4.2A,B**).

Figure 4.2. Colicin-dependent competition of *S.* Tm and *E. coli* in the gut in inflammation-induced "blooms" in gnotobiotic LCM mice. Streptomycin-treated LCM-mice were co-infected with 1:1 mixtures of *S.* Tm$^{\Delta oriT}$ and Ec^{MG1655}, *S.* Tm$^{oriT\ \Delta cib}$ and Ec^{MG1655} or *S.* Tm$^{\Delta oriT\ avir}$ and Ec^{MG1655}. **(A)** *S.* Tm (black) and *E. coli* (white) colonization density was determined at day 4 p.i. in the cecum content (cfu/g). **(B)** Competitive indices (CI; ratio of *S.* Tm / *E. coli*) as determined for individual mice shown in (A). Bars show the median. **(C)** Histopathological analysis of cecal tissue of the infected mice shown in (A). Cecal tissue sections of the mice were stained with hematoxylin/eosin and the degree of submucosal edema, neutrophil infiltration, epithelial damage and loss of goblet cells was scored.

However, both *S*. Tm strains induced similar degrees of gut inflammation (**Figure 4.2C**). These results indicated that the competitive advantage of *S*. Tm over Ec[MG1655] in the inflamed intestine is mainly ColIb-dependent. Further, to test whether ColIb is beneficial to the pathogen in the absence of inflammation, LCM mice were co-infected an avirulent *Salmonella* strain (*S*. Tm$^{\Delta oriT \text{ avir}}$). For the reason that *S*. Tm$^{\Delta oriT \text{ avir}}$ (**Table 3**) is lacking functional type three secretion systems, it is inept to trigger an inflammatory response (Hapfelmeier *et al.*, 2005). Although *S*. Tm$^{\Delta oriT \text{ avir}}$ is a ColIb-producer (**Figure 4.5**), the pathogen was incapable to overgrow Ec[MG1655] in absence of gut inflammation (**Figure 4.2**).

LCM mice serve as valuable experimental tool to investigate intrinsic bacterial and bacteria–host dynamics avoiding complexity of the species-rich natural gut microflora (Stecher *et al.*, 2013a). However, this model does not mimick the the whole diversity of the processes taking place in a conventional microbiota (Brown *et al.*, 2013). Furthermore, previous studies of colicin-dependent bacterial competition were performed using conventional mice ((Gillor *et al.*, 2009), (Kirkup & Riley, 2004)). In order to assess the ColIb-dependent competition in a more "natural" environment, streptomycin-treated mice with a conventional complex microbiota were co-infected with *S*. Tm$^{\Delta oriT}$ and *E. coli* strains. In contrast to the LCM mice, Ec[MG1655] was found to be a poor colonizer of the conventional streptomycin-treated animals (not shown). Therefore, *E. coli* Nissle (Ec[Nissle]) was used in co-infection with *S*. Tm$^{\Delta oriT}$. To investigate the importance of the ColIb as a beneficial fitness factor in the inflamed intestine, two groups of streptomycin-treated mice were set up (**Figure 4.3**). Ec[Nissle] was administrated in co-infection with either a virulent colicin producer (*S*. Tm$^{\Delta oriT}$) or a colicin–deficient *S*. Tm strain (*S*. Tm$^{\Delta oriT \ \Delta cib}$). Both groups developed strong *Salmonella*-induced gut inflammation by day 4 p.i. (**Figure 4.3E,F**). Upon inflammation, the virulent ColIb-producing *S*. Tm$^{\Delta oriT}$ grew to similar numbers as Ec[Nissle] (to ~10^8 cfu/g) while the ColIb-deficient *S*. Tm$^{\Delta oriT \ \Delta cib}$ was outcompeted by the probiotic strain (**Figure 4.3B**). This difference is displayed likewise by the competitive index (CI; ratio of *S*. Tm / *E. coli*) (**Figure 4.3D**). In respect to the aborted ColIb-dependent competitive advantage in non-inflamed intestine of the LCM mice (**Figure 4.2**), two additional groups of conventional streptomycin-treated mice were tested. Co-infection of the mice was launched with Ec[Nissle] and either an avirulent ColIb-producing *S*. Tm (*S*. Tm$^{\Delta oriT \text{ avir}}$), or an avirulent ColIb-deficient *S*. Tm (*S*. Tm$^{\text{avir P2 cured}}$). Both of these groups confronted with the avirulent strains did not develop gut inflammation (**Figure 4.3E,F**).
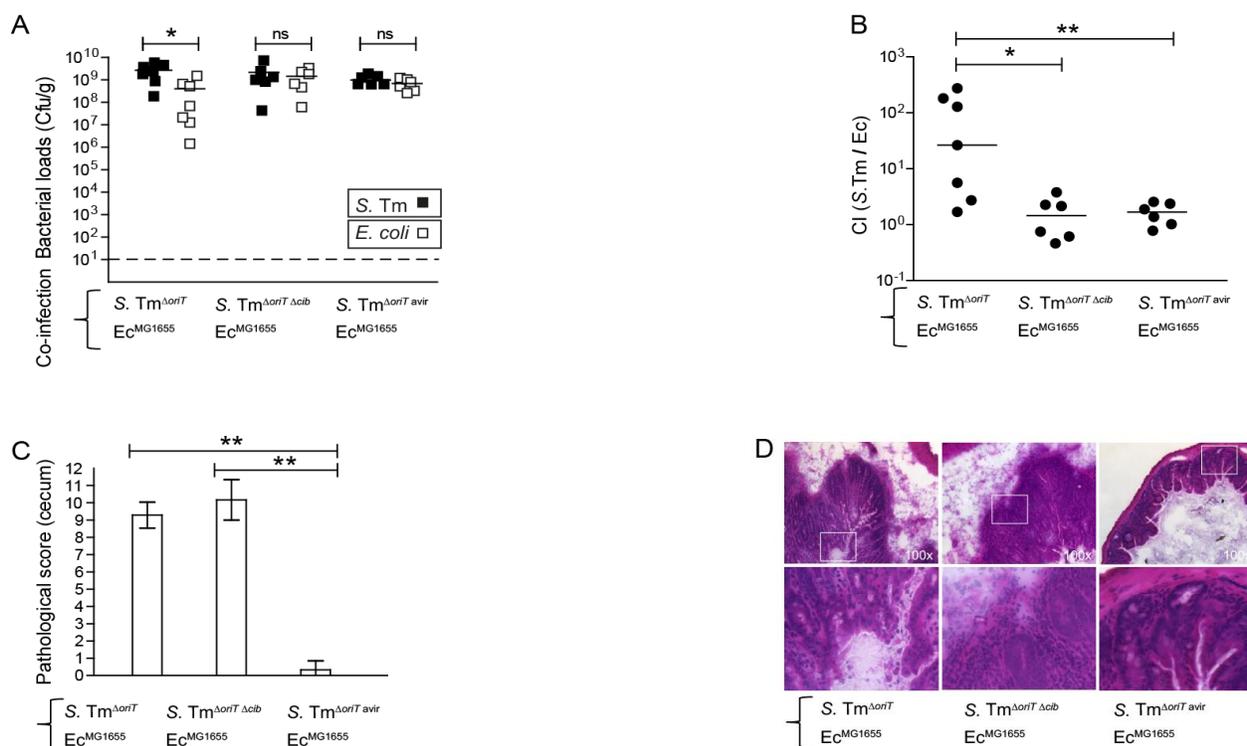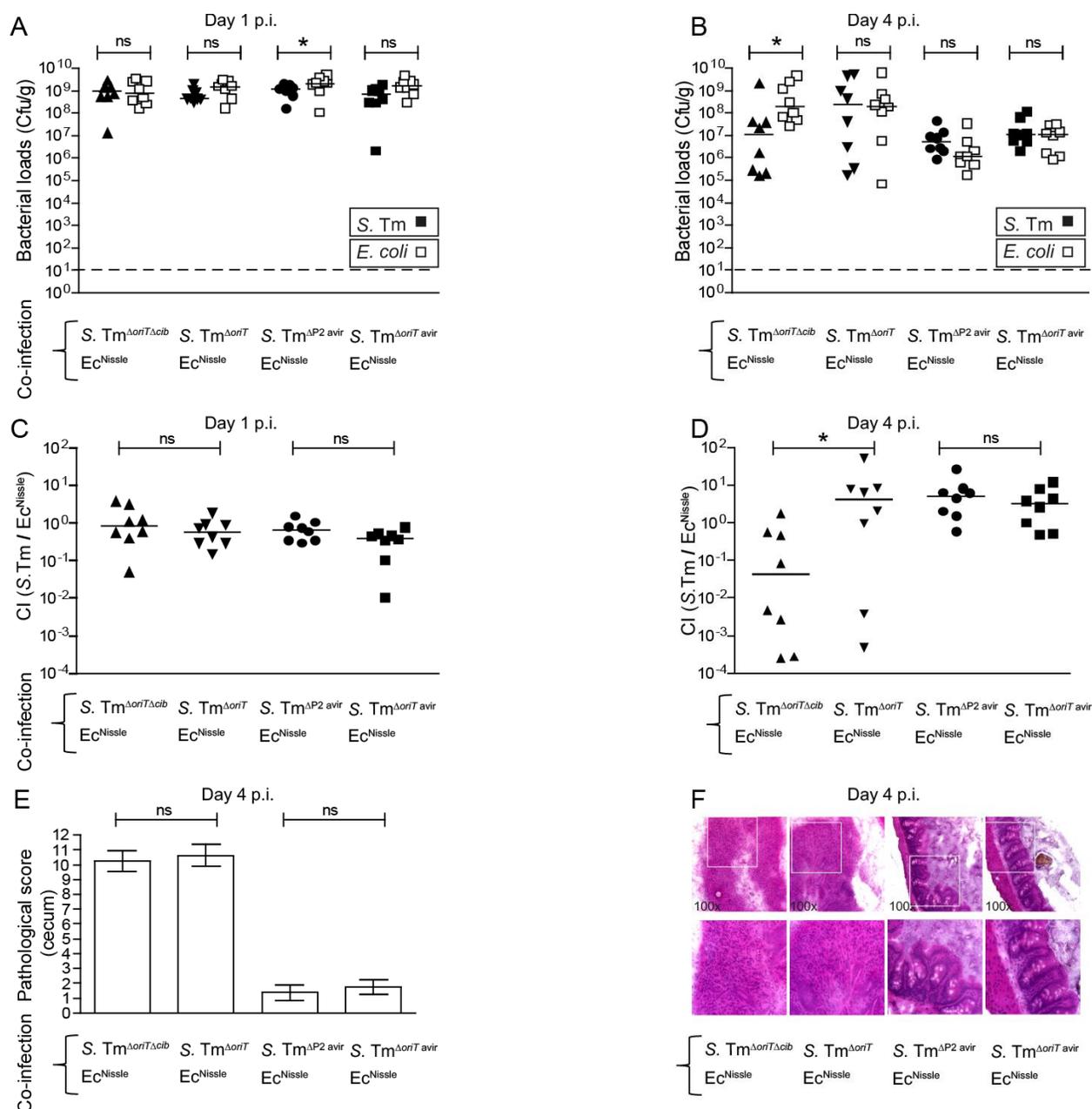
Figure 4.3. Colicin-dependent competition of *S.* Tm and *E. coli* in the gut in inflammation-induced "blooms" in conventional mice. Streptomycin-treated conventional mice were co-infected with 1:1 mixtures of *S.* Tm$^{oriT\,\Delta cib}$ and Ec^{Nissle}, *S.* Tm$^{\Delta oriT}$ and Ec^{Nissle}, *S.* Tm$^{\Delta P2\,avir}$ and Ec^{Nissle} and *S.* Tm$^{\Delta oriT\,avir}$ and Ec^{Nissle}. *S.* Tm (black) and *E. coli* (white) colonization density was determined at day 1 **(A)** and day 4 p.i. **(B)** in the feces and cecum content (Cfu/g), respectively. **(C,D)** Competitive indices (CI; ratio of *S.* Tm / *E. coli*) as determined for individual mice shown in A and B. Bars show the median. **(E)** Histopathological analysis of cecal tissue of the infected mice. Cecal tissue sections of the mice were stained with hematoxylin/eosin and the degree of submucosal edema, neutrophil infiltration, epithelial damage and loss of goblet cells was scored (Section 3.2.8). 1–3: no pathological changes; 4–7: moderate inflammation; above 8: severe inflammation. Bars shown mean and StD. **(F)** Representative hematoxylin and eosin (H&E)–stained cecal sections of mice shown in (E). Magnification 100-fold. Enlarged sections (squares) are shown in the lower panels.

At day 1 p.i., co-infecting strains (ColIb-producing *S*. Tm$^{\Delta oriT\text{ avir}}$ competing Ec$^{\text{Nissle}}$) and (ColIb-deficient *S*. Tm$^{\text{avir P2 cured}}$ competing Ec$^{\text{Nissle}}$) were colonizing the gut efficiently (**Figure 4.3A,C**). Nevertheless, in the absence of inflammation, they were out-numbered (to ~10^7 cfu/g) by the complex conventional microbiota re-growing by day 5 after streptomycin treatment (**Figure 4.3B**). Moreover, the avirulent ColIb-producer (*S*. Tm$^{\Delta oriT\text{ avir}}$) gained no advantage over Ec$^{\text{Nissle}}$ (**Figure 4.3D**). The ratio of *S*. Tm / Ec$^{\text{Nissle}}$ (competitive index (CI)) is alerted in comparison to *S*. Tm / Ec$^{\text{MG1655}}$ (**Figure 4.2B**). It could be argued that this is due to strain-specific differences between Ec$^{\text{MG1655}}$ and Ec$^{\text{Nissle}}$ as well as, due to differences between the gnotobiotic and complex gut microbiota. Nevertheless, the experiments with the conventional mice confirmed that ColIb benefits *S*. Tm when competing against Ec$^{\text{Nissle}}$ only upon gut inflammation.

Taken together, these results suggested that in the non-inflamed gut either expression of ColIb by *S*. Tm was down-regulated or the susceptibility to ColIb of *E. coli* strains was decreased. To gain further insights in the mechanism of colicin-dependent competition in the inflammation-induced blooms, the regulation of *cib* expression in *S*. Tm as well as, Ec susceptibility to ColIb were thoroughly investigated.

4.1.2 Production of *S*. Tm ColIb is induced by iron limitation and the SOS response *in vitro*

In the *cib* promoter region, two binding sites for the transcriptional repressors Fur and LexA were identified: a 17 bp-long "Fur box" and a "LexA box" of the same length, respectively (**Figure 4.4**; **Figure 4.5**).

```
-200                    -180                    -160                    -140                        fur box        -120
CCAGAGAATACCCAGACTGTGATGCTGCCACAACGTCAGCAGGCTTTCTGAACGGTTTAACACCACTTCATGTTAATGATAATCACTATCATTAAATCT

-100                   -80  -10              lexA box       -60                 -40                -20        S.D.
-35                                                                                                             -3
GACATGCCATTTTCTCCTTAATAAATTAATACTGTATATGTATCCATATACGTAAGCAGTTAATTCATTTGTTTTCCTCAGAGGATGAAGGAGATACCG

1                      20                    40                    60                    80
cib
ATGTCTGACCCTGTACGTATTACAAATCCCGGTGCAGAATCGCTGGGGTATGATTCAGATGGCCATGAAATTATGGCCGTTGATATTTATGTAAACCCT
Met Ser Asp Pro Val Arg Ile Thr Asn Pro Gly Ala Glu Ser Leu Gly Tyr Asp Ser Asp Gly His Glu Ile Met Ala Val Asp Ile Tyr Val Asn Pro

120                   140                   160                   180
cib
CACGTGTCGATGTTTTTCATGGTACCCGCCTGCATGGAGTTCCTTCGGGAACAAAACCATCTGGGGCGGAAACGAGTGGGTCGATGATTCCCCAACCC
Pro Arg Val Asp Val Phe His Gly Thr Pro Pro Ala Trp Ser Ser Phe Gly Asn Lys Thr Ile Trp Gly Gly Asn Glu Trp Val Asp Asp Ser Pro Thr

..................................................................................................

1.820                 1.840                 1.860                 1.880                 1.900
cib                                                                                              imm
TTTGCAATTATTATGGCGGCTGTGAGTGCGTTTGTTAATGATAAGTTTATTGAGCAGGTCAATAAACTTATTGGTATCTGACACATAATGATGCCCTTTC
Phe Ala Ile Ile Met Ala Ala Val Ser Ala Phe Val Asn Asp Lys Phe Ile Glu Gln Val Asn Lys Leu Ile Gly Ile Stp      Stp

1.920                 1.940                 1.960                 1.980                 2.000
imm
ATTTTCCTGAAAGGGCTTTGCAGAATATAAAAATTAAGTAAATGGCAACCACAGGAACTGATATAACGAAACAGAATAATTCAAATATTGCAGTTAAGCT
Lys Gly Ser Leu Ala Lys Cys Phe Ile Phe Ile Leu Tyr Ile Ala Val Val Pro Val Ser Ile Val Phe Cys Phe Leu Glu Phe Ile Ala Thr Leu Ser

2.020                 2.040                 2.060                 2.080                 2.100
imm
TCCGCCAACTGGATTTGTAAAGAAGTCTTTTTGCCAGAATTCTTTCCCTGTAAACCTTATTACCATTTTCTGTATTATCCTCATTGAAAAAGGAAAGTA
Gly Gly Val Pro Asn Thr Phe Phe Asp Lys Gln Trp Phe Glu Lys Gly Thr Phe Arg Ile Val Met Lys Gln Ile Ile Arg Met Ser Phe Pro Phe Thr

2.120                 2.140                 2.160                 2.180                 2.200
imm
ATGGCACTGATAATGCATCCGATGAACGCATAAAACATTCTTGCATTTTCCTGGCTATCTTTCCATCCCAGATAAAAAACTGTAAGAATAATGAGGCTTG
Ile Ala Ser Ile Ile Cys Gly Ile Phe Ala Tyr Phe Met Arg Ala Asn Glu Gln Ser Asp Lys Trp Gly Leu Tyr Phe Val Thr Leu Ile Ile Leu Ser Pro

2.220                 2.240         imm        S.D.        2.280                 2.300
GTATCAGGCTCTTCAGTAAATACTTTACAGATATATCCAGTTTCATCTGTTTTCTCCTTTATTGTTATCGTGTACCGGTGCGTGATAACATAATCACAGC
Ile Leu Ser Lys Leu Leu Tyr Lys Val Ser Ile Asp Leu Lys Met

-10   fur box     2.320              -35    2.340                 2.360
ATGATAATAATAATCAATAACAATAAGCTGTGTCACGTTTACATCATGGAACGGAGGTGCTCCT
```
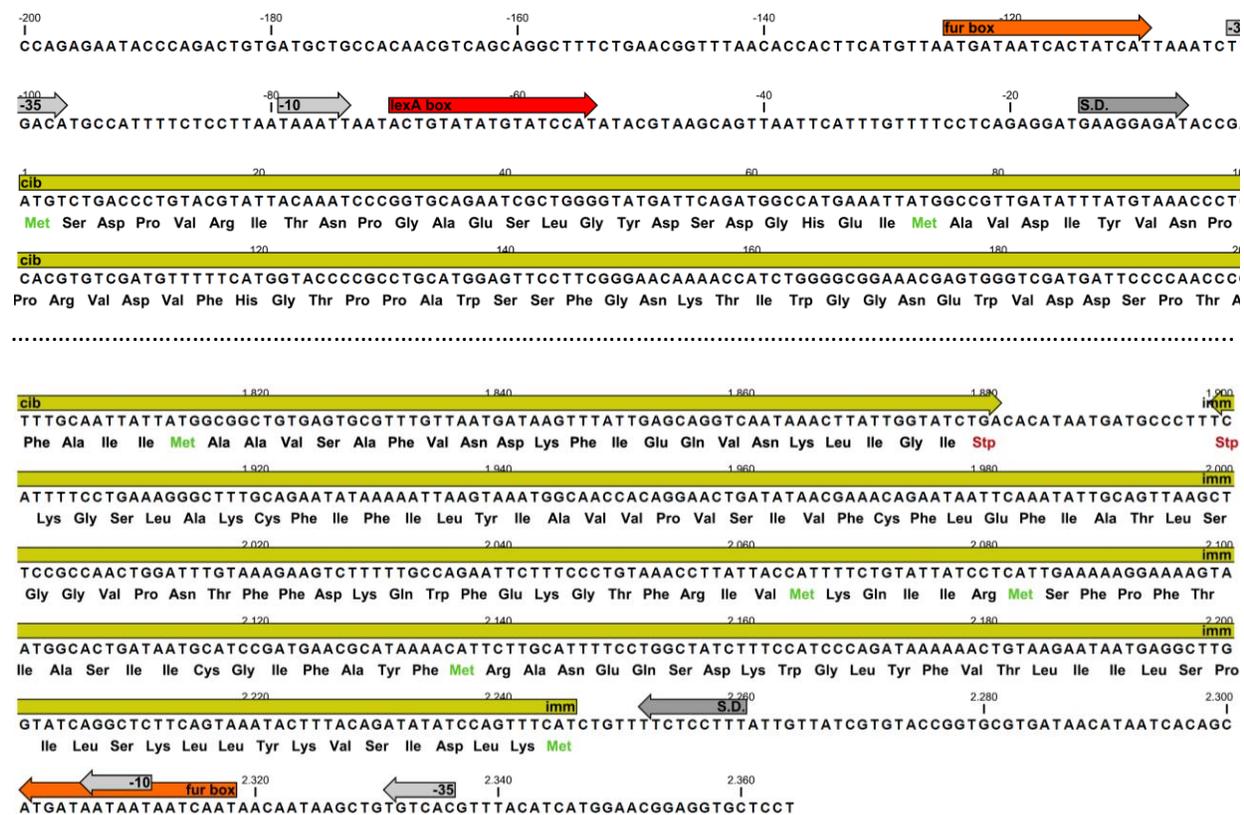
Figure 4.4. Nucleotide sequence of *S*. Tm^wt *cib imm* and its respective promoter regions. The sequence of *S*. Tm^wt *cib imm* region was searched position of the Fur- and LexA repressor binding sites as described (**Section 3.2.6.1**). The position of the Fur-box, LexA –box and major transcription start sites and their corresponding -10 and -35 regions are indicated, as well as the open reading frame and the prospective ribosome-binding site (S.D.).

To examine the regulation of the ColIb coding gene *cib*, a *cib* promoter *firefly-luciferase* (*luc*)-reporter was constructed. Furthermore, an affinity-purified polyclonal rabbit-α-ColIb antiserum was generated to quantify ColIb expression. Demonstrated by *luc*-reporter assays, as well as by immunoblot, *cib* expression was strongly up-regulated upon induction of the SOS response by the antibiotic mitomycin C (0.25 µg/ml) (**Figure 4.5B-D**). Addition of 100 µM iron chelator DTPA causes depletion of Iron(III) from the culture

media (Taylor *et al.*, 2009). This in turn also enchanced ColIb production similar to mitomycin C. Combined supplementation of mitomycin C and DTPA conveyed maximal induction of ColIb production and secretion (**Figure 4.5B-D**). These observations demonstrated that repression of *cib* is aborted in response to SOS signals and iron starvation.
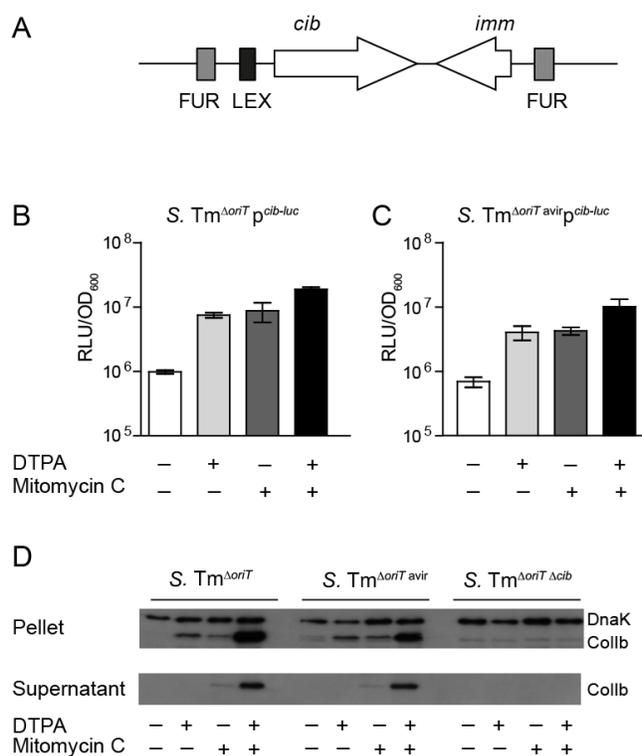

Figure 4.5. Expression of *S.* Tm ColIb is induced by iron limitation and the SOS response. (A) Organization of the ColIb locus showing location of the Fur and LexA repressor binding sites in the ColIb (*cib*) promoter and the immunity protein gene (*imm*). Overnight cultures of *S.* Tm$^{\Delta oriT}$ **(B)** and *S.* Tm$^{\Delta oriT}$ avir **(C)** carrying the reporter plasmid p$^{cib-luc}$ were re-inoculated 1:20 in fresh LB with indicated supplements (0.25 µg/ml mitomycin C; 100 mM DTPA) and grown under aeration for 4 h. OD$_{600}$ of the cultures was normalized, bacteria were harvested and luciferase-activity was measured in bacterial lysates. Relative luminescence units (RLU) per unit OD$_{600}$ are indicated. **(D)** Overnight cultures of indicated *S.* Tm strains were re-inoculated 1:20 in fresh LB with indicated supplements (0.25 µg/ml mitomycin C; 100 mM DTPA) and grown under aeration for 4 h. OD$_{600}$ of the cultures was normalized, bacteria were harvested and ColIb was detected in bacterial lysates as well as in the culture supernatant by immunoblot using an affinity-purified rabbit-α-ColIb antiserum. *S.* Tm DnaK was detected as loading control.

4.1.3 Upregulation of Ec^{wt} *cirA* under iron limitation correlates with increased ColIb suscpeptibility

The outer membrane protein CirA is the receptor for both ColIa and ColIb (Buchanan *et al.*, 2007; Cardelli & Konisky, 1974; Lazdunski *et al.*, 1998). As a component of the iron uptake system *cirA* is under negative control of the iron-sensing Fur repressor (Griggs *et al.*, 1987) (**Figure 4.6**). Binding of the specific sequence "Fur box" located in the promoter region of genes involved in iron-transport requires one Fe(II) accommodated to each monomer of the Fur dimer (Lee & Helmann, 2007).
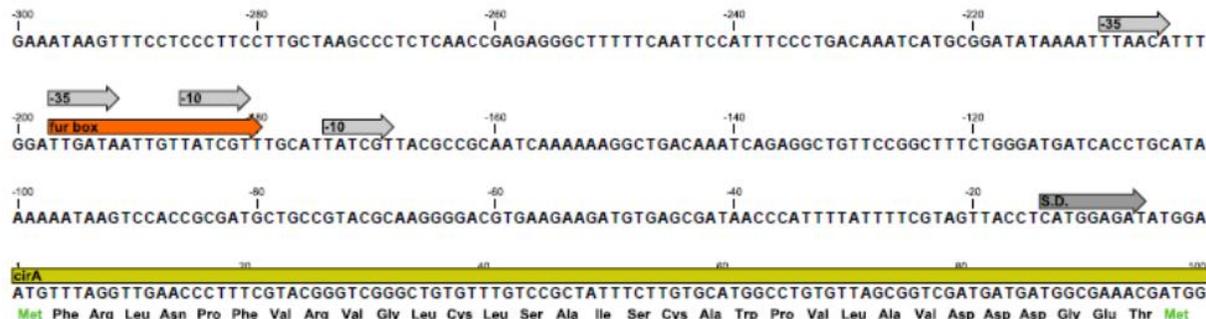
Figure 4.6. Nucleotide sequence of Ec^wt *cirA* and its promoter region. The sequence of Ec^wt *cirA* region was analyzed for the position of the Fur-repressor binding site as described (**Section 3.2.6.1**). The position of the Fur-box and major transcription start sites and their corresponding -10 and -35 regions are indicated, as well as the open reading frame and the prospective ribosome-binding site (S.D.).

A *cirA* promoter-*firefly-luciferase*-reporter and polyclonal rabbit-α-CirA antiserum were generated in order to investigate regulation of the *cirA* expression in Ec^MG1655. Confirmed by both, luciferase assay and immunoblot, iron depletion of LB medium as a result of 100 µM DTPA addition led to strong upregulation of *cirA* expression while addition of mitomycin C had no effect (**Figure 4.7A,B**). This observation verified that Ec^MG1655 *cirA* de-repression takes place in response to Fe(III)-starvation. Next, it was tested if expression of *cirA* correlates with sensitivity to ColIb-mediated killing. The Ec^MG1655 ^ΔcirA strain lacking the receptor was shown to be resistant to the bactericidal effect of ColIb (**Figure 4.11C**).
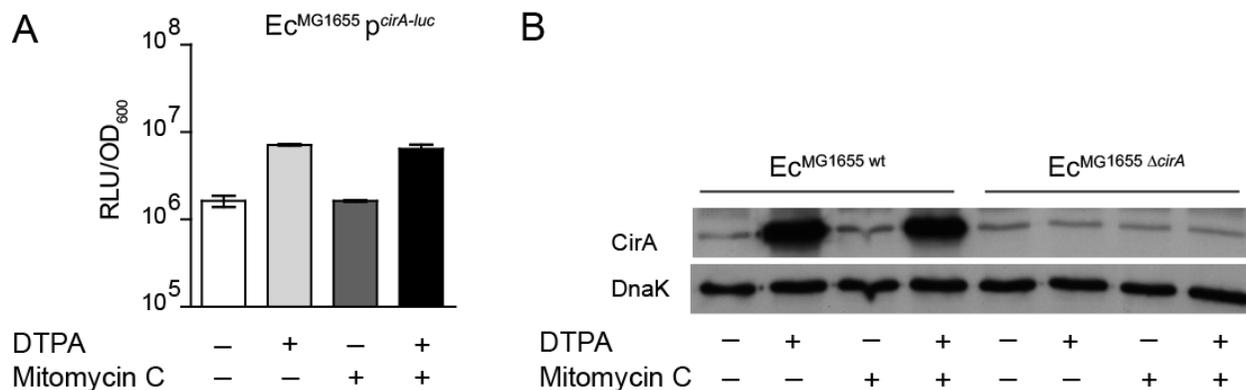
Figure 4.7. *E. coli cirA* **expression is upregulated in response to iron limitation.** (**A**) An overnight culture of Ec[MG1655] carrying the reporter plasmid p[*cirA-luc*] was re-inoculated 1:20 in fresh LB with indicated supplements (0.25 µg/ml mitomycin C; 100 mM DTPA) and grown under aeration for 4 h. OD_{600} of the cultures was normalized, bacteria were harvested and luciferase-activity was measured in bacterial lysates. Relative luminescence units (RLU) per unit OD_{600} are indicated. (**B**) Overnight cultures of Ec[MG1655] as well as Ec[MG1655 ΔcirA] were re-inoculated 1:20 in fresh LB with indicated supplements (0.25 µg/ml mitomycin C; 100 mM DTPA) and grown under aeration for 4 h. OD_{600} of the cultures was normalized, bacteria were harvested and CirA was detected in bacterial lysates by immunoblot using a rabbit-α-CirA antiserum. *E. coli* cytoplasmic protein DnaK was detected as loading control.

Moreover, ColIb-sensitivity was regained after complementation of Ec[MG1655 ΔcirA] with *cirA*-carrying plasmid (**Figure 4.11C**). To estimate whether consecutive iron depletion would lead to increased ColIb-sensitivity of Ec[MG1655], ColIb killing assays were set up. Ec[MG1655] was grown in M9 minimal media supplemented with different concentrations of $FeCl_3$. Equal amounts of purified recombinant ColIb were applied. Growth in M9 media promoted maximal sensitivity of Ec[MG1655] to ColIb, while susceptibility decreased upon $FeCl_3$ supplementation. This was consistent with reduction in CirA production by these cultures, as shown by immunoblot (**Figure 4.8B**).
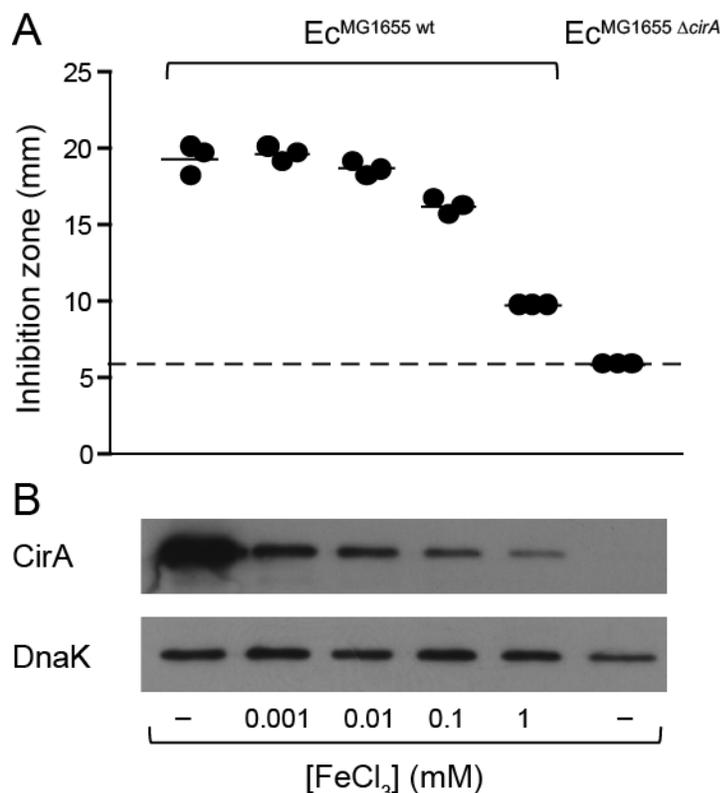
Figure 4.8. Induction of *cirA* expression increases sensitivity to ColIb of *E. coli*. (A) Ec^MG1655 and Ec^MG1655 Δ*cirA* were cultivated in M9 medium o.n., mixed with soft agar and indicated concentrations of FeCl$_3$ and overlaid on M9 agar plates. Paper discs with recombinant ColIb were placed on the agar plate and the diameter of the inhibition zone (halo) was measured after 24 h. The detection limit (dotted line) is the size of the paper-disc (6 mm). **(B)** *cirA* expression of *E. coli* grown *in vitro* in M9 medium supplemented with different concentrations of FeCl$_3$. Overnight cultures of Ec^MG1655 wt and Ec^MG1655 Δ*cirA* grown in M9 medium for 12 h were used for inoculation of 2 ml M9 medium supplemented with 1μM, 10μM, 0.1mM or 1mM FeCl$_3$ and subcultured for 7 h. From each subculture, 250 μl (for an OD$_{600}$ of 1) was taken, spun down at 4 °C, 10 min, 10, 000 rpm. CirA was detected by immunoblot in bacterial lysates using affinity-purified rabbit-α-CirA-antiserum. *E. coli* DnaK was detected as loading control.

Further, ColIb-meditated killing of Ec^MG1655 grown in rich LB medium upon addition of 100 μM DTPA was investigated using live-dead staining and FACS (**Section 3.2.1.5**). High rates of killing were detected among bacteria grown for 1 hour in Fe(III)-depleted media and consequently challenged with the purified recombinant ColIb. Interestingly, same amount of ColIb was shown to be more deadly for Ec^MG1655 grown for 1 hour in the iron-depleted medium compared to bacteria enduring long-terme (4 h) iron starvation (**Figure 4.9A**). However, an increase in *cirA* expression as a response to addition of DTPA was confirmed after both, short (1 h) and long (4 h) growth (**Figure 4.9B**). Taken together, the results above

demonstrated that elevated *cirA* expression increases ColIb sensitivity of Ec^{MG1655}. At late time point, siderophores may compete with ColIb for CirA receptor.
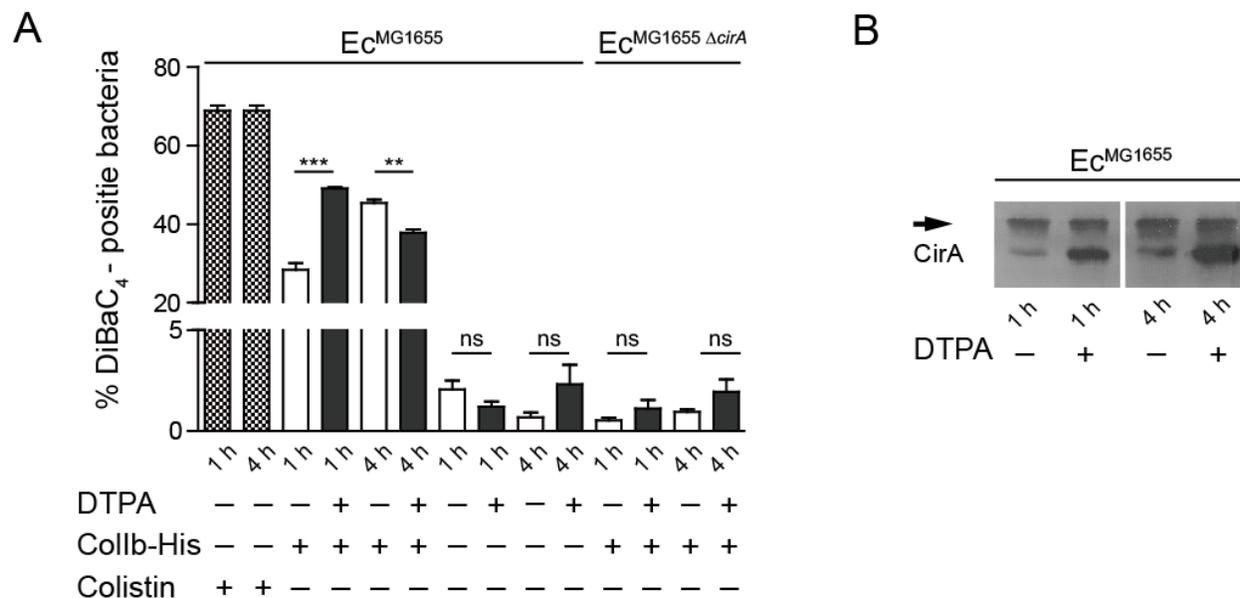
Figure 4.9. *E. coli* **exposed for a short time to iron starvation is highly susceptible to ColIb-mediated killing**. *E. coli* strains; $Ec^{MG1655\ wt}$ and $Ec^{MG1655\ \Delta cirA}$ were inoculated in 3 ml LB medium, grown for 12 h and subsequently used for inoculation of subculture I supplemented with 100 μM DTPA, which was grown for either 1, or 4 h. (**A**). Subculture I was diluted and normalized to an OD_{600} of 0.01 in LB medium supplemented with colistin sulphate (killing control) or ColIb-His and incubated for 2 h. Thereafter, bacteria were stained with $DiBaC_4$ and analyzed by FACS, % $DiBaC_4$-positive bacteria of the bacterial population is shown. (**B**) CirA in the cell lysates of subculture I (grown for 1 h or 4 h) was detected by immunoblot using rabbit-α-CirA-antiserum. The black arrow points an unspecific protein recognized by the rabbit-α-CirA-antiserum.

4.1.4 ColIb-dependent competition of *S*. Tm and Ec^{wt} *in vitro* is boosted by iron starvation and SOS-stress

Co-culture experiments were performed *in vitro* to further address the importance of the environmental conditions for ColIb-dependent competition between *S*. Tm$^{\Delta oriT}$ and Ec^{MG1655}. The ColIb-producer (*S*. Tm$^{\Delta oriT}$) was co-cultured with Ec^{MG1655} or Ec$^{MG1655\,\Delta cirA}$ under different conditions (**Figure 4.10**).
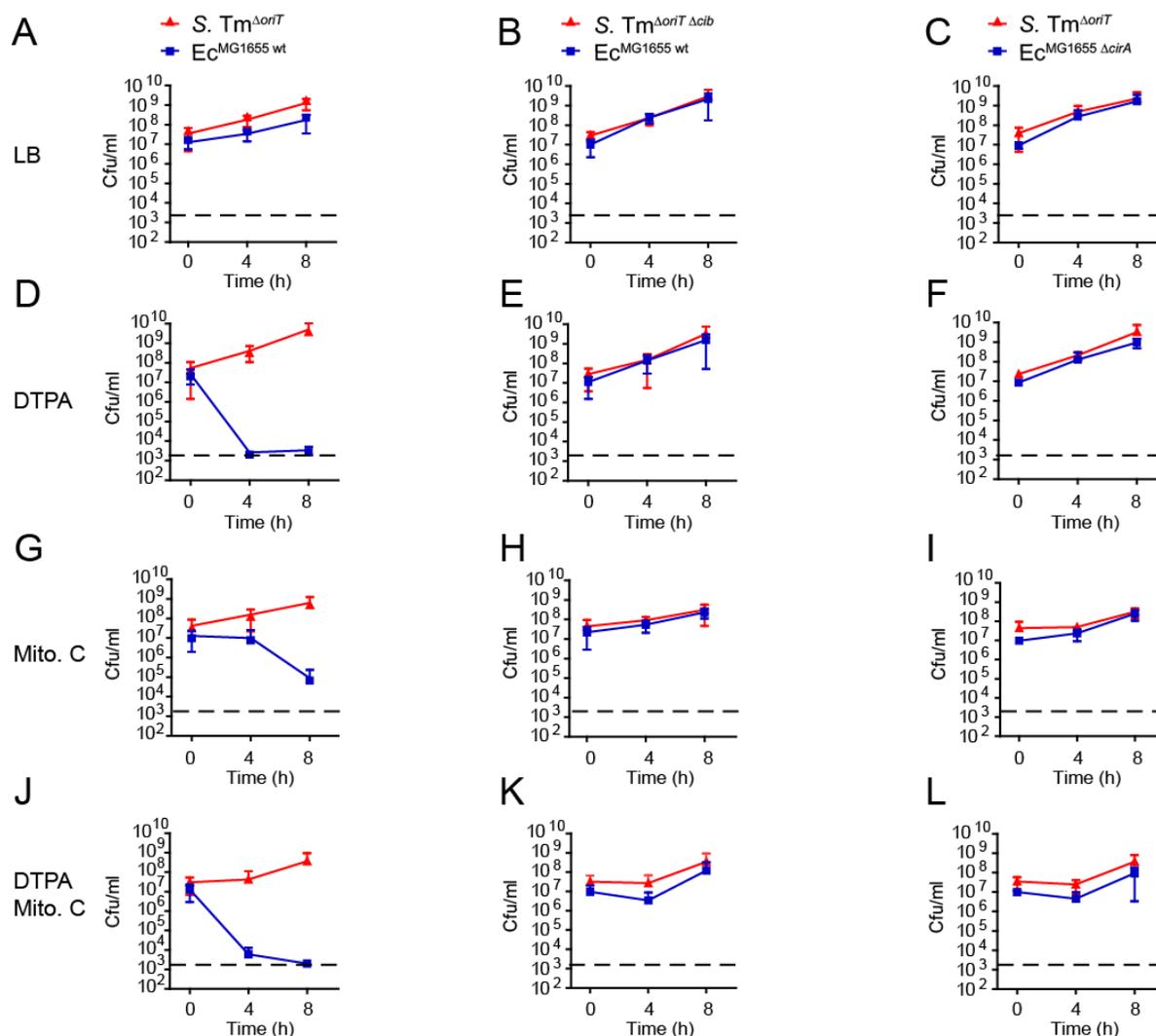
Figure 4.10. ColIb dependent competition of *S*. Tm and *E. coli in vitro*. Overnight cultures of *S*. Tm$^{\Delta oriT}$ and Ec^{MG1655} (**A, D, G, J**), *S*. Tm$^{\Delta oriT\,\Delta cib}$ and Ec^{MG1655} (**B, E, H, K**) and *S*. Tm$^{\Delta oriT}$ and Ec$^{MG1655\,\Delta cirA}$ (**C, F, I, L**) were diluted and normalized to an OD$_{600}$ of 0.05 for each strain in fresh LB with indicated supplements (0.25 µg/ml mitomycin C; 100 µM DTPA). Cfu/ml of both strains was determined at 0 h, 4 h, and 8 h after start of the subculture. Red lines: *S*. Tm strains, blue lines: *E. coli* strains. Dotted line: detection limit (2000 cfu/ml).

65

Additionally, competition between *S*. Tm$^{\Delta oriT\ \Delta cib}$ and Ec^{MG1655} was tested. Similar growth rates were observed for *S*. Tm$^{\Delta oriT}$ and Ec^{wt} co-cultured in the absence of supplements. After 8 h, *S*. Tm$^{\Delta oriT}$ overgrew Ec^{MG1655} by ~7-fold (mean titer *S*. Tm$^{\Delta oriT}$: 1.7 x 10^9 cfu/ml and Ec^{MG1655}: 2.3 x 10^8 cfu/ml) (**Figure 4.10A**). In contrast, Ec^{MG1655} was outnumbered by several orders of magnitude when either DTPA (7 x 10^7-fold), mitomycin C (1 x 10^4-fold) or both supplements (6 x 10^6-fold) were added to the co-culture (**Figure 4D,G,J**). Furthermore, comparable growth of the competitors was observed in the absence of ColIb (*S*. Tm$^{\Delta oriT\ \Delta cib}$) or its receptor CirA (Ec$^{MG1655\ \Delta cirA}$) independent of the conditions (**Figure 4.10B,C,E-L**). This indicated that *S*. Tm overgrowth *in vitro* was clearly ColIb-dependent. Interestingly, there was a discrepancy between the comparable ColIb expression levels (**Figure 4.5D**), but the more exuberant killing of Ec^{MG1655} upon addition of DTPA compared to the mitomycin C supplementation. These observations argued that iron depletion has a greater impact for ColIb-dependent competition (i.e. by enhancing Ec^{MG1655} *cirA* expression resulting in increased susceptibility to ColIb). Further, *S*. Tm *cib* mutant and the Ec^{MG1655} *cirA* mutant were complemented with plasmids carrying the respective genes missing leading to a reversed phenotype, as shown by ColIb killing assay (**Figure 4.11A,C**) and immunoblot (**Figure 4.11B,D**). Complemented strains were further tested in co-culture experiments. In absence of inducers, Ec$^{MG1655\ \Delta cirA}$ p$^{compl.\ cirA}$ was overgrown by *S*. Tm$^{\Delta oriT}$ (**Figure 4.12A**) and Ec^{MG1655} was completely outcompeted by *S*. Tm$^{\Delta oriT\ \Delta cib}$ p$^{compl.\ cib}$ after 8 hours (**Figure 4.12C**). This could be due to the difference between the complemented and the background trains. Nevertheless, upon addition of inducers similarly to the respective wild type strain Ec$^{MG1655\ \Delta cirA}$ p$^{compl.\ cirA}$ was outcompeted by *S*. Tm$^{\Delta oriT}$ (**Figure 4.12D,G,J**), but grew unaffected by *S*. Tm$^{\Delta oriT\ \Delta cib}$ (**Figure 4.12E,H,K**). Likewise, *S*. Tm$^{\Delta oriT\ \Delta cib}$ p$^{compl.\ cib}$ was overgrowing Ec^{MG1655} as result of iron depletion, mitomycin C supplementation, or both (**Figure 4.12F,I,L**). These results further supported ColIb-dependent overgrowth of *S*. Tm as well as, CirA-required killing of Ec on the account of ColIb.
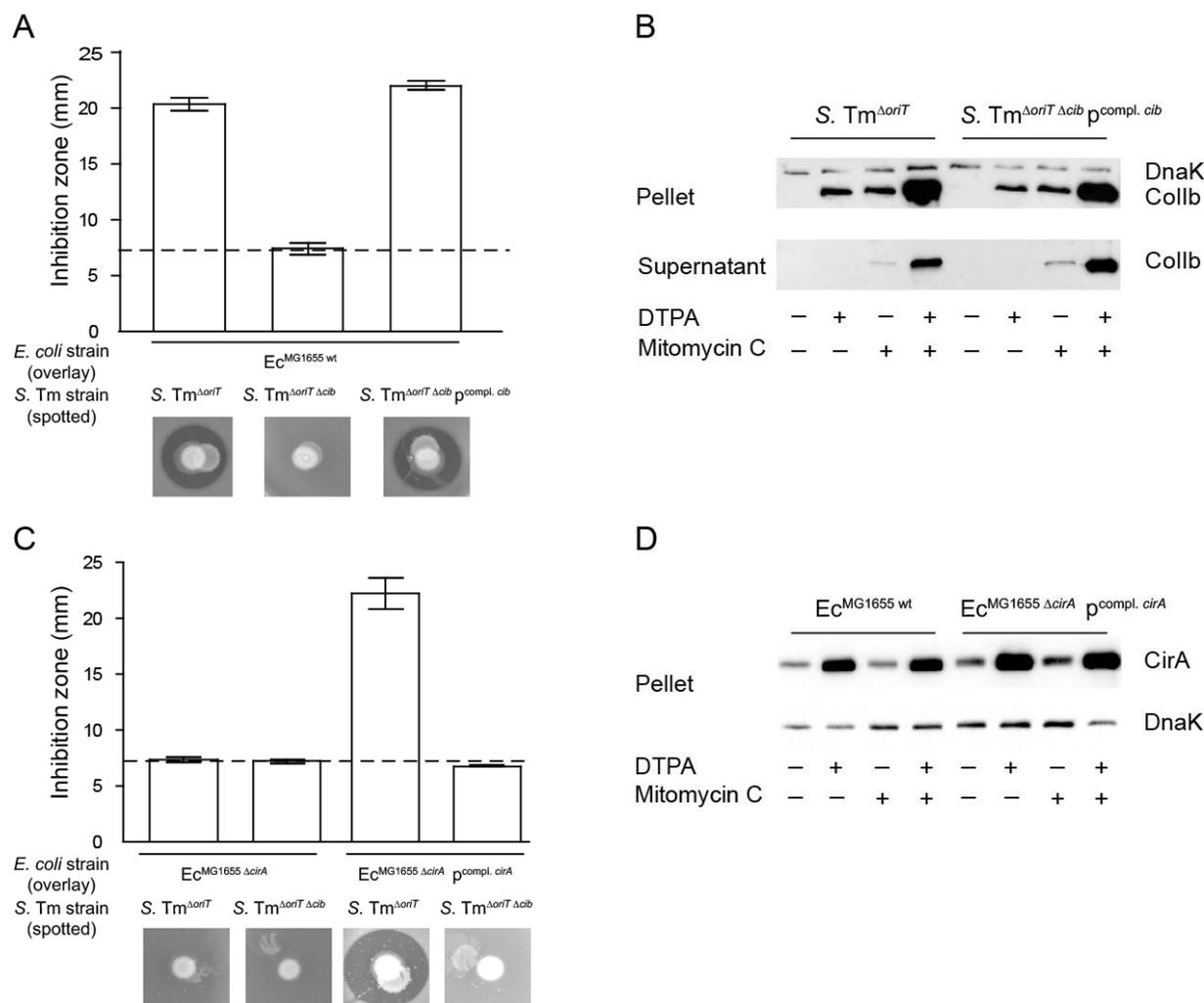
Figure 4.11. Characterization of plasmid-based complementation of *S*. Tm$^{oriT\ \Delta cib}$ and Ec$^{MG1655\ \Delta cirA}$ mutant strains. (**A**) Plasmid-based complementation of the ColIb-deficient *S*. Tm mutant *S*. Tm$^{oriT\ \Delta cib}$. *S*. Tm^{oriT}, *S*. Tm$^{oriT\ \Delta cib}$ and *S*. Tm$^{oriT\ \Delta cib}$ p$^{compl.\ cib}$ were spotted on LB agar plates containing mitomycin C and incubated o.n. to induce ColIb secretion. Ec^{MG1655} was cultivated in LB medium o.n., mixed with soft agar and overlaid on the agar plates. (**C**) Plasmid-based complementation of the CirA-deficient Ec$^{MG1655\ \Delta cirA}$ mutant. *S*. Tm^{oriT}, and *S*. Tm$^{oriT\ \Delta cib}$ were spotted on LB agar plates containing mitomycin C and incubated o.n. to induce ColIb secretion. Ec$^{MG1655\ \Delta cirA}$ and Ec$^{MG1655\ \Delta cirA}$ p$^{compl.\ cirA}$ were cultivated in LB medium o.n., mixed with soft agar and overlaid on the agar plates. The experiments were done in triplicates and the diameter of the ColIb inhibition zone (halo) was measured after 24 hours. The detection limit (dotted line) is the average size of the *S*. Tm^{wt} colony. Characterization of plasmid-based complementation of *S*. Tm$^{oriT\ \Delta cib}$ and Ec$^{MG1655\ \Delta cirA}$ mutant strains by Western Blot was done. Overnight cultures of indicated *S*. Tm (**B**) and Ec^{MG1655} (**D**) strains were re-inoculated 1:20 in fresh LB with indicated supplements (0.25 µg/ml mitomycin C; 100 µM DTPA) and grown under aeration for 4 h. OD$_{600}$ of the cultures was normalized, bacteria were harvested and ColIb was detected in bacterial lysates as well as in the culture supernatant by immunoblot using an affinity-purified rabbit-α-ColIb antiserum. *S*. Tm DnaK was detected as loading control. Ec^{MG1655} CirA was detected in bacterial lysates by immunoblot using a rabbit-α-CirA antiserum. *E. coli* cytoplasmic protein DnaK was detected as loading control.
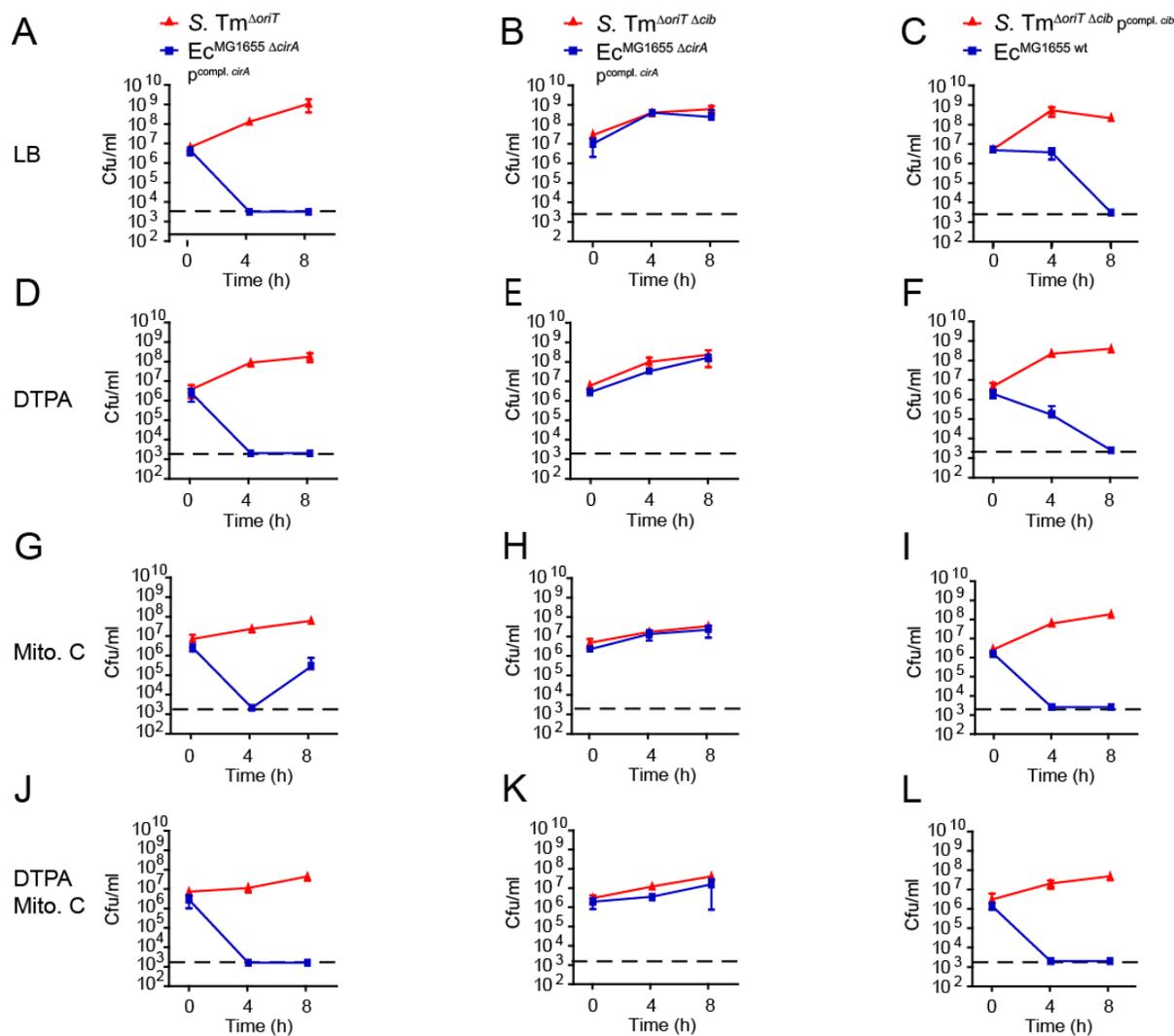
Figure 4.12. ColIb dependent competition of complemented *S.* Tm and *E. coli* mutant strains *in vitro*. Overnight cultures of *S.* Tm$^{\Delta oriT}$ and Ec$^{MG1655\ \Delta cirA}$ p$^{compl.cirA}$ (**A, D, G, J**), *S.* Tm$^{\Delta oriT\ \Delta cib}$ and Ec$^{MG1655\ \Delta cirA}$ p$^{compl.cirA}$ (**B, E, H, K**) and *S.* Tm$^{\Delta oriT\ \Delta cib}$ p$^{compl.cib}$ and Ec^{MG1655} (**C, F, I, L**) were diluted and normalized to an OD$_{600}$ of 0.05 for each strain in fresh LB with indicated supplements (0.25 µg/ml mitomycin C; 100 µM DTPA). Cfu/ml of both strains was determined at 0 h, 4 h, and 8 h after start of the subculture. Red lines: *S.* Tm strains, blue lines: *E. coli* strains. Dotted line: detection limit (2000 cfu/ml). Plasmid-based reconstitution of *cib* and *cirA* to the mutant strains leads to an over-complementation apparent by ColIb-dependent killing of *E. coli* in LB in the absence of supplements which is attributed to the multi-copy nature of the complementation-plasmid (A, C).

4.1.5 Inflammation-induced enterobacterial blooms foster *cib* and *cirA* expression *in vivo*

Initial co-infection experiments in mice established that colicin-dependent competition was taking place only in the inflamed gut. *In vitro S.* Tm and Ec^MG1655 grew alike independent of ColIb upon sufficient iron and no activator of the SOS response. In contrast, Fe(III)-limitation or DNA damaging mitomycin C promoted *S.* Tm overgrowth, based on ColIb production by the pathogen and *cirA* expression by *E. coli.* In consistence with these observations it could be argued that ColIb-dependent dominance of *S.* Tm over Ec^MG1655 in the inflamed gut could be attributed likewise to the increased production of ColIb by *S.* Tm, or up-regulation of the colicin receptor CirA by *E. coli*, or both. To verify this, expression of Ec^MG1655 receptor (*cirA*) and *S.* Tm ColIb (*cib*) using *firefly-luciferase* reporter-constructs was evaluated in the streptomycin mouse colitis model.
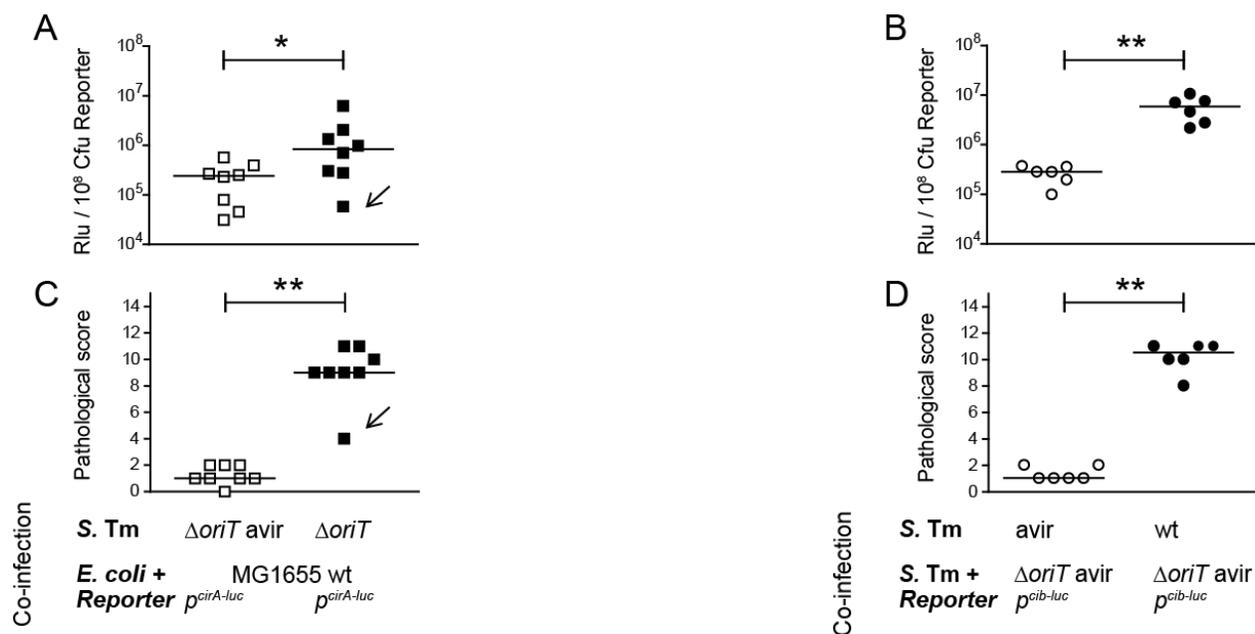
Figure 4.13. *S.* **Tm ColIb and and the** *E. coli* **ColIb receptor CirA are induced in the inflamed gut.** To measure *in vivo* regulation of *E. coli cirA* expression, streptomycin-treated LCM-mice were co-infected with 1:1 mixtures of *S.* Tm$^{\Delta oriT}$ avir (avirulent) or *S.* Tm$^{\Delta oriT}$ (wildtype) and the luciferase-reporter strain Ec^MG1655 p$^{cirA-luc}$ (**A, C**). To measure *in vivo* regulation of *S.* Tm *cib* expression, streptomycin-treated LCM-mice were co-infected with *S.* Tm^{avir} (avirulent) or with *S.* Tm^{wt} (wildtype) and the luciferase-reporter strain *S.* Tm$^{\Delta oriT}$ p$^{cirA-luc}$ (**B, D**). Bacteria were harvested from cecal content and luciferase-activity was measured in cecum content (**A, B**). Relative luminescence units (rlu) per 10^8 cfu of the reporter strain are indicated (**C, D**). Gut inflammation as determined by pathological score of cecal tissue sections of the infected mice. 1–3: no pathological changes; 4–7: moderate inflammation; above 8: severe inflammation. Bars show the median. Arrow in A and C points at one animal with atypically mild inflammatory symptoms.

Virulent (*S*. Tm$^{\Delta oriT}$ or *S*. Tm^{wt}) pathogen inflicting gut inflammation was administrated to LCM mice. To test expression of the reporters in non-inflammatory conditions LCM mice were infected with the avirulent *S*. Tm$^{\Delta oriT\,avir}$ or *S*. Tm^{avir} strains. Co-infection with Ec^{MG1655} carrying the p$^{cirA-luc}$-reporter plasmid, granted assesssment of *cirA* expression by Ec^{MG1655} (**Figure 4.13A,C**). Regulation of *S*. Tm *cib* expression was tested by co-infection with the avirulent *S*. Tm$^{\Delta oriT\,avir}$ carrying the p$^{cib-luc}$-reporter plasmid (**Figure 4.13B,D**). In contrast to the non-inflammatory conditions, significantly increased luciferase levels were detected for both the p$^{cirA-luc}$- and the p$^{cib-luc}$-reporters in the inflamed intestine (**Figure 4.13A-D**). These findings confirmed the initial conception of increased side by side ColIb production by *S*. Tm and CirA-dependent susceptibility of Ec^{MG1655} as a response to the gut inflammation. Thus, disclosing the means in which inflammation promotes ColIb-dependent competition of *S*. Tm and commensal *E. coli*.

4.2 Prophage-mediated ColIb release

4.2.1 Activation of temperate phages affects ColIb release in *S*. Tm

Along with the activation of ColIb expression, the SOS-response promotes numerous other events in the jeopardized bacterial cell. Facing the risk of the host-cell death, temperate phages enter the lytic mode (N.J. Dimmock, 2001). DNA damage in bacteria leads to the activation of RecA coprotease (RecA*) which in turn triggers self cleavage of LexA repressor followed by de-repression of genes involved in the SOS response (Little & Mount, 1982). The lambdoid prophage repressor protein CI is adapted to recognize host RecA* as a signal for impaired cell viability. RecA* directed cleavage of CI promotes successive expression of prophage genes required for assembly and lysis-directed release of new phage particles. Phage-mediated cell lysis could either conduct leakage of the cytoplasmic compounds through a holin-formed pore in the inner membrane or trigger instant release of the whole cytoplasmic content as a result of massive membrane disruption (Desvaux, 2012). The mechanism for release of ColIb is unclear. It was hypothesized that upon phage-mediated lysis ColIb may be released alongside the rest of the cytoplasmic content.

To address this, release of ColIb was compared between the *S*. Tm SL1344 strain (*S*. Tm^{MA6118}) lysogenic for four temperate phages (Gifsy-1, Gifsy-2, SopEΦ and ST64B) (Figueroa-Bossi & Bossi, 2004) and its isogenic prophage-cured derivatives *S*. Tm^{ΔG1ΔG2}, *S*. Tm^{ΔG1ΔG2ΔST} and *S*. Tm^{ΔPh}, lacking all four prophages(Alonso *et al.*, 2005), in a ColIb-dependent killing assay ("halo assay") using the ColIb-sensitive *E. coli* strain Ec^{MG1655} (Nedialkova *et al.*, 2014). Comperable inhibition zones were observed for *S*. Tm^{MA6118} and *S*. Tm^{ΔG1ΔG2} (cured from Gifsy-1, Gifsy-2 prophages) (**Figure 4.14**). In contrast, *S*. Tm^{ΔG1ΔG2ΔST} cured from three prophages (Gifsy-1, Gifsy-2 and ST64B) displayed a significant decrease in halo size (**Figure 4.14**). This was even more pronounced in case of the quadruple prophage mutant *S*. Tm^{ΔPh}.
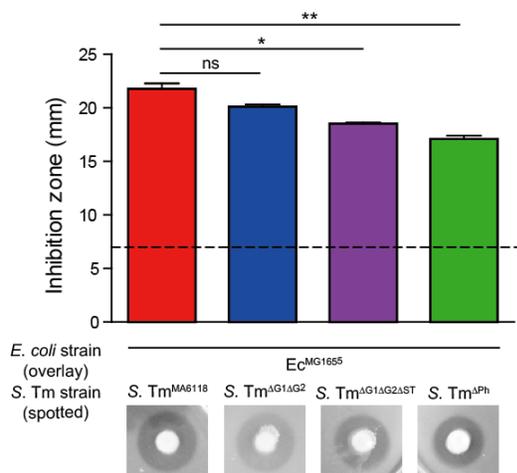
Figure 4.14. Prophage depletion leads to decrease in ColIb-dependent killing. *S.* Tm strains: *S.* Tm^MA6118 (red), *S.* Tm^ΔG1ΔG2 (blue), *S.* Tm^ΔG1ΔG2ΔST (violet), *S.* Tm^ΔPh (green) were spotted on a LB agar plate supplemented with 0.25 µg/ml mitomycin C. Plates were incubated o.n. to induce production of ColIb and phage lytic mode. Next, plates were overlaid with Ec^MG1655 (grown in 10 ml LB medium and mixed with LB soft agar). After 12 hours incubation, the ColIb inhibition zone (halo) was measured. The detection limit (dotted) line denotes the average diameter of *S.* Tm colony.

Decreased halo size could be the result of reduced ColIb release or of attenuated growth of the producing strain. Therefore the growth dynamics of the four *S.* Tm strains upon addition of 0.5 µg/ml mitomycin C was analyzed. Initial experiments were performed in Erlenmeyer flasks in 10 ml culture volume (**Figure 4.15**). In the absence of mitomycin C, all four strains grew at equal rate. Addition of mitomycin C led to an overall decrease of growth (600 ηm) of all strains.
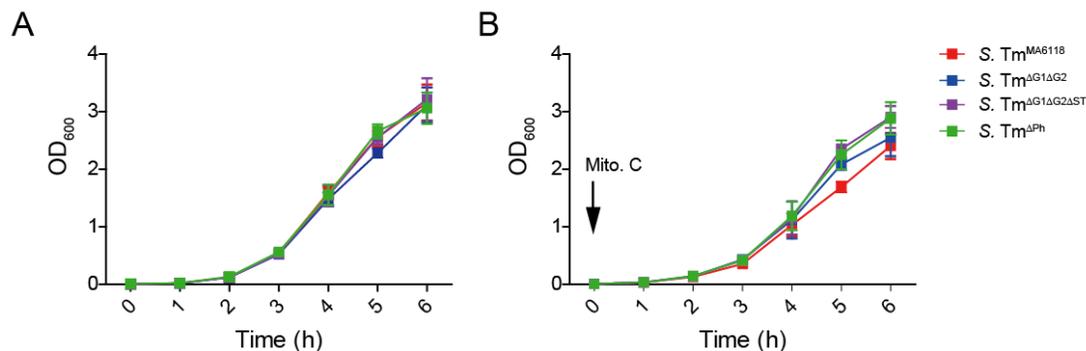
Figure 4.15. Prophage deletion results in slightly diminished cell lysis. *S.* Tm strains: *S.* Tm^MA6118 (red), *S.* Tm^ΔG1ΔG2 (blue), *S.* Tm^ΔG1ΔG2ΔST (violet), *S.* Tm^ΔPh (green) grown for 12 h in LB medium were separately diluted and normalized to an OD$_{600}$ of 0.0025 in 10 ml fresh LB (subcultures I). Subcultures I (grown in Erlenmeyer flasks for 3 h) were used for inoculation of 10 ml LB (subculture II) without (**A**) or without 0.25 µg/ml mitomycin C (**B**). Subcultures II were grown for 6 h. OD$_{600}$ values of the subculture were measured each hour.

However, no significant difference in growth of the four strains was observed. Interestingly, cultivation of the bacteria in a smaller volume (200 µl) in 96-well plates led to a notable enhancement of bacterial lysis upon addition of mitomycin C (**Figure 4.16B**). Cell density values decreased as soon as 2 hours after addition of mitomycin C for *S*. Tm^{MA6118}, but also for the *S*. Tm$^{\Delta G1\Delta G2}$ indicating that activation of the Gifsy-phages only has a minor impact on prophage-induced *S*. Tm lysis. In contrast, *S*. Tm$^{\Delta G1\Delta G2\Delta ST}$ and *S*. Tm$^{\Delta Ph}$ growth was not significantly affected 4 hours after induction. This suggests that either SopEΦ or ST64B alone, or both prophages together promote extensive lysis.

Next, ColIb production and release by *S*. Tm^{MA6118} and prophage-mutant strains was analyzed by immunoblot. For the analysis of intra-bacterial and secreted ColIb levels, a culture-volume normalized to an equal OD$_{600}$ was used. ColIb–release into supernatant was detected in an equal volume of culture supernatant (not normalized). Colicin expression, in response to mitomycin C, was comparable in the lysates of the four strains grown in Erlenmeyer flasks (**Figure 4.17A**). In the culture supernatant, ColIb was detected for *S*. Tm^{MA6118} and *S*. Tm$^{\Delta G1\Delta G2}$. In contrast, no release of ColIb was detected for *S*. Tm$^{\Delta G1\Delta G2\Delta ST}$ and *S*. Tm$^{\Delta Ph}$.
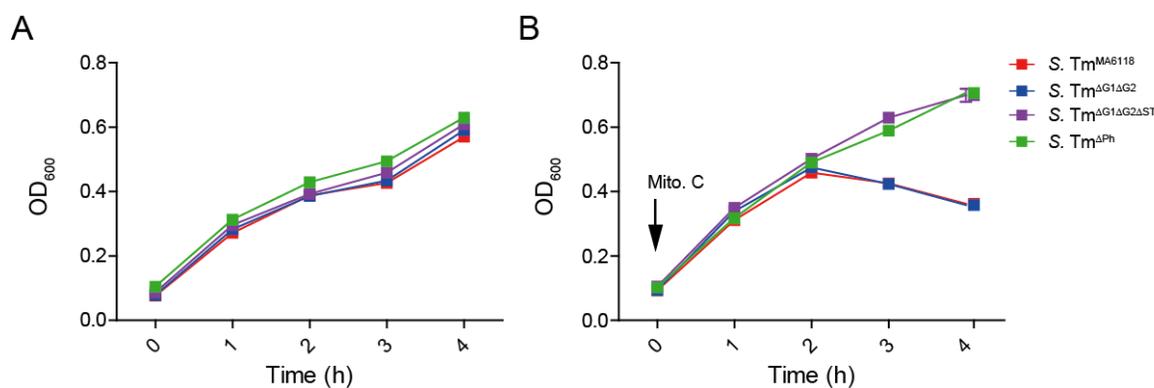

Figure 4.16. Prophage deletion results in significant reduction of the cell lysis. . *S*. Tm strains: *S*. Tm^{MA6118} (red), *S*. Tm$^{\Delta G1\Delta G2}$ (blue), *S*. Tm$^{\Delta G1\Delta G2\Delta ST}$ (violet), *S*. Tm$^{\Delta Ph}$ (green) were grown for 12 h in LB medium, separately diluted and normalized to an OD$_{600}$ of 0.025 in 3 ml fresh LB (subcultures I). After 2 h growth in glass tubes, on a wheel rotor, subcultures I were diluted and normalized to an OD$_{600}$ of 0.2 in LB medium (subcultures II) without (**A**) or supplemented with 0.5 µg/ml mitomycin C (**B**). Subcultures II were grown in 96-well plate for 4 h measuring OD$_{600}$ each hour. Bars shown mean and StD. The OD$_{600}$ values (4 h) separately analyzed for the non induced and mitomycin C-induced cultures are significantly different (***$p<0.0001$) (ANOVA test). Statistical analysis by unpaired Student's t-test for non induced cultures: *S*. Tm^{MA6118} and *S*. Tm$^{\Delta G1\Delta G2}$ ($p>0.05$), *S*. Tm^{MA6118} and *S*. Tm$^{\Delta G1\Delta G2\Delta ST}$ (***$p<0.0001$), *S*. Tm^{MA6118} and *S*. Tm$^{\Delta Ph}$ (*** $p<0.0001$). Statistical analysis by unpaired Student's t-test for mitomycin C-supplemented cultures: *S*. Tm^{MA6118} and *S*. Tm$^{\Delta G1\Delta G2}$ (*$p<0.05$), *S*. Tm^{MA6118} and *S*. Tm$^{\Delta G1\Delta G2\Delta ST}$ (** $p<0.006$), *S*. Tm^{MA6118} and *S*. Tm$^{\Delta Ph}$ (*** $p<0.0001$).
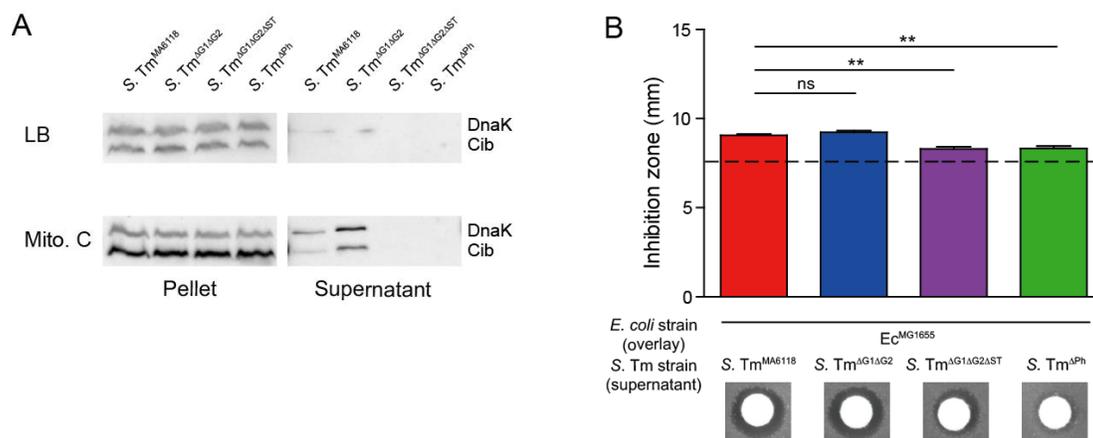
Figure 4.17. ColIb secretion is reduced in prophage-deficient strains. Subcultures II of *S*. Tm strains: *S*. Tm^{MA6118} (red), *S*. Tm$^{\Delta G1\Delta G2}$ (blue), *S*. Tm$^{\Delta G1\Delta G2\Delta ST}$ (violet) and *S*. Tm$^{\Delta Ph}$ (green) were grown in Erlenmeyer flasks. Cultured for 6 h bacteria were harvested from subculture II (**Section 3.2.2.2**). (**A**) ColIb was detected in cell lysates and culture supernatants by immunoblot using affinity-purified rabbit-α-ColIb-antiserum. *S*. Tm DnaK was detected as loading control. (**B**) Bactericidal activity of extracellular ColIb was tested. Paper disks soaked with sterile spent culture supernatant (mitomycin C supplemented (0.25 µg/ml) subculture II (6) h) were set on LB agar plates overlaid with Ec^{MG1655} (grown in LB medium and mixed with soft agar). Following 12 h incubation, ColIb inhibition zone (halo) was measured. The detection limit (dotted) line indicates the size of the paper disks.

Of note, DnaK was detected in the supernatant fraction alongside with ColIb. This suggests that indeed ColIb may be not actively secreted, but rather is released by phage-mediated bacterial lysis. Similar results were obtained for strains grown in a 96-well plate (**Figure 4.18A,B**). To determine ColIb-levels in bacterial cultures in 96-well plates, pellet fraction was not normalized to an equal OD$_{600}$. This way, the relative bacteria-associated and released ColIb-levels can be directly compared. These results again showed that ColIb secretion mainly correlated with the lysis triggered by the SopEΦ and (or) ST64B prophages.
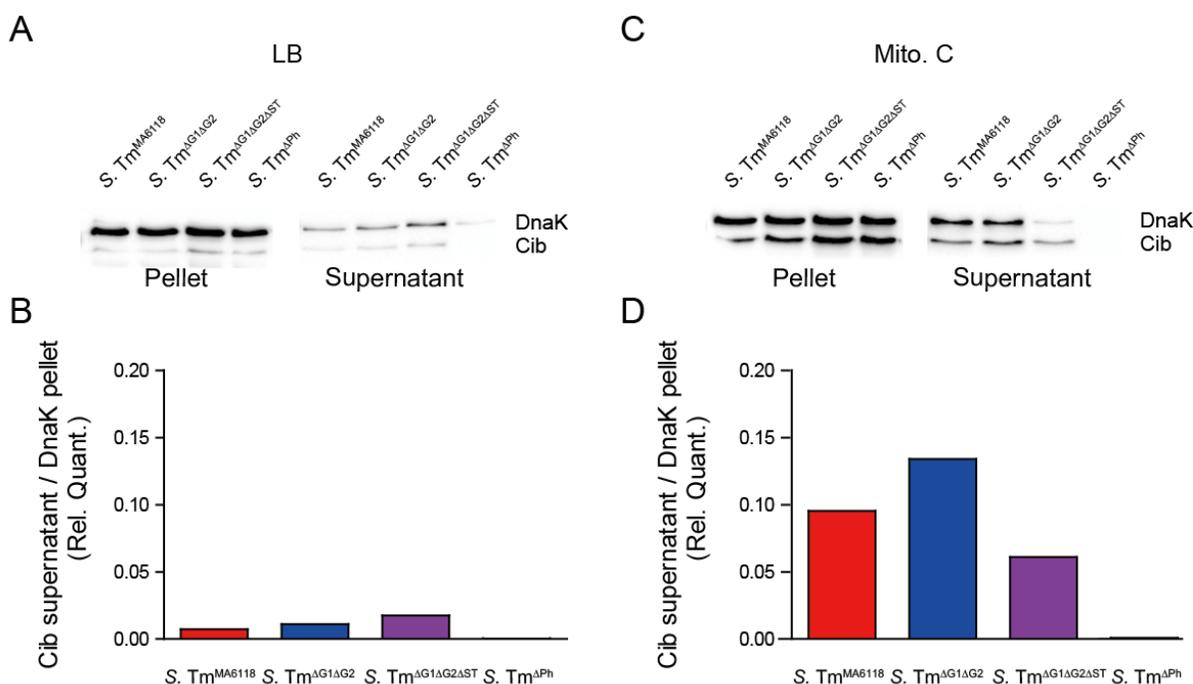
Figure 4.18. Temperate phage induction enhances ColIb release. Subculture II of *S*. Tm strains: *S*. Tm^{MA6118} (red), *S*. Tm$^{\Delta G1\Delta G2}$ (blue), *S*. Tm$^{\Delta G1\Delta G2\Delta ST}$ (violet), *S*. Tm$^{\Delta Ph}$ (green) were grown for 4 h in a 96-well plate without (**A**) or with addition of mitomycin C (**C**) (**Section 3.2.1.3**). Next, bacteria were harvested from 100 μl of subculture II and ColIb was detected in cell lysates and culture supernatants by immunoblot using affinity-purified rabbit-α-ColIb-antiserum. *S*. Tm DnaK was detected as loading control. The relative quantity of ColIb and DnaK was determined by densitometry using Image Lab software (Bio-Rad). The ratio of relative quantity of ColIb (found in the supernatant) divided by the relative quantity of DnaK (found in the bacterial lysate) for non induced (**B**) and mitomycin C-induced (**D**) culture is shown.

Next, it was assessed, weather ColIb released in the culture supernatant in the course of the prophage-mediated lysis retains full bactericidal activity. Therefore, culture supernatant was tested in the colicin-killing assay. In consistence with the previous observations, only extracellular fractions of *S*. Tm^{MA6118} and *S*. Tm$^{\Delta G1\Delta G2}$ cultures supplemented with mitomycin C mediated killing of Ec^{MG1655} (**Figure 4.17B**; **Figure4.19**). No inhibition zone was observed for supernatant of *S*. Tm$^{\Delta G1\Delta G2\Delta ST}$ and *S*. Tm$^{\Delta Ph}$ cultures, suggesting that they don't contain active ColIb. Taken together, these results suggested that induction of the bacterial SOS response leads to activation of the lytic stage of ST64B and SopEΦ prophages, thereby enhancing the release of bactericidal ColIb into the surrounding environment.
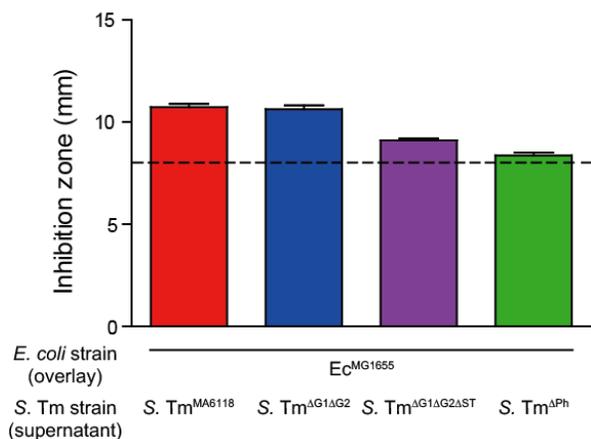
Figure 4.19. Bactericidal activity of extracellular ColIb is reduced in prophage-depleted strains. Mitomycin C supplemented (0.5 µg/ml) subcultures II of *S.* Tm strains: *S.* Tm^{MA6118} (red), *S.* Tm$^{\Delta G1\Delta G2}$ (blue), *S.* Tm$^{\Delta G1\Delta G2\Delta ST}$ (violet) and *S.* Tm$^{\Delta Ph}$ (green) were grown in a 96-well plate for 4 h (**Section 3.2.1.3**). Next, bacteria were harvested and bactericidal activity of extracellular ColIb was tested (**Section 3.2.3.3**). Paper disks soaked with sterile spent culture supernatant were set on LB agar plates overlaid with Ec^{MG1655} (grown in LB medium and mixed with soft agar). Following 12 h incubation, ColIb inhibition zone (halo) was measured. The detection limit (dotted) line indicates the size of the paper disks.

4.2.2 SopEΦ does not contribute to ColIb release in *S.* Tm^{MA6118}

Lysis genes are expressed in the final phase of the phage lytic. In the course of virion morphogenesis a small phage-encoded protein termed holin accumulates in the inner membrane of gram negative bacteria. When reaching a critical concentration, holins form a micro-scale hole in the inner membrane. Next, phage encoded muralyitic enzymes termed endolysins pass through the holin-formed membrane lesion and degrade the peptidoglycan. Finally, a third class of lysis proteins termed spanins trigger outer membrane disruption and subsequently bacterial lysis (Young, 2013). Lysis genes arranged as a "cassette" are highly conserved across lambdoid phage genomes (Wang *et al.*, 2000). Therefore, they can be identified by homology searches. Based on the observation that SopEΦ- or (and) ST64B–deficient *S.* Tm strains release significantly less ColIb, it was reasoned that deletion of the lysis genes of these phages would be sufficient to cause a decreased ColIb release. Using the lambda Red recombinase system (Datsenko & Wanner, 2000) SopEΦ lysis genes in strains *S.* Tm^{MA6118} and *S.* Tm$^{\Delta G1\Delta G2}$ were replaced by a chloramphenicol resistance cassette (**Figure 2.1A,B**; **Table 30**). ColIb-mediated killing of Ec^{MG1655} by *S.* Tm$^{\Delta lysS\phi C}$ and *S.* Tm$^{\Delta G1\Delta G2\Delta lysS\phi C}$ was attenuated compared to the respective background strains (**Figure 4.20A**).
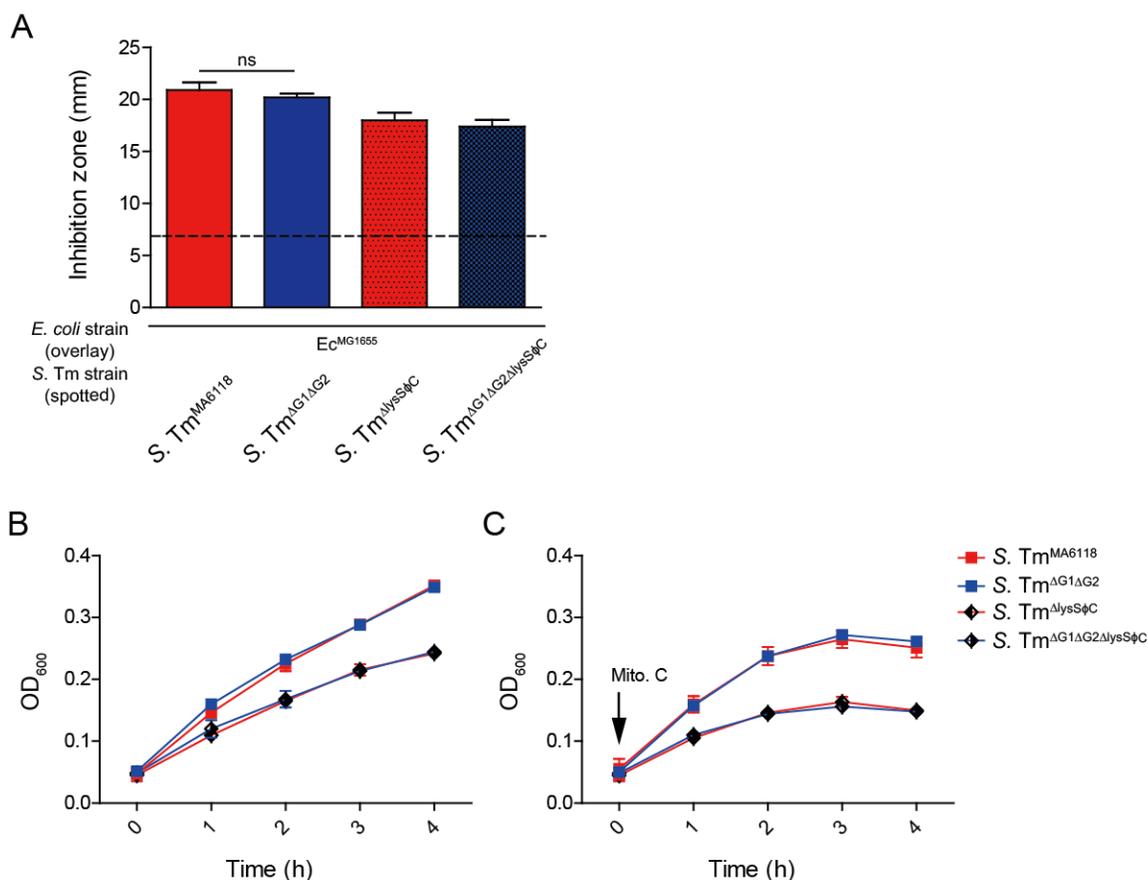
Figure 4.20. Replacement of SopEΦ lytic genes with a *cat* cassette leads to attenuated growth. (**A**). *S.* Tm strains: *S.* Tm^{MA6118} (red), *S.* Tm$^{\Delta G1\Delta G2}$ (blue), *S.* Tm$^{\Delta lysS\phi C}$ (dotted red) and *S.* Tm$^{\Delta G1\Delta G2\Delta lysS\phi C}$ (dotted blue) were spotted on a LB agar plate supplemented with 0.25 µg/ml mitomycin C. Plates were incubated o.n. to induce production of ColIb and phage lytic mode. Next, plates were overlaid with Ec^{MG1655} (grown in LB medium and mixed with LB soft agar). Following 12 hours incubation, the ColIb inhibition zone (halo) was measured. The detection limit (dotted) line denotes the average diameter of *S.* Tm colony. Subculture II of *S.* Tm strains: *S.* Tm^{MA6118} (red squares), *S.* Tm$^{\Delta G1\Delta G2}$ (blue squares), *S.* Tm$^{\Delta lysS\phi C}$ (black rhombs, red connecting lines) and *S.* Tm$^{\Delta G1\Delta G2\Delta lysS\phi C}$ (black rhombs, blue connecting lines) were grown in LB in a 96-well plate without (**B**) or supplemented with 0.5 µg/ml mitomycin C (**C**). OD$_{600}$ of the subculture II was measured each hour. Mean and SD of replicates are shown.

However, both *S.* Tm$^{\Delta lysS\phi C}$ and *S.* Tm$^{\Delta G1\Delta G2\Delta lysS\phi C}$ displayed impaired growth both in presence and absence of mitomycin C (**Figure 4.20B,C**). This could explain the decrease in ColIb-mediated killing of Ec^{MG1655} observed in the "halo" assay (**Figure 4.20A**). The attenuated growth kinetics of *S.* Tm$^{\Delta lysS\phi C}$ and *S.* Tm$^{\Delta G1\Delta G2\Delta lysS\phi C}$ could be due to a polar effect caused by the introduction of the cat-cassette or disruption of the lysis genes (in case they would be required for bacterial growth). To test this, the chloramphenicol-resistance cassette, flanked by FRT-sites (Datsenko & Wanner, 2000) was eliminated from the *S.* Tm$^{\Delta lysS\phi C}$

and *S*. Tm$^{\Delta G1\Delta G2\Delta lysS\phi C}$ using the Flp-recombinase. Additionally, SopEΦ lysis genes of *S*. Tm$^{\Delta G1\ \Delta G2}$ were substituted with a FRT-flanked kanamycin-resistance cassette. The newly generated strains grew at rates similar to the background strains, suggesting that the chloramphenicol resistance cassette was the reason for the impaired growth of *S*. Tm$^{\Delta lysS\phi C}$ and *S*. Tm$^{\Delta G1\Delta G2\Delta lysS\phi C}$. Interestingly, comparison between growth kinetics of a *S*. Tm strain and isogens carrying a chloramphenicol-resistance cassette in the flagella genes did not shown any difference (data not shown), suggesting that attenuated growth caused by introduction of chloramphenicol-resistance is related specifically to the SopEΦ lysis genes. However, this was not further investigated. *S*. Tm$^{\Delta lysS\phi}$, *S*. Tm$^{\Delta G1\Delta G2\Delta lysS\phi}$ and *S*. Tm$^{\Delta G1\Delta G2\Delta lysS\phi K}$ displayed ColIb-mediated kilning phenotypes comparable to the background strains (**Figure 4.21**).
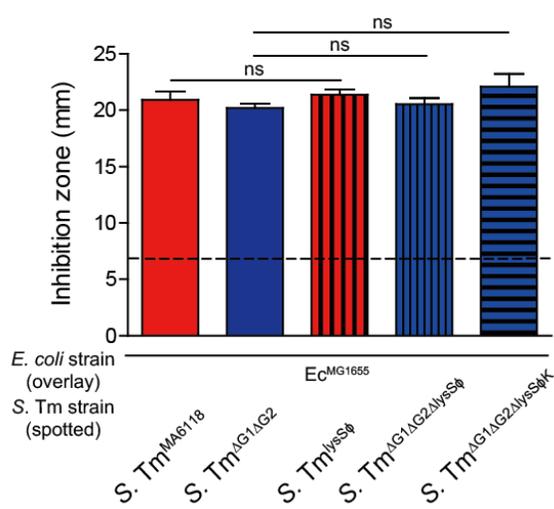
Figure 4.21. SopEΦ does not significantly contribute to the ColIb-dependent killing. *S*. Tm strains: *S*. Tm^{MA6118} (red), *S*. Tm$^{\Delta G1\Delta G2}$ (blue), *S*. Tm$^{\Delta lysS\phi}$ (red, vertical stripes), *S*. Tm$^{\Delta G1\Delta G2\Delta lysS\phi}$ (blue, vertical stripes) and *S*. Tm$^{\Delta G1\Delta G2\Delta lysS\phi K}$ (blue, horizontal stripes) were spotted on LB agar plate containing 0.5 µg/ml mitomycin C and incubated overnight. Next, plates were overlaid with Ec^{MG1655} (grown in LB medium and mixed with LB soft agar) and incubated for 12 h. Further, ColIb inhibition zone (halo) was measured. The detection limit (dotted) line indicates the average diameter of *S*. Tm colony.
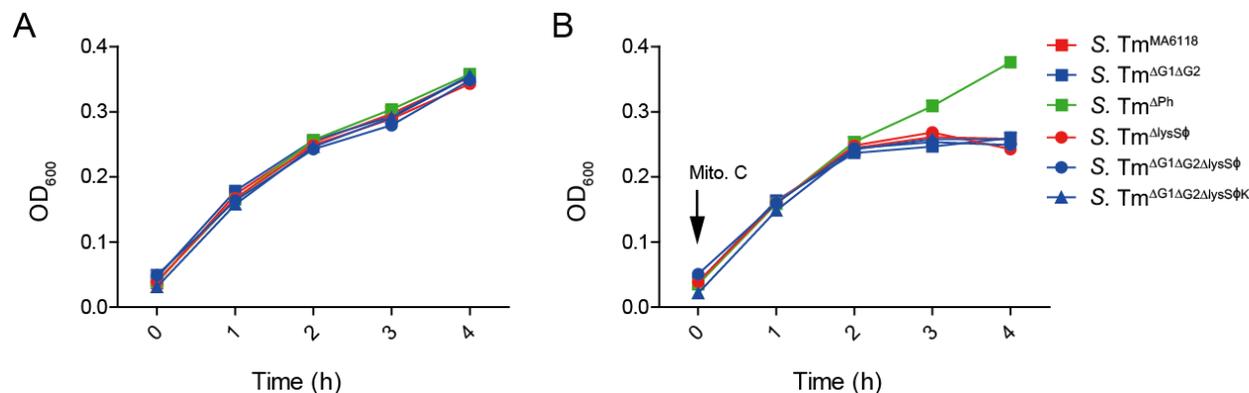
Figure 4.22. SopEΦ does not siginificantly contribute to the lysis. Subcultures II of *S.* Tm strains: *S.* Tm^{MA6118} (red squares), *S.* Tm$^{\Delta G1\Delta G2}$ (blue squares), *S.* Tm$^{\Delta lysS\phi}$ (red circles), *S.* Tm$^{\Delta G1\Delta G2\Delta lysS\phi}$ (blue circles), *S.* Tm$^{\Delta G1\Delta G2\Delta lysS\phi K}$ (blue triangle) and *S.* Tm$^{\Delta Ph}$ (green squares) were grown for 4 h in a 96-well plate without (**A**) or supplemented with 0.5 µg/ml mitomycin C (**B**). OD$_{600}$ of the subculture II was measured each hour. Bars shown mean and StD. OD$_{600}$ values (4 h) of the mitomycin C-induced cultures are significantly different (***$p<0.0001$) (ANOVA test). Statistical analysis by unpaired Student's *t*-test for mitomycin C-supplemented cultures: *S.* Tm^{MA6118} and *S.* Tm$^{\Delta G1\Delta G2}$ ($p>0.05$), *S.* Tm^{MA6118} and *S.* Tm$^{\Delta Ph}$ (***$p<0.0001$), *S.* Tm^{MA6118} and *S.* Tm$^{\Delta lysS\phi}$ (**$p<0.006$), *S.* Tm$^{\Delta G1\Delta G2}$ and *S.* Tm$^{\Delta G1\Delta G2\Delta lysS\phi}$ ($p>0.05$), *S.* Tm$^{\Delta G1\Delta G2}$ and *S.* Tm$^{\Delta G1\Delta G2\Delta lysS\phi K}$ ($p>0.05$).

Upon induction with mitomycin C, strains lacking SopEΦ lysis genes lysed to the same degree as *S.* Tm^{MA6118} and *S.* Tm$^{\Delta G1\Delta G2}$ (**Figure 4.22B**). Furthermore, upon induction similar amounts of ColIb were produced and released by *S.* Tm$^{\Delta lysS\phi}$, *S.* Tm$^{\Delta G1\Delta G2\Delta lysS\phi}$ and the background strains as detected by immunoblot (**Figure 4.23**). This suggests that SopEΦ lysis genes do not contribute to ColIb release.

Further, a prophage-deficient *S.* Tm strain (*S.* Tm^{A36}) and its SopEΦ lysogen (*S.* Tm^{M4}) were used to compare ColIb-release. Both strains were transformed with the p2^{cm} by conjugation. No significant difference in ColIb-dependent "halo" size was detected (Figure 4.24). In conclusion, no evidence for the contribution of SopEΦ-mediate lysis to the release of ColIb was found.
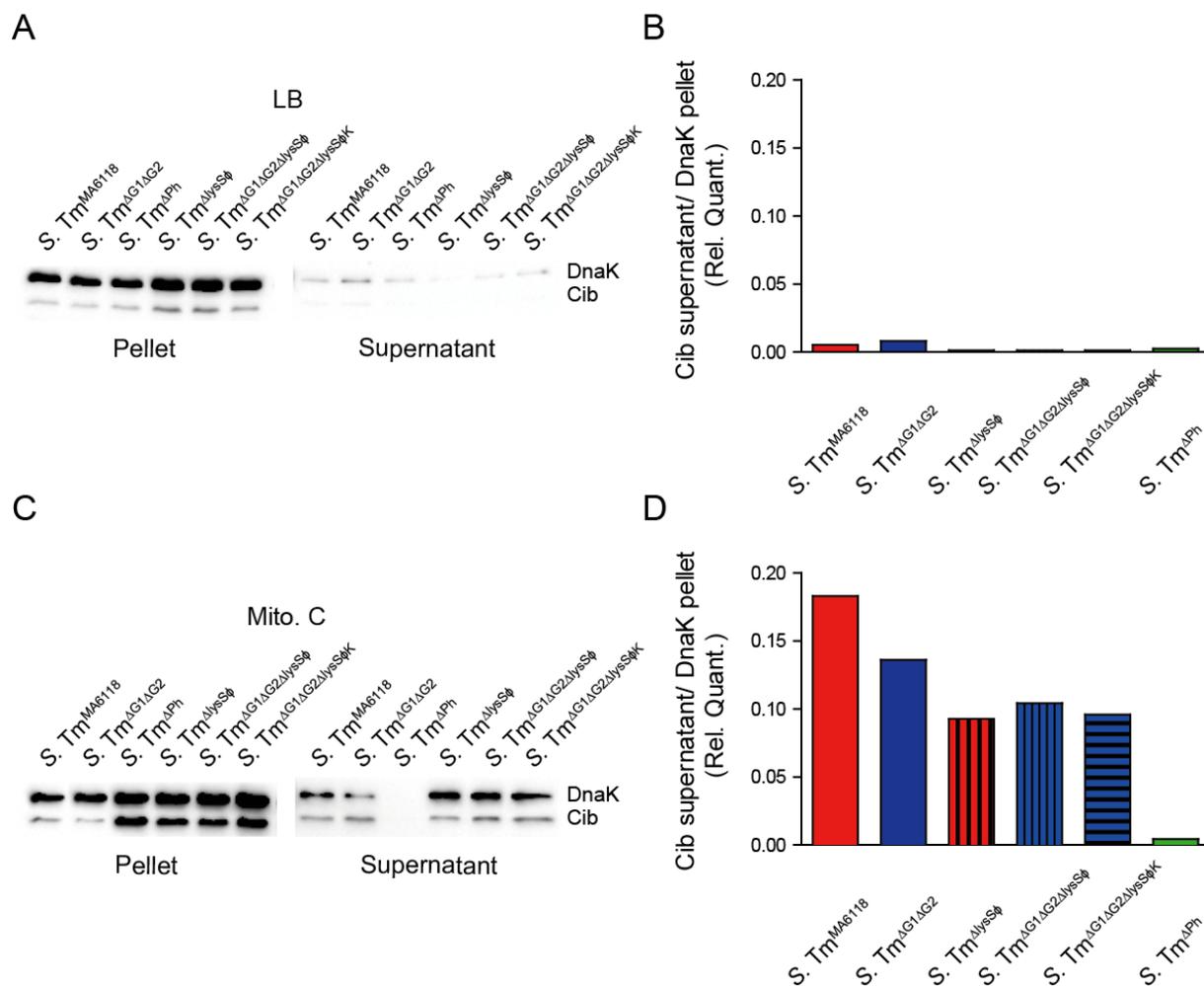
Figure 4.23. Release of ColIb is not affected by the lytic activity of SopEΦ prophage. Subculture II of *S*. Tm strains: *S*. Tm^{MA6118}, *S*. Tm^{ΔG1ΔG}, *S*. Tm^{ΔlysSφ}, *S*. Tm^{ΔG1ΔG2ΔlysSφ}, *S*. Tm^{ΔG1ΔG2ΔlysSφK} and *S*. Tm^{ΔPh} were grown for 4 h in a 96-well plate without (**A**) or with addition of mitomycin C (**C**) (**Section 3.2.1.3**). Next, bacteria were harvested from 100 μl of subculture II and ColIb was detected in the cell lysate and culture supernatant by immunoblot using affinity-purified rabbit-α-ColIb-antiserum. *S*. Tm DnaK was detected as loading control. The relative quantity of ColIb and DnaK was determined by densitometry using Image Lab software (Bio-Rad). The ratio of relative quantity of ColIb (found in the supernatant) divided by the relative quantity of DnaK (found in the bacterial lysate) for non induced (**B**) and mitomycin C-induced (**D**) culture is shown.
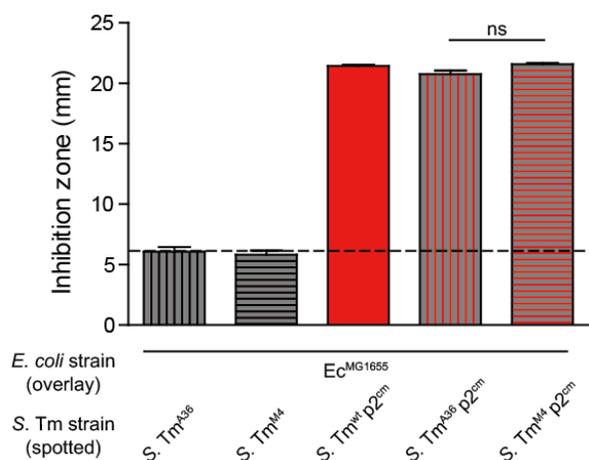
Figure 4.24. ColIb-dependent killing is not influenced by SopEΦ prophage. *S.* Tm strains: *S.* Tm^{A36} (vertical black stripes), *S.* Tm^{M4} (horizontal black stripes), *S.* Tm^{wt} p2^{cm} (red), *S.* Tm^{A36} p2^{cm} (vertical red stripes), *S.* Tm^{M4} p2^{cm} (horizontal red stripes) were spotted on LB agar plate containing 0.5 μg/ml mitomycin C and incubated overnight. Next, plates were overlaid with Ec^{MG1655} (grown in LB medium and mixed with LB soft agar). Following incubation for 12 h, ColIb inhibition zone (halo) was measured. The detection limit (dotted) line denotes the average diameter of *S.* Tm colony.

4.2.3 Deletion of ST64B lysis genes leads to decreased ColIb-release in *S.* Tm^{ΔG1ΔG2} background strain

Decreased cell lysis and impaired ColIb release by *S.* Tm^{ΔG1ΔG2ΔST} suggested that ST64B prophage might be involved in ColIb-release. To investigate this further, three lysis-related genes of the ST64B prophage encoding, a hypothetical holin, lysozyme and lysis related protease were replaced with a kanamycin resistance cassette in strains *S.* Tm^{MA6118} and *S.* Tm^{ΔG1ΔG2} (**Figure 2.1C,D**; **Table 31**). Indeed, deletion of the putative ST64B putative lysis genes led to diminished ColIb-mediated killing of the susceptible *E. coli* strain (**Figure 4.25**).
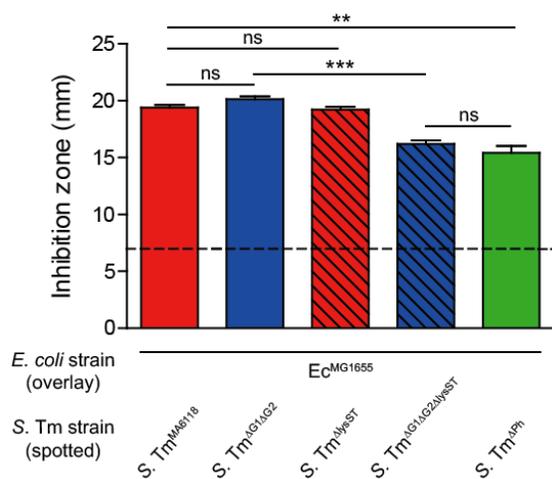
Figure 4.25. Deletion of ST64B prophage lysis genes leads to decrease in ColIb-dependent killing *S.* Tm strains: *S.* Tm^{MA6118} (red), *S.* Tm^{ΔG1ΔG2} (blue), *S.* Tm^{ΔlysST} (red striped), *S.* Tm^{ΔG1ΔG2ΔlysST} (blue striped) and *S.* Tm^{ΔPh} (green) were spotted on LB agar plate supplemented with 0.5 μg/ml mitomycin C. ColIb producers were grown o.n. and then overlaid with Ec^{MG1655} (grown in LB medium and mixed with LB soft agar). Following incubation for 12 h, the ColIb inhibition zone (halo) was measured. The detection limit (dotted) line indicates the average diameter of *S.* Tm colony.

81

Interestingly, this effect was only significant for the Gifsy-1 and Gifsy-2 deficient *S.* Tm strain (*S.* Tm$^{\Delta G1\Delta G2\Delta lysST}$) and not for the *S.* Tm$^{\Delta lysST}$ (**Figure 4.25**). However, in the growth assay upon induction with mitomycin C, *S.* Tm$^{\Delta lysST}$ lysis was significantly reduced compared to the *S.* Tm^{MA6118} (**Figure 4.26B**). In contrast, *S.* Tm$^{\Delta G1\Delta G2\ \Delta lysST}$ and *S.* Tm$^{\Delta Ph}$ strains was not affected by addition of mitomycin C (**Figure 4.26B**).

Figure 4.26. Cell lysis is impaired in strains with deleted lysis genes of ST64B prophage. Subculture II of *S.* Tm strains: *S.* Tm^{MA6118} (red square), *S.* Tm$^{\Delta G1\Delta G2}$ (blue square), *S.* Tm$^{\Delta lysST}$ (red rhomb), *S.* Tm$^{\Delta G1\Delta G2\Delta lysST}$ (blue rhomb) and *S.* Tm$^{\Delta Ph}$ (green square) were grown for 4 h in a 96-well plate without (**A**) or supplemented with 0.5 µg/ml mitomycin C (**B**). OD$_{600}$ of the subculture II was measured each hour. Bars shown mean and StD. OD$_{600}$ values (4 h) of the mitomycin C-induced cultures are significantly different (***$p<0.0001$) and no significant difference was found for the non induced cultures ($p>0.05$) (ANOVA test). Statistical analysis by unpaired Student's *t*-test for non induced cultures: *S.* Tm^{MA6118} and *S.* Tm$^{\Delta G1\Delta G2}$ ($p>0.05$), *S.* Tm^{MA6118} and *S.* Tm$^{\Delta Ph}$ (**$p<0.01$), *S.* Tm^{MA6118} and *S.* Tm$^{\Delta lysST}$ ($p>0.05$), *S.* Tm$^{\Delta G1\Delta G2}$ and *S.* Tm$^{\Delta G1\Delta G2\Delta lysST}$ (*$p<0.05$). Statistical analysis by unpaired Student's *t*-test for mitomycin C-supplemented cultures: *S.* Tm^{MA6118} and *S.* Tm$^{\Delta G1\Delta G2}$ ($p>0.05$), *S.* Tm^{MA6118} and *S.* Tm$^{\Delta Ph}$ (**$p<0.003$), *S.* Tm^{MA6118} and *S.* Tm$^{\Delta lysST}$ (*$p<0.05$), *S.* Tm$^{\Delta G1\Delta G2}$ and *S.* Tm$^{\Delta G1\Delta G2\Delta lysST}$ (***$p<0.0001$).

No ColIb release was detected for *S.* Tm$^{\Delta G1\Delta G2\Delta lysST}$ and *S.* Tm$^{\Delta Ph}$ strains (**Figure 4.27B**). Finally, the impaired colicin release was confirmed by the reduced or fully lost bactericidal activity displayed by the extracellular fractions of *S.* Tm$^{\Delta lysST}$ or *S.* Tm$^{\Delta G1\Delta G2\Delta lysST}$ mitomycin C supplemented cultures (**Figure 4.27B**). Together, these results identified the ST64B temperate phage as a key-player in the process of ColIb release in *S.* Tm SL1344. Remarkably, the ST64B impact was further augmented by the Gifsy-phages.
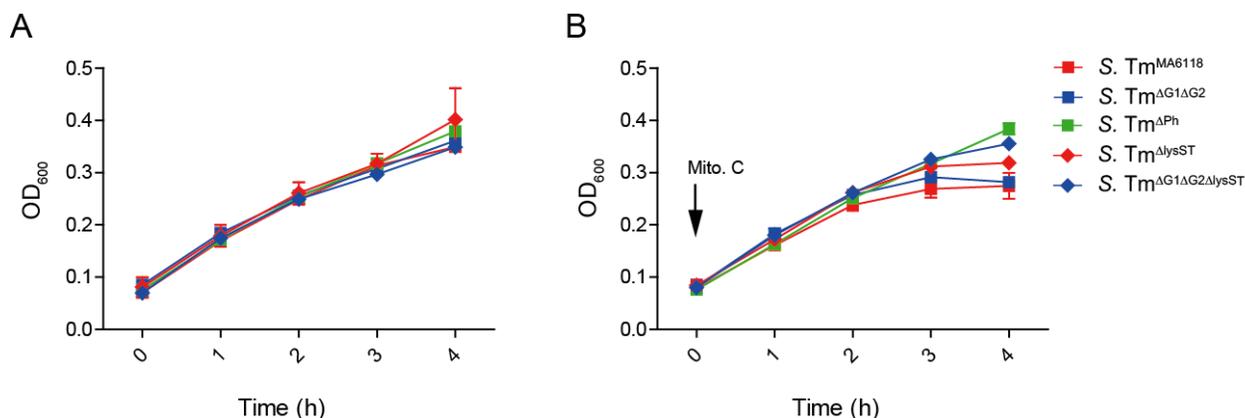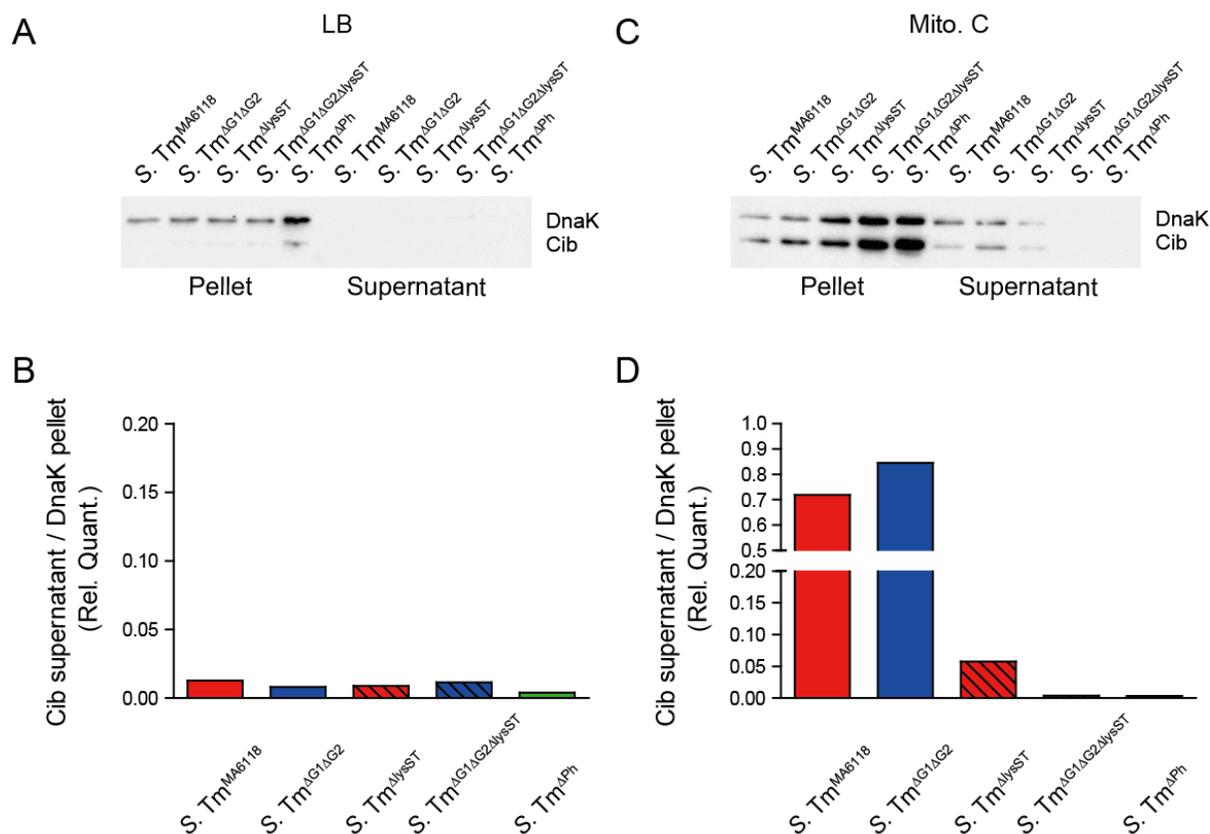
Figure 4.27. Deletion of ST64B prophage lysis genes leads to decrease in extracellular ColIb. Subcultures II of *S.* Tm strains: *S.* Tm^{MA6118} (red), *S.* Tm$^{\Delta G1\Delta G2}$ (blue), *S.* Tm$^{\Delta lysST}$ (red striped), *S.* Tm$^{\Delta G1\Delta G2\Delta lysST}$ (blue striped) and *S.* Tm$^{\Delta Ph}$ (green) were grown for 4 h in a 96-well plate without (**A**) or with addition of mitomycin C (**C**) (**Section 3.2.1.3**). Next, bacteria were harvested from 100 µl of subculture II and ColIb was detected in the cell lysate and culture supernatant by immunoblot using affinity-purified rabbit-α-ColIb-antiserum. *S.* Tm DnaK was detected as loading control. The relative quantity of ColIb and DnaK was determined by densitometry using Image Lab software (Bio-Rad). The ratio of relative quantity of ColIb (found in the supernatant) divided by the relative quantity of DnaK (found in the bacterial lysate) for non induced (**B**) and mitomycin C-induced (**D**) culture is shown.
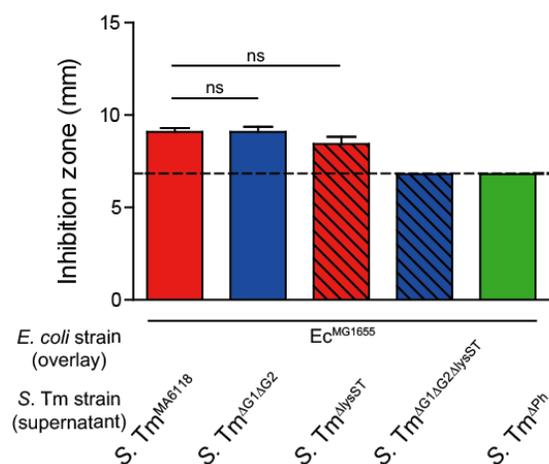
Figure 4.28. Bactericidal activity of extracellular ColIb is reduced in *S*. Tm$^{\Delta G1\Delta G2\Delta lysST}$. Mitomycin C supplemented (0.5 µg/ml) subcultures II of *S*. Tm strains: *S*. Tm^{MA6118} (red), *S*. Tm$^{\Delta G1\Delta G2}$ (blue), *S*. Tm$^{\Delta lysST}$ (red striped), *S*. Tm$^{\Delta G1\Delta G2\Delta lysST}$ (blue striped) and *S*. Tm$^{\Delta Ph}$ (green) were grown in a 96-well plate for 4 h (**Section 3.2.1.3**). Next, bacteria were harvested and bactericidal activity of extracellular ColIb was tested (**Section 3.2.3.3**). Paper disks soaked with sterile spent culture supernatant were set on LB agar plates overlaid with Ec^{MG1655} (grown in LB medium and mixed with soft agar). Following 12 h incubation, ColIb inhibition zone (halo) was measured. The detection limit (dotted) line indicates the size of the paper disks.

4.2.4 ColIb release by *S*. Tm$^{\Delta G1\Delta G2\Delta lysST}$ is not enhanced by SopEΦ-mediated lysis.

In order to test whether deletion of SopEΦ lysis genes would result in further reduction of ColIb release in the background strain *S*. Tm$^{\Delta G1\Delta G2\Delta lysST}$, the ΔlysST allele (lysis genes replaced with kanamycin resistance cassette) was introduced into *S*. Tm$^{\Delta G1\Delta G2\Delta lysS\phi}$ via P22-transduction. Both *S*. Tm$^{\Delta G1\Delta G2\Delta lysS\phi\Delta lysST}$ and *S*. Tm$^{\Delta G1\Delta G2\Delta lysST}$ exhibited similar ColIb-dependent halo sizes with the Ec^{MG1655} strain (**Figure 4.29**).
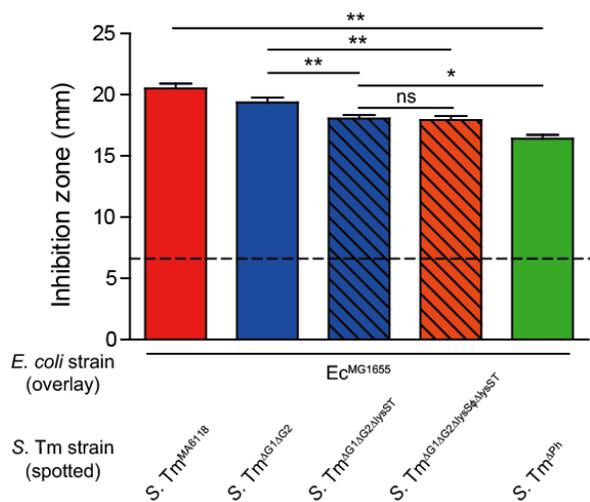
Figure 4.29. Deletion of SopEΦ lysis genes has no effect on ColIb-dependent killing by *S*. Tm$^{\Delta G1\Delta G2\Delta lysS\phi\Delta lysST}$. *S*. Tm strains: *S*. Tm^{MA6118} (red), *S*. Tm$^{\Delta G1\Delta G2}$ (blue), *S*. Tm$^{\Delta G1\Delta G2\Delta lysST}$ (blue striped), *S*. Tm$^{\Delta G1\Delta G2\Delta lysS\phi\Delta lysST}$ (orange striped) and *S*. Tm$^{\Delta Ph}$ (green) were spotted on LB agar plate supplemented with 0.5 µg/ml mitomycin C. ColIb producers were grown o.n. and thereon overlaid with Ec^{MG1655} (grown in LB medium and mixed with LB soft agar). Following incubation for 12 h, the ColIb inhibition zone (halo) was measured. The detection limit (dotted) line indicates the average diameter of *S*. Tm colony.

Comparison of the growth dynamics of these strains in liquid cultures with or without mitomycin C showed that elimination of SopEΦ lysis genes did not further reduce lysis of *S.* Tm$^{\Delta G1\Delta G2\Delta lysST}$ (**Figure 4.30B**). Furthermore, no ColIb release was detectable for both, *S.* Tm$^{\Delta G1\Delta G2\Delta lysST}$ and *S.* Tm$^{\Delta G1\Delta G2\Delta lysS\phi\Delta lysST}$, as demonstrated by immunoblot (**Figure 4.31**). Interestingly, weak extracellular bactericidal activity was observed for *S.* Tm$^{\Delta G1\Delta G2\Delta lysST}$, but not for *S.* Tm$^{\Delta G1\Delta G2\Delta lysS\phi\Delta lysST}$ (**Figure 4.32**).
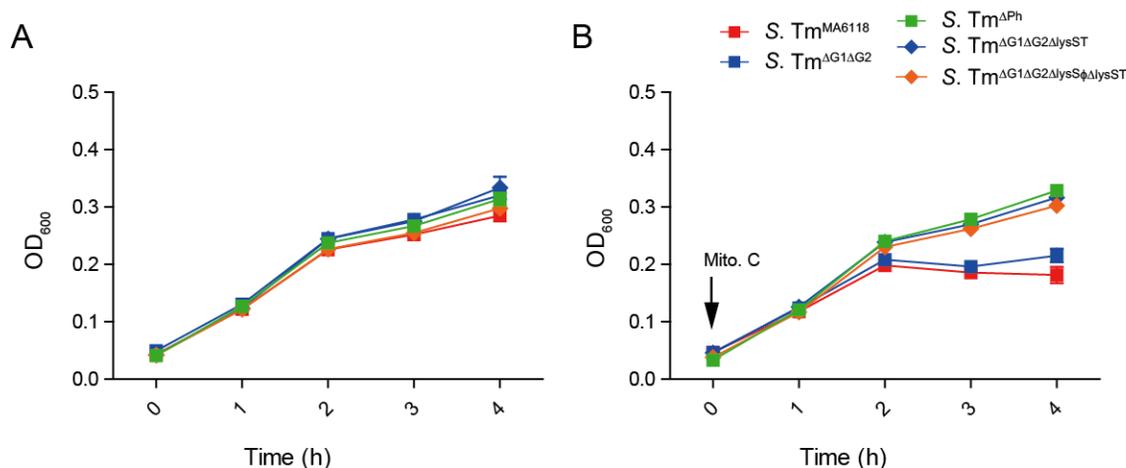
Figure 4.30. Deletion of SopEΦ lysis genes has no effect on *S.* Tm$^{\Delta G1\Delta G2\ \Delta lysS\phi\Delta lysST}$ lysis. Subculture II of *S.* Tm strains: *S.* Tm^{MA6118} (red squares), *S.* Tm$^{\Delta G1\Delta G2}$ (blue squares), *S.* Tm$^{\Delta G1\Delta G2\Delta lysST}$ (blue rhombs), *S.* Tm$^{\Delta G1\Delta G2\Delta lysS\phi\Delta lysST}$ (orange rhombs) and *S.* Tm$^{\Delta Ph}$ (green squares) were grown for 4 h in a 96-well plate without (**A**) or with addition of mitomycin C (0.5 µg/ml) (**B**). OD$_{600}$ of the subculture II was measured each hour. Bars shown mean and StD. OD$_{600}$ values (4 h) of the mitomycin C-induced (***p<0.0001) and non induced (**p<0.002) culture are significantly different (ANOVA test). Statistical analysis by unpaired Student's *t*-test for non induced cultures: *S.* Tm^{MA6118} and *S.* Tm$^{\Delta G1\Delta G2}$ (**p<0.002), *S.* Tm^{MA6118} and *S.* Tm$^{\Delta Ph}$ (*p<0.05), *S.* Tm$^{\Delta G1\Delta G2}$ and *S.* Tm$^{\Delta G1\Delta G2\Delta lysST}$ (*p*>0.05), *S.* Tm$^{\Delta G1\Delta G2}$ and *S.* Tm$^{\Delta G1\Delta G2\Delta lysS\phi\Delta lysST}$ (**p<0.007), *S.* Tm$^{\Delta G1\Delta G2\Delta lysST}$ and *S.* Tm$^{\Delta G1\Delta G2\Delta lysS\phi\Delta lysST}$ (*p<0.05). Statistical analysis by unpaired Student's *t*-test for mitomycin C-supplemented cultures: *S.* Tm^{MA6118} and *S.* Tm$^{\Delta G1\Delta G2}$ (*p<0.05), *S.* Tm^{MA6118} and *S.* Tm$^{\Delta Ph}$ (***p<0.0001), *S.* Tm$^{\Delta G1\Delta G2}$ and *S.* Tm$^{\Delta G1\Delta G2\Delta lysST}$ (***p<0.0001), *S.* Tm$^{\Delta G1\Delta G2}$ and *S.* Tm$^{\Delta G1\Delta G2\Delta lysS\phi\Delta lysST}$ (***p<0.0001), *S.* Tm$^{\Delta G1\Delta G2\Delta lysST}$ and *S.* Tm$^{\Delta G1\Delta G2\Delta lysS\phi\Delta lysST}$ (*p<0.05).

In conclusion, deletion of the SopEΦ lysis genes did not influence the ColIb release of a *S.* Tm mutant lacking Gifsy-1, Gifsy-2 and the lysis genes of ST64B prophage.

In combination with the results that transduction of SopEΦ into a prophage-deficient *S.* Tm strain did not increase its ability to release ColIb, these data suggest, that SopEΦ-mediated lysis does not contribute to ColIb release in *S.* Tm SL1344.
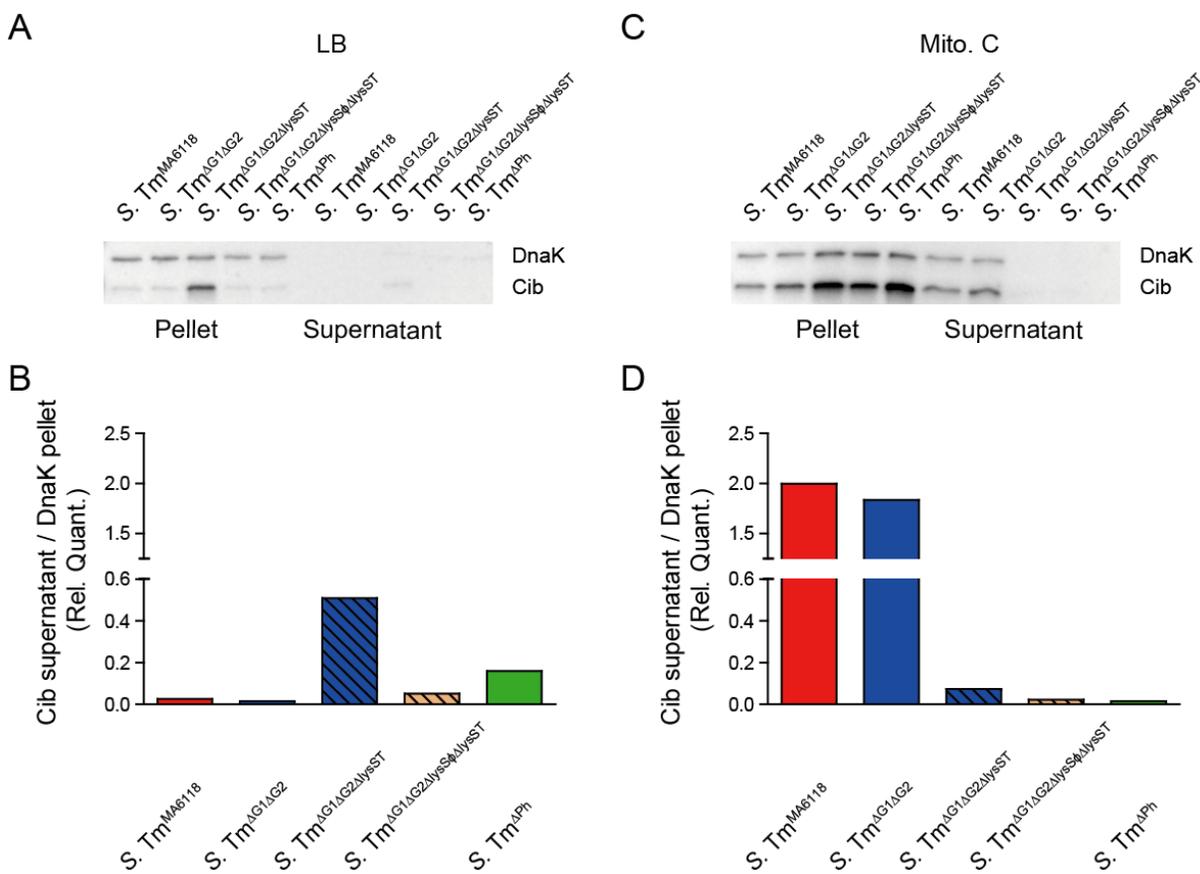
Figure 4.31. ColIb release by *S*. Tm^{ΔG1ΔG2ΔlysST} is not further affected by the deletion of SopEΦ lysis genes. Subcultures II of *S*. Tm strains: *S*. Tm^{MA6118} (red), *S*. Tm^{ΔG1ΔG2} (blue), *S*. Tm^{ΔG1ΔG2ΔlysST} (blue striped), *S*. Tm^{ΔG1ΔG2ΔlysSφΔlysST} (orange striped) and *S*. Tm^{ΔPh} (green) were grown for 4 h in a 96-well plate without (**A**) or with addition of mitomycin C (**C**) (**Section 3.2.1.3**). Next, bacteria were harvested from 100 µl of subculture II and ColIb was detected in the cell lysate and culture supernatant by immunoblot using affinity-purified rabbit-α-ColIb-antiserum. *S*. Tm DnaK was detected as loading control. The relative quantity of ColIb and DnaK was determined by densitometry using Image Lab software (Bio-Rad). The ratio of relative quantity of ColIb (found in the supernatant) divided by the relative quantity of DnaK (found in the bacterial lysate) for non induced (**B**) and mitomycin C-induced (**D**) culture is shown.
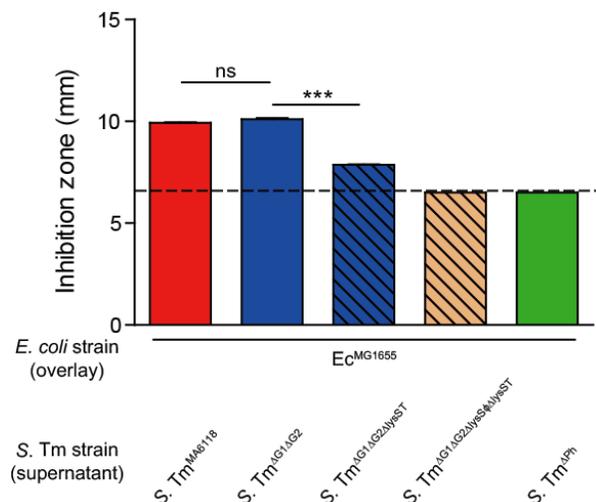
Figure 4.32. No bactericidal activity of ColIb was detected for *S*. Tm$^{\Delta G1\Delta G2\Delta lysS\phi\Delta lysST}$. Subcultures II of *S*. Tm strains: *S*. Tm^{MA6118} (red), *S*. Tm$^{\Delta G1\Delta G2}$ (blue), *S*. Tm$^{\Delta G1\Delta G2\Delta lysST}$ (blue striped), *S*. Tm$^{\Delta G1\Delta G2\Delta lysS\phi\Delta lysST}$ (orange striped) and *S*. Tm$^{\Delta Ph}$ (green) were grown in a 96-well plate for 4 h (**Section 3.2.1.3**). Next, bacteria were harvested and bactericidal activity of extracellular ColIb was tested (**Section 3.2.3.3**). Paper disks soaked with sterile spent culture supernatant were set on LB agar plates overlaid with Ec^{MG1655} (grown in LB medium and mixed with soft agar). Following 12 h incubation, ColIb inhibition zone (halo) was measured. The detection limit (dotted line) indicates the size of the paper disks.

4.2.5 ColIb-dependent competition of *S*. Tm against Ec^{MG1655} *in vitro* is strongly enhanced by prophage-mediated lysis

The presence of prophages and their encoded lysis genes strongly affects ColIb-release by *S*. Tm *in vitro*. Next, it was determined whether prophages may also increase *S*. Tm fitness in direct competition against a colicin-sensitive opponent. Of note, it was found that pRSF1010-SL1344 plasmid, which confers resistance to streptomycin, was present in *S*. Tm^{MA6118} but not in its phage-cured isogens *S*. Tm$^{\Delta G1\Delta G2}$, *S*. Tm$^{\Delta G1\Delta G2\Delta ST}$ and *S*. Tm$^{\Delta Ph}$. Therefore, pRSF1010-SL1344 was isolated from *S*. Tm^{MA6118} and transformed in *S*. Tm$^{\Delta Ph}$ (*S*. Tm$^{\Delta Ph\ smR}$) and *S*. Tm$^{\Delta G1\Delta G2\Delta lysST}$ (*S*. Tm$^{\Delta G1\Delta G2\Delta lysST\ smR}$) strains. The ColIb-sensitive, Ec$^{MG1655\ amp}$ was co-cultured with *S*. Tm^{MA6118} and the respective mutants in LB or *cib*-inducing conditions (100 µM DTPA and (or) 0.5 µg/ml mitomycin C) (**Figure 4.33**). The strain lacking all four prophages (*S*. Tm$^{\Delta Ph\ smR}$) and a Gifsy-1, Gifsy-2 double mutant carrying a mutation in the ST64B lysis genes (*S*. Tm$^{\Delta G1\Delta G2\Delta lysST\ smR}$) were employed. To better assess the competitive advantage of *S*. Tm over Ec$^{MG1655\ amp}$, the CI (ratio of *S*. Tm / *E. coli*) was determined under all conditions (**Figure 4.34**).
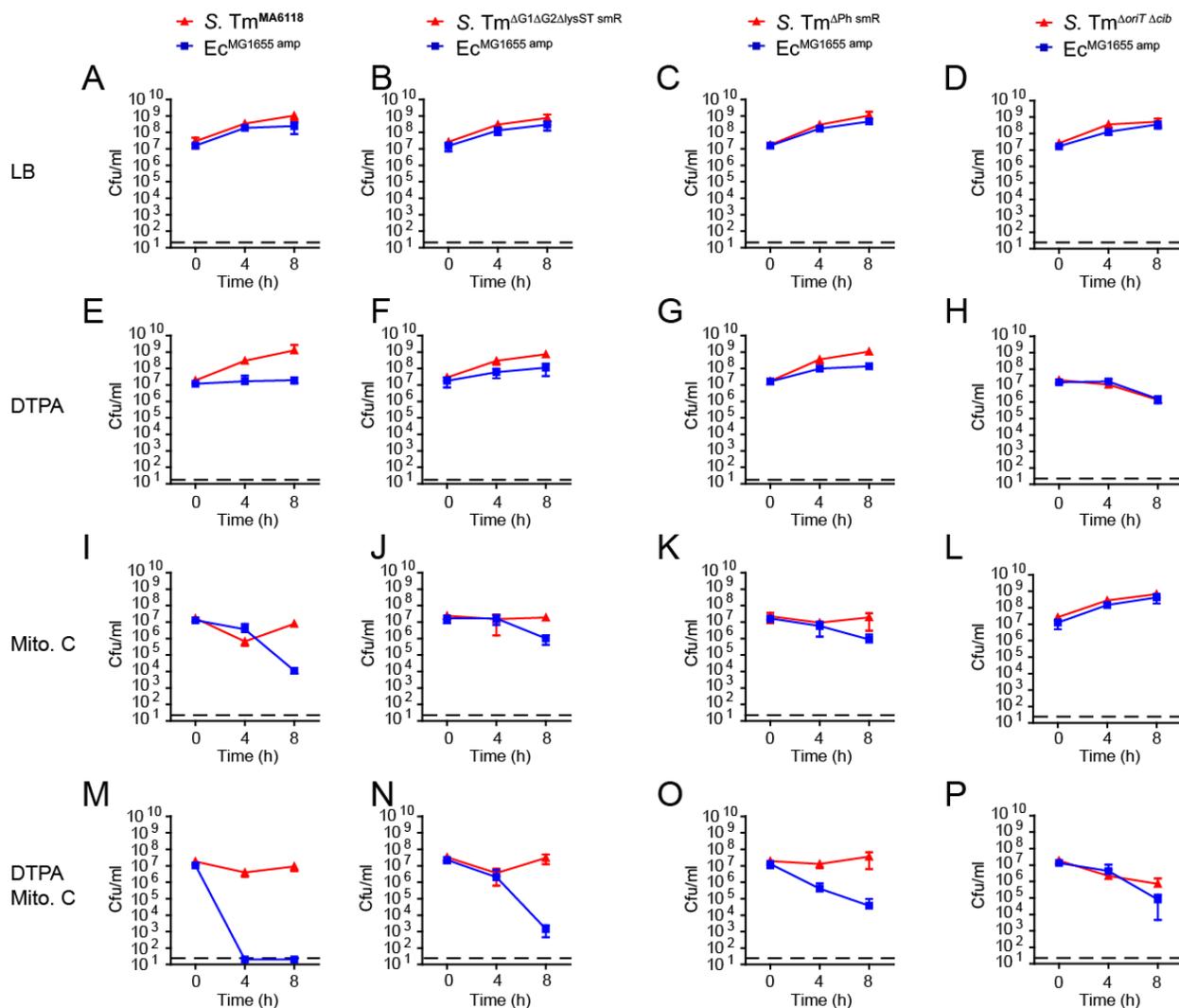
Figure 4.33. Temperate phages enhance ColIb-dependent competitive advantage of *S*. Tm. *S*. Tm (red triangles) and *E. coli* strains (blue squares) were grown separately for 12 h in LB medium and thereafter diluted and normalized to an OD_{600} of 0.025 in 3 ml fresh LB (subculture I). After 2 h growth the subcultures I were diluted and normalized to an OD_{600} of 0.4 in LB medium with or without supplements (100 µM DTPA, 0.5 µg/ml mitomycin C, or both) (Subculture II). Further, the subculture II of *S*. Tm[MA6118] and Ec[MG1655 amp] (**A,E,I,M**), *S*. Tm[ΔG1ΔG2ΔlysST smR] and Ec[MG1655 amp] (**B,F,J,N**), *S*. Tm[ΔPh smR] and Ec[MG1655 amp] (**C,G,K,O**), *S*. Tm[ΔoriT Δcib] and Ec[MG1655 amp] (**D,H,L,P**) were mixed (1:1) to a final volume of 200 µl/well and grown in a 96-well plate for 6 hours. The cfu/ml of both strains were determined at 0 h, 3 h and 6 h after the addition of supplements by plating on selective agar to distinguish Ec[MG1655 amp] and *S*. Tm strains. The detection limit (20 cfu/ml) is indicated with a line. Bars shown mean and StD.

In absence of supplements, all combinations of competing Ec[MG1655 amp] and *S*. Tm strains grew to similar densities after 6 h (mean titer of *S*. Tm[MA6118]: 1.05×10^9 and Ec[MG1655 amp]: 2.4×10^8; *S*. Tm[ΔG1ΔG2ΔlysST smR]: 7.53×10^8 and Ec[MG1655 amp]: 2.93×10^8; *S*. Tm[ΔPh smR] 1.05×10^9 and Ec[MG1655 amp] 4.6×10^8) (**Figure 4.33A,B,C**).
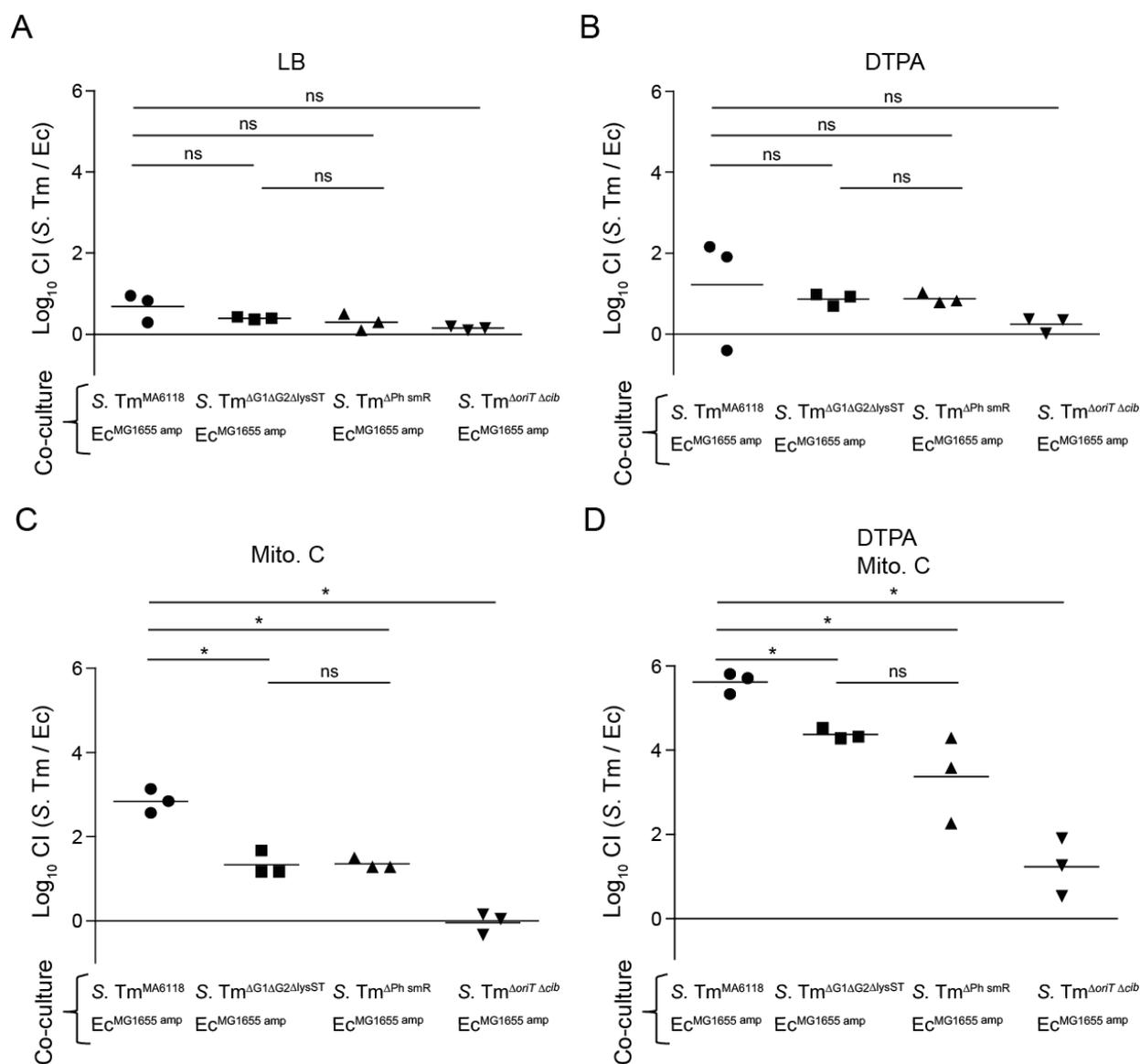

Figure 4.34. Competitive index of the co-culture assays. CI (ratio of *S*. Tm / *E. coli*) were determined at 6 h growth of the co-cultures (Figure 4.33) of; *S*. Tm[MA6118], *S*. Tm[ΔG1ΔG2ΔlysST smR], *S*. Tm[ΔPh smR] or *S*. Tm[ΔoriT Δcib] with Ec[MG1655 amp] in absence of inducers (**A**), supplemented with 100 μM DTPA (**B**), 0.5 μg/ml mitomycin C (**C**), or both (**D**). Values are Log$_{10}$ transformed and the geometric mean is shown with a line. Statistical analysis by unpaired Student's *t*-test was done: *$p<0.05$.

As shown before (Nedialkova *et al.*, 2014) $Ec^{MG1655\ amp}$ does not exhibit any colonization disadvantage against *S.* Tm (**Figure 4.33D,H,L,P**). In contrast to *S.* $Tm^{\Delta oriT\ \Delta cib}$, *S.* Tm^{MA6118} outcompeted $Ec^{MG1655\ amp}$ by 6-fold, while prophage-deficient strain *S.* $Tm^{\Delta Ph}$ exhibited only 2-fold higher numbers compered to $Ec^{MG1655\ amp}$ (**Figure 4.34A**). Fe(III) depletion by DTPA, which induces *cib* expression, lead to 7.4 x 10-fold higher cfu of *S.* Tm^{MA6118} compared to $Ec^{MG1655\ amp}$, but almost 10 times lower values (7.9-fold) in case of prophage-deficient *S.* $Tm^{\Delta Ph\ smR}$ (**Figure 4.34B**). Addition of mitomycin C and concomitant induction of both, *cib* expression and prophage activation (**Figure 4.33I,L**) led to a 8 x 10^2-fold higher cfu of *S.* Tm^{MA6118} (**Figure 4.34C**). Under the same conditions, *S.* $Tm^{\Delta Ph\ smR}$ outcompeted $Ec^{MG1655\ amp}$ only by 2.3 x10-fold. Furthermore, addition of both supplements (**Figure 4.33M,O**) lead to overgrowth of *S.* Tm^{MA6118} over $Ec^{MG1655\ amp}$ by 4.5 x 10^5-fold. In contrast, $Ec^{MG1655\ amp}$ was outcompeted by *S.* $Tm^{\Delta Ph\ smR}$ only by 7.8 x 10^3-fold (**Figure 4.34D**). Similar results were observed for *S.* $Tm^{\Delta G1\Delta G2\Delta lysST\ smR}$ as *S.* $Tm^{\Delta Ph\ smR}$ in competition with $Ec^{MG1655\ amp}$ (**Figure 4.33B,F,K,N**).

In summary, these results argued that functional lytic activity of temperate phages strongly facilitates the ColIb-dependent competition against a colicin-sensitive competitor, in particular upon activation of SOS response.

4.2.6 Phage transduction boosts release of ColIb by a prophage-deficient *E. coli* strain.

To further support the concept of prophage-enhanced release of ColIb, it was investigated whether transduction of a colicin producing strain with a functional prophage would lead to enhancement of colicin release. To this end, the shiga-like toxin–producing lambdoid prophage 933W isolated from an enterohemorrhagic *E. coli* strain (O'Brien *et al.*, 1984) was used. The *stx2A* and *stx2B* genes (encoding the Shiga toxin 2 subunits) are located downstream of the phage late promoters (*pR'*) followed by the lysis genes a S (holin)-like and a R (endolysin)-like gene (Neely & Friedman, 1998). Hence, transition of the prophage to the lytic mode results in expression of *stx(2)AB* genes along with the lysis genes (Wagner *et al.*, 2001). Reporters of p(R') were constructed by lysogenisation of Ec^{MG1655} with a modified 933W prophage containing a firefly-luciferase gene replacing either the gene s*tx2A* alone or the s*tx2A* plus the downstream located S- and R-like genes. Next, the ColIb plasmid $p2^{cm}$ was introduced into Ec^{MG1655} or its lysogenic variants with intact (Ec^{Stx}) or deleted phage lysis genes ($Ec^{Stx\Delta SR}$). ColIb-mediated killing of Ec^{MG1655} was only observed for Ec^{Stx} $p2^{cm}$ but not for $Ec^{Stx\Delta SR}$ $p2^{cm}$ and Ec^{MG1655} $p2^{cm}$ (**Figure 4.35**).
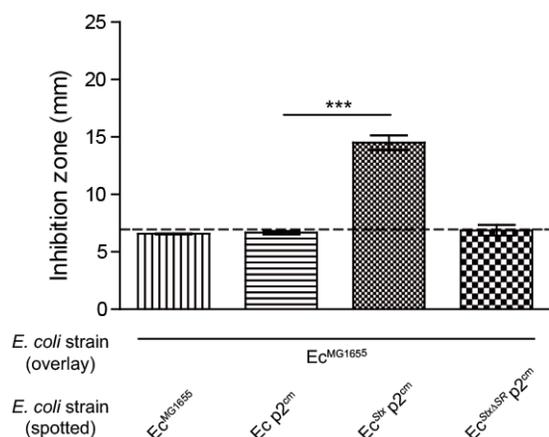
Figure 4.35. Prophage-mediated cell lysis is required for ColIb-dependent killing. *E. coli* strains: Ec^{MG1655} (vertical stripes), Ec^{P2} (white), Ec^{Stx} p2^{cm} (checkered, small) and $Ec^{Stx\Delta SR}$ p2^{cm} (checkered, large) were spotted on LB agar plate supplemented with a prophage and ColIb expression activator mitomycin C (0.5 µg/ml). Plates were incubated o.n. and thereon overlaid with Ec^{MG1655} (grown in LB medium and mixed with LB soft agar). After 12 hours incubation, ColIb inhibition zone (halo) was measured. The detection limit (dotted) line indicates the average diameter of *E. coli* colony.
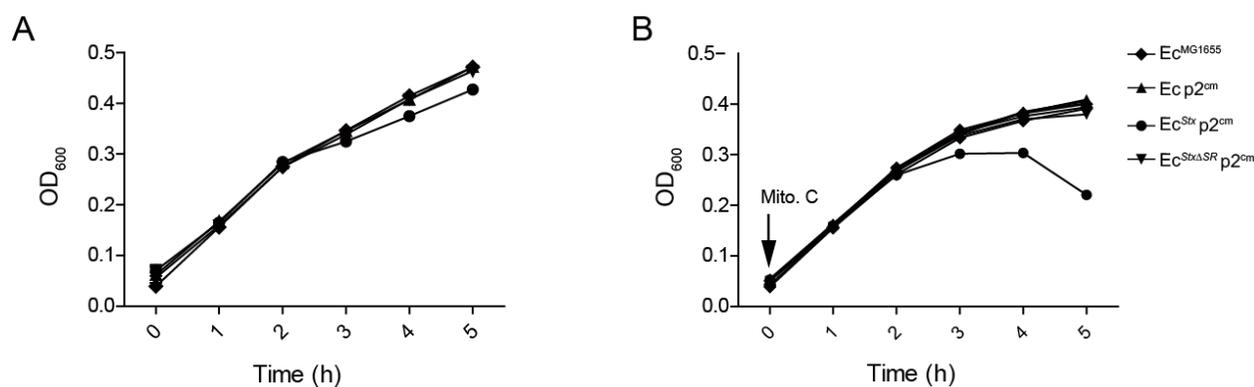

Figure 4.36. Deletion of the phage lysis gene leads to significant decrease of the lysis. Subculture II of *E. coli* strains: Ec^{MG1655} (rhomb), Ec p2^{cm} (triangle), Ec^{Stx} p2^{cm} (circle) and $Ec^{Stx\Delta SR}$ p2^{cm} (inverted triangle) were grown for 5 h in a 96-well plate without (**A**) or with addition of mitomycin C (0.5 µg/ml) (**B**). OD_{600} of the subculture II was measured each hour. Bars shown mean and StD. OD_{600} values (5 h) of the mitomycin C-induced (***$p<0.0001$) and non induced (***$p<0.0001$) culture are significantly different (ANOVA test). Statistical analysis by unpaired Student's *t*-test for non induced cultures: Ec p2^{cm} and Ec^{Stx} p2^{cm} (**$p<0.002$), Ec p2^{cm} and $Ec^{Stx\Delta SR}$ p2^{cm} ($p>0.05$), and Ec^{Stx} p2^{cm} and $Ec^{Stx\Delta SR}$ p2^{cm} (***$p<0.0001$). Statistical analysis by unpaired Student's *t*-test for mitomycin C-supplemented cultures: Ec p2^{cm} and Ec^{Stx} p2^{cm} (***$p<0.0001$), Ec p2^{cm} and $Ec^{Stx\Delta SR}$ p2^{cm} (***$p<0.0001$), and Ec^{Stx} p2^{cm} and $Ec^{Stx\Delta SR}$ p2^{cm} (***$p<0.0001$).

Upon induction with mitomycin C (0,5 µg/ml) lysis of Ec^{Stx} p2^{cm} was detected (**Figure 4.36B**), which correlated with release of active ColIb into the culture supernatant (**Figure 4.37A**). A variant lacking *S*- and *R*-like genes ($Ec^{Stx\Delta SR}$ p2^{cm}) did not lyse in the presence of mitomycin C and no extracellular ColIb was detected by immunoblot or bactericidal activity tests.
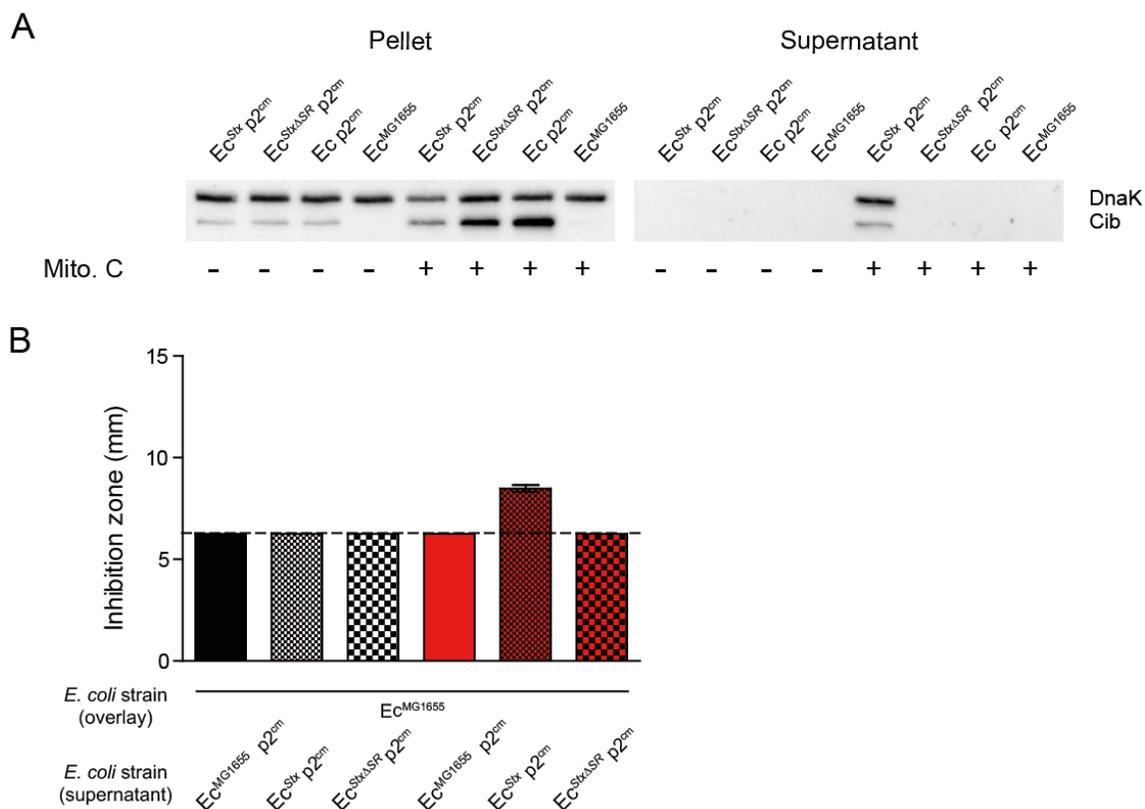
A

Mito. C   − − − − + + + +   − − − − + + + +

B

Figure 4.37. Active ColIb is released only by a lysogen with intact phage lysis genes. (**A**). Mitomycin C supplemented subculture II of *E. coli* strains: Ec^{MG1655} (vertical stripes), Ec p2^{cm} (white), Ec^{Stx} p2^{cm} (checkered, small) and Ec$^{Stx\Delta SR}$ p2^{cm} (checkered, large) were grown for 5 h in 96-well plates. Further, 100 µl were taken from subculture II and spun down. ColIb was detected by immunoblot in bacterial lysates and culture supernatants using affinity-purified rabbit-α-ColIb-antiserum. *E. coli* DnaK was detected as loading control. (**B**) Bactericidal activity of extracellular ColIb was tested (**Section 3.2.3.3**). Paper disks soaked with sterile spent culture supernatant (subculture II (5 h) supplemented with mitomycin C (0.5 µg/ml)) were set on LB agar plates overlaid with Ec^{MG1655} (grown in LB medium and mixed with soft agar). Following 12 h incubation, ColIb inhibition zone (halo) was measured. The detection limit (dotted) line indicates the size of the paper disks.

Expression of the prophage late genes was induced in both, Ec^{Stx} p2^{cm} and Ec^{Stx} p2^{cm}, as confirmed by firefly-luciferase assay. Significantly higher levels of extracellular luciferase activity was detected for Ec^{Stx} p2^{cm}, which correlated with deficient lysis of Ec$^{Stx\Delta SR}$ p2^{cm} (**Figure 4.38A,B**). Taken together, these results fully supported the assumption that release of ColIb, is enhanced by temperate phage-implemented lysis.
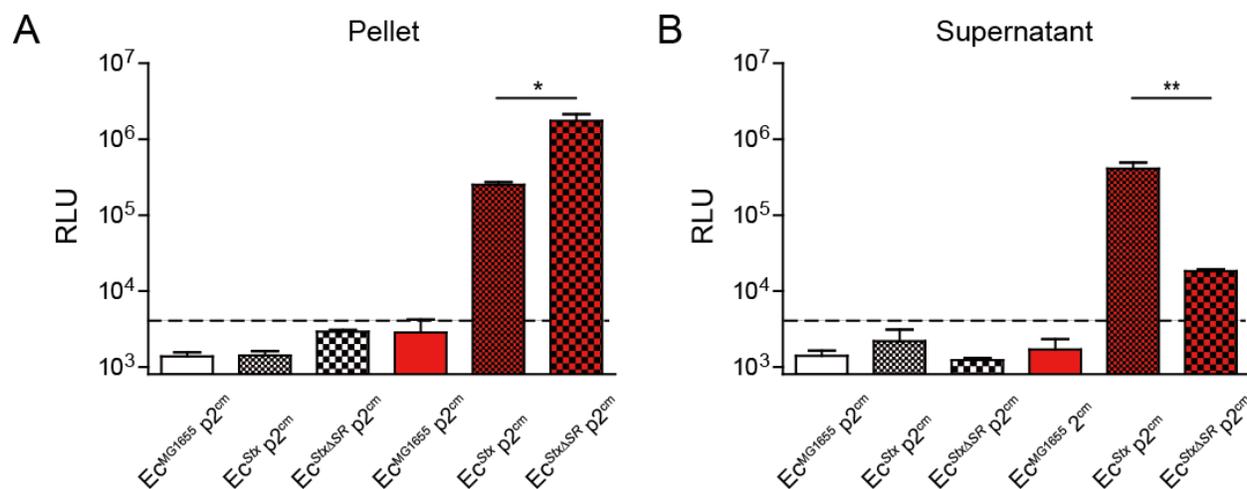
Figure 4.38. Deletion of the lysis genes prophage 933W leads to significant attenuation of the lysis. Subcultures II of *E. coli* strains: Ec[MG1655] (vertical stripes), Ec p2[cm] (white), Ec[Stx] p2[cm] (checkered, small) and Ec[StxΔSR] p2[cm] (checkered, large).were grown for 5 h in 96-well plates. Non-induced cultures are displayed in black and these supplemented with mitomycin C in red color. After 4 h, bacteria were harvested from 100 μl subculture II and luciferase-activity was measured in bacterial lysates (**A**) or culture supernatants (**B**). Relative luminescence units (RLU) are indicated. The detection limit (dotted) line represents the background luminescence detected in Ec p2[cm].

5 Discussion

5.1 Colicin production and sensitivity upon inflammation-induced *Enterobacteriaceae* blooms

Intestinal inflammation leads to dysbiosis which is characterized by the shift of obligate anaerobic bacteria (Bacteroidetes and Firmicutes) dominating a healthy microbiota to otherwise low numbered facultative anaerobic bacteria belonging to the *Enterobacteriaceae* family (Eckburg *et al.*, 2005; Stecher *et al.*, 2013b; Winter *et al.*, 2013a). Expansion of *Enterobacteriaceae* including *E. coli* takes place upon intestinal inflammation triggered by enteric pathogens (*S.* Tm, *Citrobacter rodentium)* (Lupp *et al.*, 2007; Stecher *et al.*, 2007a; Stecher *et al.*, 2012). Furthermore, *Enterobacteriaceae* are increased in the intestine of patients with inflammatory bowel diseases (Crohn's disease) (Walker *et al.*, 2011). Pathogenic and commensal *Enterobacteriaceae* overgrow in the inflamed gut as they have developed adaptation mechanisms to exploit inflammation-derived metabolites, such as ethanolamine and the anaerobic electron acceptors nitrate and tetrathionate (Thiennimitr *et al.*, 2011; Winter *et al.*, 2010; Winter *et al.*, 2013b). Competing for the available nutrients in the intestine, distinct *Enterobacteriaceae* strains employ various competition strategies. Our study revealed that colicin production is an effective fitness trait of *Enterobacteriaceae* in inflammation-inflicted blooms. The current study showed that both production of ColIb and concomitant upregulation of the ColIb receptor-CirA take place only in the inflamed gut. This leads to a tremendous fitness gain of the ColIb producer over the sensitive strain. *In vitro*, *cib* is upregulated under iron limitation conditions and by SOS response induction, which will be reviewed in the context of the inflamed intestine. Next, this discussion will focus on colicins acting as a "Trojan horse" of the siderophore-uptake machinery, which is induced in the inflamed gut. Finally, the importance of the intestinal inflammation as a new environmental niche, favoring colicinogenic bacteria, will be discussed.

5.1.1 Environmental conditions leading to colicin expression upon inflammation

Iron limitation, a defense-measure against pathogen infection, is mediated by several host factors in the inflamed intestine. For instance, the iron-binding protein lactoferrin is secreted by the epithelial cells into

gastric fluids. Further, it is delivered and released at the site of inflammation by degranulating neutrophils (Legrand *et al.*, 2005). Another protein secreted by neutrophils, Lcn-2, restricts growth of commensal *E. coli* and relatives, relying on iron-uptake via catechol siderophores, such as ferric-enterochelin. Lcn-2 binds enterochelin and thereby couples with the siderophore-mediated iron acquisition (Flo *et al.*, 2004; Goetz *et al.*, 2002). Of note, some Gram-negative pathogens (*S.* Tm and pathogenic *E. coli*) produce a glucosylated derivative of enterochelin, termed salmochelin, along with a salmochelin-specific secretion and uptake system. Lcn-2 can not bind the ferric-salmochelin complex and thus is unable to interfere with the salmochelin-based iron acquisition of *Enterobacteriaceae* (Fischbach *et al.*, 2006). Therefore, induction of inflammation and concominant secretion of Lcn-2 is a competitive strategy of *S*. Tm against commensal *E. coli* (Raffatellu *et al.*, 2009). Albeit being an essential element, high concentrations of iron can be toxic for the cell. Due to the Fenton chemistry, iron catalyzes generation of hydroxyl radicals, which destroy various cellular components. Therefore, bacterial iron uptake and storage systems need to be tightly regulated. This is governed by the global Fur repressor (Braun & Hantke, 2011). Iron-bound Fur dimers occupy consensus sequences (Fur box) located in the promoters of multiple genes involved not only in iron homeostasis, but also in oxidative stress and acid resistance responses, as well as virulence factors expression. Depletion of iron leads to disengagement of the iron-free repressor and de-repression of Fur-regulated genes (Braun & Hantke, 2011; Carpenter *et al.*, 2009). The *cib* promoter contains a Fur box and ColIb expression is upregulated upon iron limitation (**Section 4.1.2**). Therefore, it could be expected that inflammation-driven iron limitation would lead to induction of ColIb production.

Furthermore, *cib* expression, as with most other colicins, is regulated by a second repressor, LexA. De-repression of LexA takes place upon induction of the SOS response by various agents such as UV light, DNA-damaging antibiotics (mitomycin C, ciprofloxacin) and cell-wall active β-lactams (Kelley, 2006). Inflammatory mediators likewise induce the SOS response, e.g. hydrogen peroxyde along with other ROS, which are products of neutrophil oxidative activity (Segal, 2005). In addition, pro-inflammatory cytokine stimulation of the intestinal epithelium leads to upregulation of iNOS and production of RNS. (Winter *et al.*, 2013a). In a recent study, expression of stress-related proteins, such as GroL, RecA, and NfuA by intestinal *E. coli* was shown to be induced upon inflammation (Schumann *et al.*, 2012). Of note, NfuA, as a protein involved in biogenesis of iron-sulfur clusters, is engaged in survival upon conditions of oxidative stress and iron starvation (Angelini *et al.*, 2008). Therefore, the upregulation of *nfuA in vivo* further confirms that both iron deprivation and production of inducers of SOS response takes place in the inflamed intestine. These environmental changes in the inflamed intestine might be the trigger of *cib* expression observed in the *Salmonella* colitis model (**Figure 4.13**).

5.1.2 Colicins: The Trojan horse of iron-siderophore uptake system employed in the competition between close relatives in the inflamed gut

Expression of *E. coli cirA* encoding an outer membrane receptor protein is likewise induced upon inflammation (**Figure 4.13**). CirA mediates a TonB-dependent uptake of monomeric catecholate siderophores, several bacteriocins and bacteriophages. Expression of genes encoding both, CirA and the TonB-ExbB-ExbD protein complex is repressed by Fur protein (McHugh *et al.*, 2003; Nikaido & Rosenberg, 1990; Noinaj *et al.*, 2010). Depletion of iron *in vitro* resulted in gradually increased sensitivity of *E. coli* to ColIb, which was directly proportional to increased amounts of CirA (**Figure 4.8**). Furthermore, iron limitation provided a significant competitive advantage to ColIb-producing *S*. Tm against a colicin-sensitive *E. coli* strain *in vitro* (**Figure 4.10**). Interestingly, that was significantly higher compared to SOS response induction alone or in combination with iron depletion. Notably, iron limitation and SOS response induction alone resulted in comparable amounts of ColIb produced by *S*. Tm (**Figure 4.5**). Furthermore, de-repression of both LexA and Fur led to higher ColIb concentrations than iron-dependent Fur release alone. Taken together these results argue that elevated CirA production by *E. coli* is of more importance for the ColIb-dependent competition of *S*.Tm and *E. coli*, than the amount of ColIb produced by *S*. Tm.

Of note, it was observed, albeit not further investigated, that a ColIb-sensitive strain is resistant against very high concentrations of recombinant ColIb (data not shown). A similar observation was made for ColIa and attributed to the colicin uptake process (Jakes & Finkelstein, 2010). Two CirA molecules are required for ColIa uptake: one for ColIa binding and a second molecule for ColIb translocation through the outer membrane. Consequently, if all available receptors are occupied by bound ColIa molecules, there are no free receptors left to execute ColIa translocation (Jakes & Finkelstein, 2010).

Another observation made in the current study further supports the importance of high numbers of CirA to ensure ColIb action. ColIb-sensitivity of Ec[MG1655] differed depending on the time during which bacteria were cultured at low iron concentrations. Short time iron starvation resulted in increased ColIb-susceptibility. In contrast, although more CirA was produced compared to the short term culturing, upon extended iron deprivation, significantly less bacteria were killed by ColIb (**Figure 4.9**). This effect could be linked to the competition between the natural ligands (catecholate siderophores) and colicins for the common receptor (Cascales *et al.*, 2007). Further investigations are required to confirm that siderophores compete with colicin-receptor interaction and thereby prevent colicin-mediated killing.

Ec[Nissle] showed reduced ColIb-sensitivity compared to Ec[MG1655] *in vitro* and *in vivo* (**Figure 4.1;Figure 4.3**). This is maybe another hint for the crucial role of CirA-mediated colicin-sensitivity. Recently it was

shown that probiotic Ec[Nissle] suffers less from iron limitation in the inflamed intestine, compared to Ec[MG1655]. This was attributed to the multiple iron uptake systems of Ec[Nissle], particularly to the salmochelin uptake system conferring resistance to Lpc-2 (Behnsen *et al.*, 2013). Therefore, it might be suggested that this efficient iron acquisition could result in downregulation of CirA and consequently decreased ColIb-susceptibility. Nevertheless, *cirA* expression of both Ec[Nissle] and Ec[MG1655] was not evaluated in the course of this work to further support this notion.

Interestingly, a ColIb homologue ColIa was found frequently in combination with microcin V in human faecal *E. coli* isolates (Prof. Dr. Margaret A. Riley & Chavan, 2007). The ColIa promoter contains a CRP binding sequence, a LexA box (identical to ColIb) and a Fur box (identical to ColIb, with an exception of one nucleotide) (Mankovich *et al.*, 1986). Microcins are small size (<10 kDa) colicin-like antimicrobial peptides, expressed upon nutrient depletion or iron limitation (Duquesne *et al.*, 2007). Frequently expressed by enteric pathogens, microcin V is induced at low iron concentrations and likewise acts via the CirA receptor (Braun *et al.*, 2002; Pinou & Riley, 2001). It was proposed that a combination of ColIa and microcin V is required for colonization of two distinct ecological niches: the nutrient-depleted lower intestinal tract, which promotes CRP-cAMP-mediated upregulation of ColIa expression, and on the other side, generally iron-depleted extra-intestinal body sights inducing microcin V production (Prof. Dr. Margaret A. Riley & Chavan, 2007). Our results suggest that inflammatory conditions in the intestine could be another niche where a strain could benefit from the ColIa and microcin V couple.

Other bacteriocins likewise exploit iron-siderophore uptake receptors, such as the ferric enterobactin receptor FepA (colicin D and colicin B), the ferrichrome receptor FhuA (colicin M), the yersiniabactin receptor FyuA (pesticin) and the CirA receptor (ColIa). Furthermore, several microcins, such as E492, H47 and M, bind siderophore receptors FepA, Fiu, CirA and IroN (Braun *et al.*, 2002), suggesting that enhanced killing of bacteriocin-sensitive competitors upon low iron concentrations could be a common strategy of bacteriocin producers. This concept is further supported by the increased bacteriocin (pyocin S2)-sensitivity of a targeted strain (*Pseudomonas aeruginosa*), observed upon iron limitation (Ohkawa *et al.*, 1980). Nevertheless, it should be tested if other colicins induced exclusively by SOS response, follow this scenario in the inflamed intestine.

5.1.3 Intestinal inflammation as a new environmental niche favouring colicinogenic bacteria

Colicins were found in 24% of human and 33% of other mammalian intestinal *E. coli* isolates, (Riley, 2011). This high frequency was explained by the importance of colicins for invasion and establishment of a bacterial population in the gut, protection of the resident microbiota against invading strains (e.g. pathogens), restriction of neighboring cell growth and promotion of microbial diversity (Kirkup & Riley, 2004; Riley, 2011). Furthermore, colicins are expected to be an important feature of probiotic *E. coli* strains (Gillor *et al.*, 2009).

Despite the evident benefits, colicinogeny is a costly trait associated with metabolic expenses by replication and maintenance of the colicin plasmid, colicin production and finally lethality by colicin release (Riley, 2011). Therefore, transcription of many colicin genes is tightly repressed by two overlapping LexA binding sites and in some cases additional negative regulatory mechanisms (Butala *et al.*, 2012). In the absence of exogenous DNA damage, colicin expression was observed only for a small fraction (~3%) of the colicinogenic population (Mulec *et al.*, 2003). The latter was attributed to a spontaneous SOS response activation, differential affinity of the repressor to the LexA box, fluctuating LexA concentrations as well as the involvement of additional transcriptional repressors (Kamensek *et al.*, 2010; Mrak *et al.*, 2007).

Despite the extensive research, conditions affecting the balance of colicinogeny "pros and cons" remained unclear. Only a part of the experimental *in vivo* studies confirmed that bacteriocins expression confers a benefit to the colicinogenic strain. A colicin producer dominated over its sensitive adversary during a long-term colonization experiment (5-16 weeks) in the mouse intestine (Gillor *et al.*, 2009; Kirkup & Riley, 2004) and *E. coli* expressing microcin V outcompeted a microcin-sensitive strain after 24-72 h growth (McCormick *et al.*, 1989; Wadolkowski *et al.*, 1988). In contrast, other studies failed to show that production of colicin is of any advantage for colonization of healthy (noninflamed) intestine after 1-6 weeks (Craven *et al.*, 1971; Kelstrup & Gibbons, 1969). Colicin production was even detrimental for a colicinogenic *E. coli* competing against the colicin-sensitive strain (Ikari *et al.*, 1969). The lack of phenotype for colicinogeny was attributed to colicin inactivation by intestinal proteolytic enzymes (Kelstrup & Gibbons, 1969) and the block of energy dependent colicin-uptake upon anaerobiosis (Braun *et al.*, 1980; de Graaf, 1973; Kelstrup & Gibbons, 1969). In agreement with these studies, ColIb-expressing *S.* Tm[avir] did not outcompete a colicin-sensitive Ec[MG1655] in the noninflamed mouse intestine (**Figure 4.2**). However, *S.* Tm[wt] retains a ColIb-dependent competitive advantage in the inflamed intestine, due to the SOS response induction by inflammation-derived ROS and RNS. Along with the host-mediated

iron-limitation, SOS response leads to increased production of ColIb. Even more important, upon inflammation ColIb-sensitive strain was outcompeted by the producer (*S*. Tm^wt^) due to the increased sensitivity of Ec^MG1655^. Therefore, our current work highlights the importance of the environmental conditions *in vivo* for the colicin-dependent competition.

The mammalian colon represents a structured environment with localized interactions, which favors colicinogenic bacteria (Majeed *et al.*, 2011). *E. coli* strains could form biofilms via secretory IgA-mediated adhesion to the epithelial surface (Orndorff *et al.*, 2004), growing on mucin-derived sugars (Chang *et al.*, 2004). It has been shown that a colicinogenic bacteria could outgrow a colicin-sensitive strain competing in structured environment (e.g. agar plate and biofilms) (Chao & Levin, 1981). In contrast, growing in a well-mixed liquid culture with randomly distributed nutrients (i.e. equally well accessible by both competitors), the producer strain is outcompeted by the faster growing colicin-sensitive rival because the latter is not suffering from the burden of colicin production (Chao & Levin, 1981; Greig & Travisano, 2008). Furthermore, high initial numbers of the colicin-producing strain were found to be another prerequisite for the success of a colicinogenic strain. Later studies on *Saccharomyces cerevisiae* producing K1 toxin (killing K1-sensitive *S. cerevisiae*) confirmed the importance of high densities of both producing and toxin-sensitive strains, because numerous producers release a high amount of the toxin, which easily finds sensitive-bacteria presented at high numbers (Greig & Travisano, 2008). Furthermore, it was shown that high abundance of nutrients supports invasion of the yeast killer strain, compensating the fitness costs of the K1 production (Brown *et al.*, 2009; Wloch-Salamon *et al.*, 2008). The discussed environmental settings should be even more important for the success of a colicin-producing strain, because the latter is undergoing a cell lysis, in contrast to *S. cerevisiae*, where K1 secretion is not lethal for the producer (Cascales *et al.*, 2007; Wloch-Salamon *et al.*, 2008). Thereby, the exuberant growth of *Enterobacteriaceae* thriving on the inflammation-derived metabolites (Thiennimitr *et al.*, 2011; Winter *et al.*, 2010; Winter *et al.*, 2013b) sets up the inflamed intestine as an environment favoring the colicin-producing bacteria over the colicin-sensitive competitors.
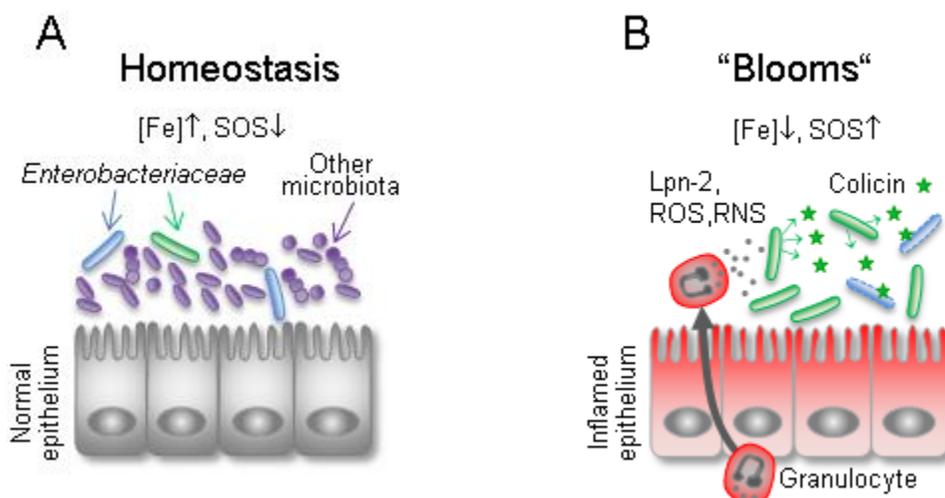
Figure 5.1. Model for the role of colicins for bacterial competition in inflammation-induced blooms. (A) Under homeostatic conditions, *Enterobacteriaceae* (blue, green) are reduced in numbers as they are kept in check by the obligate anaerobic microbiota (violet-blue). Under this condition, colicin expression as well as expression of the colicin surface receptors are relatively repressed (high iron, no triggers of the SOS response). **(B)** Upon induction of an inflammatory response, gut microbial ecology is altered leading to enterobacterial blooms. Neutrophils transmigrate into the gut lumen and produce iron-depleting agents (lipocalin, lactoferrin) and reactive oxygen and nitrogen species (ROS, RNS). This triggers SOS-and Fur-dependent transcriptional responses in *Enterobacteriaceae* and colicin- and colicin-receptor expression is induced. Thereby, the inflammatory response drives colicin-dependent enterobacterial competition.

In summary, the current work identifies inflammation-induced *Enterobacteriaceae* blooms as a new ecological niche favoring colicin-dependent competition. This is illustrated by a model, where both colicin expression by the producer and colicin sensitivity of the competitor, are upregulated upon *Salmonella*-elicited inflammation (**Figure 5.1**). Moreover, high density of the competitors, along with the abundant resources upon inflammation (Stecher *et al.*, 2007a; Stecher *et al.*, 2013b), promotes colicin-mediated competitive advantage of the producer over the colicin-sensitive strain.

5.2 The novel concept of phage-mediated colicin release

Despite the interest in colicin's biology and possible medical application of these toxins, up to date, it is not know how numerous colicins belonging to group B colicins are released. Our study showed that induction of temperate phages encoded within *S*. Tm genome leads to cell lysis and release of various cellular components, including the ColIb. Moreover, it was observed that prophages display differential contributions to the cell lysis and release of ColIb. Along with these findings, the importance of an accurate timing of production of colicin and prophage induction would be discussed. Finally, this discussion will focus on the impact of prophages on colicin-dependent bacterial fitness.

5.2.1 The enigma of the release of group B colicins

Up to date, the mechanism of release of group B colicins remains an open question. In contrast, release of group A colicins of various sizes (20-60 kDa) is associated with the action of a conserved lysis protein encoded within the colicin operon. The lysis protein is proposed to assist colicin accumulation in the periplasm and subsequent extracellular release of a small amount of colicin, defined as "basal" colicin release (Cascales *et al.*, 2007; Chen *et al.*, 2011). As shown for colicin A and E7, at the second stage lysis proteins could interact with colicins, outer membrane porins (OmpC or OmpF), as well as with the outer membrane phospholipase A (OMPLA) (Cavard, 2004). Lysis protein-mediated activation of OMPLA leads to membrane permeabilization and a secondary massive release of the colicin followed by cell death (Cascales *et al.*, 2007; Chen *et al.*, 2011). Hitherto, no release mechanism is known for the majority of group B colicins (including ColIb), which do not encode a lysis protein (Cascales *et al.*, 2007).

It was observed that ColIb was detected in the culture supernatant upon supplementation of mitomycin C, but not DTPA (**Figure 4.5**), suggesting that mitomycin C induces another process leading to ColIb release.

Common traits shared by colicins and lysogenic phages were discussed more than half a century ago (Lwoff *et al.*, 1952). This includes: induction by SOS agents, lethality of production and attack of competitors via Tol- or Ton B-dependent outer membrane receptors (Brown *et al.*, 2009; Cascales *et al.*, 2007). Comparison between group A colicins- and prophage-mediated cell lysis shows some similarities, though the exact mechanism are rather different. Release of λ prophages is mainly associated with five proteins leading to formation of holes in the inner membrane (holins), degradation of the peptidoglycan layer (muramidases) and permeabilization of the outer membrane (Rz integral membrane protein and Rz1

lipoprotein) (Young, 2013). Group A colicins trigger only quasilysis of the host cell, employing a single lysis protein, which is a lipoprotein and has no muralytic activity. Of note, some ssDNA and ssRNA phages encode for single lysis proteins (Young *et al.*, 2000) suggested to be functionally and evolutionarily related to the colicin lysis proteins, based on sequence and structural similarity (Lau *et al.*, 1987). Furthermore, in support to this phage-colicin relationship, another class of bacteriocins (F- and R-type pyocins) was shown to be phage tail proteins, evolved as bacteriocins (Nakayama *et al.*, 2000).

5.2.2 Prophage-mediated release of ColIb

Our experiments have shown a significant decrease in colicin release by *S*. Tm lacking four prophages compared to the wild type strain (**Figure 4.14**). Furthermore, colicin release correlated with cell lysis of the wild type *S*. Tm (**Figure 4.16; Figure 4.18**). Interestingly, different phages had distinct effects on the ColIb release and lysis; e.g. deletion of Gifsy-1 and Gifsy-2 phages had no detectable impact, in contrast to the decreased ColIb release and lysis in absence of Gifsy phages along with ST64B prophage (**Figure 4.14**). Differential contribution of prophages to the host physiology has been previously observed. Deletion of each cryptic prophage encoded by *E. coli* K-12 led to reduction in biofilm formation between 3- and 11-fold. Three out of nine prophages (e14, Rac and CP4-44) mostly contributed to this effect (Wang *et al.*, 2010). Of note, induction of lambdoid prophages differs depending on CI repressor sensitivity and concentration (Refardt & Rainey, 2010). Evaluation of four *S*. Tm LT2 prophages showed that following mitomycin C treatment Fels-1 prophage is significantly stronger induced compared to Gifsy-1 and Gifsy-2 (Frye *et al.*, 2005; Garcia-Russell *et al.*, 2009). Furthermore, Gifsy-1 temperate phage was found to be repressed upon DNA damage, while Gifsy-2 displayed constant low induction albeit mitomycin C supplementation (Garcia-Russell *et al.*, 2009). These observations were in agreement with no detectable release of infectious Gifsy-1 and Gifsy-2 particles upon DNA damage, in contrast to Fels-1 and Fels-2 prophages (Frye *et al.*, 2005). Based on these observations, it could be suggested that ColIb release and cell lysis remained unchanged upon Gifsy-1 and Gifsy-2 deletion due to weak response of these phages to mitomycin C treatment.

SopEΦ is a P2 phage, homologous to Fels-2 (Pelludat *et al.*, 2003). Interestingly, despite the strong induction observed for *S*. Tm LT2 Fels-2 prophage (Frye *et al.*, 2005), deletion of the SopEΦ lysis genes had no detectable impact on *S*. Tm lysis or ColIb release in response to mitomycin C treatment (**Figure 4.22; Figure 4.23**). This could be a result of the incomplete deletion of one of the proposed lysis protein genes (**Section 3.2.6**) or the presence of yet another lysis gene that had not been annotated so far.

However, this is not very likely explanation, since transduction of SopEΦ did not lead to increased release of ColIb by *S*. Tm isolate A36 (**Figure 4.24**). Possibly, unlike Fels-2, DNA damage does not provoke strong induction of SopEΦ prophage.

In contrast, cell lysis and ColIb release were decreased for *S*. Tm strain with lysis deficient ST64B prophage (**Figure 4.26; Figure 4.27**). These results suggest that ST64B lytic activity is induced upon mitomycin C supplementation, leading to cell lysis and ColIb release. Increased expression of genes of the ST64B prophage is detected at 3 h after mitomycin C induction (Frye *et al.*, 2005; Garcia-Russell *et al.*, 2009). Furthermore, following ~10 min exposure to stress-inducing agents ST64B alone out of four phages displayed a slightly elevated gene expression in *S*. Tm^{MA6118} (Kroger *et al.*, 2013). Of note, the effect of ST64B prophage on lysis-mediated ColIb release was much more prominent in absence of Gifsy-1 and Gifsy-2 prophages than in *S*. Tm wild type. This suggests that Gifsy-1 and Gifsy-2 have an inhibitory effect on ST64B lysis or that activation of ST64B induces lysis by Gifsy-1 and Gifsy-2. Gifsy-1 and Gifsy-2 prophages are under negative control of small size global repressor proteins that, unlike RecA-stimulated cleavage of CI, are deactivated by antirepressor proteins (Lemire *et al.*, 2011). It has been shown that antirepressor protein FsoA of the lambdoid prophage Fels-1 deactivates the temperate phage repressor of Gifsy-2. It could be possible that a similar crosstalk takes place between an antirepressor of ST64B and Gifsy-1 / Gifsy-2 repressor proteins. Thereby, despite the deletion of ST64B lysis genes, the antirepressor is still present within the prophage genome and can activate Gifsy-1- or Gifsy-2-mediated lysis. The contribution of the latter two prophages could be rather insignificant compared to the ST64B-mediated lysis and therefore not detectable for a strain lacking Gifsy-1 / Gifsy-2 (**Figure 4.27**). Alternatively, lysis proteins may enhance each other's function. It is known that heterogeneous endolysins and holins can substitute each other and boost cell lysis and toxin release (Hodak & Galan, 2013; Wang *et al.*, 2000). Therefore, enhancement of ST64B-assisted ColIb release by Gifsy-1 / Gifsy-2 prophages could be due to the additive interactions between prophage lysis proteins.

The concept of ColIb release as a result of phage-mediated cell lysis is even better illustrated by Ec^{MG1655} strain carrying the ColIb plasmid p2^{cm} and a variant of a Shiga-toxin expressing prophage 993W. Remarkably, in the absence of prophage or deletion of *S*- and *R*-like phage lysis genes neither cell lysis, extracellular ColIb, nor ColIb-directed bactericidal activity were detected for Ec^{MG1655} (**Figure 4.35; Figure 4.36; Figure 4.37**).

Interestingly, in contrast to the Ec^{MG1655} strains carrying no or a lysis-deficient prophage, *S*. Tm^{ΔPh} retained, albeit significantly reduced, ColIb-dependent bactericidal activity, even if no cell lysis and extracellular ColIb were detected (**Figure 4.14**). Why would *S*. Tm^{ΔPh} be able to release tiny amounts of

103

ColIb leading to killing of the colicin-sensitive strain, unlike prophage-depleted Ec^{MG1655}? Apart from the functional prophages (Gifsy-1, Gifsy-2, SopEΦ and ST64B) *S.* Tm SL1344 encodes approximately 80 bacteriophage-related proteins, some of them belonging to prophage remnant SLP443, degenerate bacteriophage SLP28 and a P4-family bacteriophage gene cluster (Kroger *et al.*, 2012). Particularly, the prophage-associated genes *SL1344_2210-SL1344_2219* (among them a holin-homologue *SL1344_2213*) located between the ST64B and the Gifsy-1 prophage could correspond to a SOS-induced gene cluster, previously detected in this region (Frye *et al.*, 2005). Assuming that some of these genes encode lysis proteins, these prophage genes may be responsible for the "left-over" ColIb release observed in *S.* Tm^{ΔPh}.

Ec^{MG1655} strain cured of the single inducible phage lambda contains various bacteriophage-like elements, among them nine cryptic prophages (Blattner *et al.*, 1997; Canchaya *et al.*, 2003; Wang *et al.*, 2010). Moreover, some of these phages encode lysis proteins: DLP-12 (putative lipoprotein, murein endopeptidase and lysozyme); Rac (a prophage endopeptidase); Qin (a lysozyme and an S-like protein) (Blattner *et al.*, 1997). It is unclear if any of these proteins could cause cell lysis. Nevertheless, only cryptic prophage e14, but not the remaining eight, can be excised upon SOS induction (Wang *et al.*, 2010), questioning whether the expression of the cryptic prophage lysis genes is induced by DNA damaging agents. Cryptic prophages are generally inactive in terms of cell lysis, phage particle production and plaque formation (Wang *et al.*, 2010). This could be the reason why Ec^{MG1655} carrying p2^{cm} requires an inducible prophage with intact lysis genes to support ColIb release. Thereby, acquisition of a group B colicin-encoding plasmid could be expected to benefit only a recipient, which has retained functional prophage lysis genes within its genome.

5.2.3 Prophage-independent ColIb release

Release of colicin A, which belongs to group A colicins, was linked to production of outer membrane vesicles (OMV), introducing another distinct mechanism for colicin release (Cavard, 2004). Colicin A could block the host cell proteins of the Tol–Pal system, which is involved in outer membrane stabilization during cell division (Gerding *et al.*, 2007; Kleanthous, 2010). Interception of this system results in production of OMV, a feature observed for *tol–pal* deficient strains (Bouveret *et al.*, 2002). Colicins are separated into two groups (A and B), based on their ability to interact with either the TolA-TolQ-TolR or the TonB-ExbB-ExbD systems, respectively (Kleanthous, 2010). Interestingly, alteration of the TolA binding site of a group A colicin (colicin U) enabled the interaction of this colicin with distinct components of both, Ton and Tol system (Pilsl & Braun, 1998). Nevertheless, to our knowledge, this

effect has not been tested for any Ton-dependent colicin. Therefore, interaction of ColIb (a group B colicin) with Tol proteins leading to OMV-dependent release is a rather unlikely event. Furthermore, Ec^{MG1655} *tol-pal* mutants were shown to produce OMV (Bernadac *et al.*, 1998), yet no detectable ColIb release is observed for Ec^{MG1655} in absence of a functional prophage.

In summary, the current study confirmed that phage-mediated cell lysis promoted colicin release. Further experiments would be required to determine if there are other, phage-independent ColIb release mechanisms.

5.2.4 Time-management of ColIb release

Colicin release via prophage-triggered cell lysis would require precise timing of colicin and phage lysis genes expression upon induction of the SOS response. It could be expected that to achieve an optimal cost–effect (cell lysis-colicin toxicity) ratio, it has to be ensured that a dying bacterium releases a maximal amount of colicin. Therefore, the lysis should take place only when bacteria have accumulated high amounts of colicin intracellularly. This concept is further supported by an observation that typhoid toxin is expressed before bacteriophages-like muramidase lysis protein, which is involved in the toxin release (Hodak & Galan, 2013). Of note, *cib* expression is downregulated not only by SOS response repressor LexA, but also by Fur repressor. Thereby, maximal benefit from the lysis could be attained upon Fur de-repression triggered by iron limitation.

What would be the control mechanisms of an efficient prophage-mediated colicin release? Group A colicin release takes place late after colicin synthesis, after reaching a critical concentration of colicin lysis protein. Furthermore, a terminator upstream of the lysis gene (**Figure 5.2**) ensures that colicin will be always expressed in higher amounts and earlier than the lysis protein (Cascales *et al.*, 2007). Likewise, lambda prophage lysis genes belong to the group of late genes, which are tightly controlled by *pR'* promoter and *tR'* terminator. Transcription of these genes takes place at high threshold concentration of Q antiterminator (Court *et al.*, 2007). DNA damage leads to sequential expression of prophage genes: initial expression of DNA binding components, antirepressor proteins, virulence factors and transcriptional regulators is followed by expression of genes involved in DNA replication, recombination, integration, excision and host lysis (Frye *et al.*, 2005). The requirement for a critical concentration of holins and pinholins coordinates the cell lysis timing is similarly to the colicin lysis protein "high threshold" behavior (Cascales *et al.*, 2007; Young, 2013). Furthermore, it was shown on a single cell level that activation of

the SOS response precedes prophage induction (Nanda *et al.*, 2014). Generally, colicin expression is likewise correlated with SOS induction on a single cell level (Kamensek *et al.*, 2010; Zgur-Bertok, 2012).

How are SOS response, ColIb expression and phage activity coordinated in *S*. Tm? This could be investigated via analysis of a microarray of transcriptome sequencing following induction of the SOS response. Alternatively, gene reporters (green fluorescent protein (GFP)) could not only follow the timing, but further verify at a single cell level that all these events take place in the same bacterium (Nanda *et al.*, 2014). Possible candidates as reporters for the SOS response could be *sulA*, *lexA* or *recA* (McCool *et al.*, 2004; Zgur-Bertok, 2012) and ColIb activity *cib* reporter. Based on the strong impact of ST64B prophage observed, a ST64B early gene reporter and a single lysis gene reporter for the late events could be suitable to trace activation of prophage genes; e.g. an early gene expression reporter could be ST64B encoded excisionase, shown to be one of the first genes expressed upon DNA damage (Frye *et al.*, 2005; Mmolawa *et al.*, 2003). Other relevant early gene candidates could be an N antiterminator homologue, as well as O protein coding gene upregulated before and after the excisionase, respectively (Court *et al.*, 2007; Frye *et al.*, 2005; Mmolawa *et al.*, 2003).
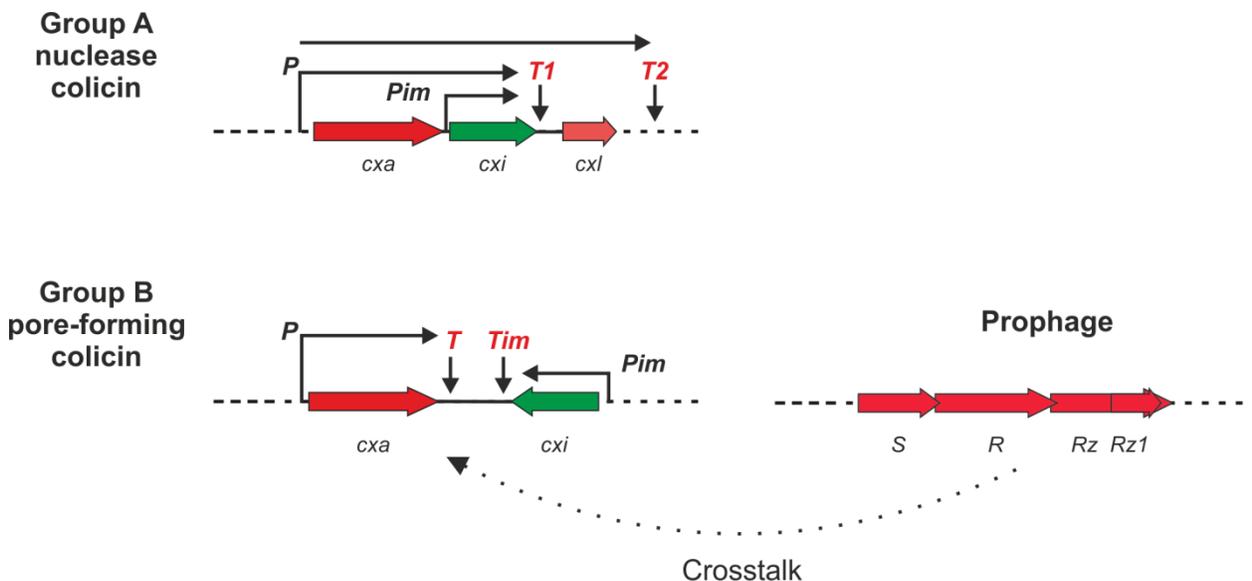

Figure 5.2. The crosstalk between group B colicins and prophages. Release of group A colicins (encoded by *cxa*) is mediated by the action of a conserved lysis protein (encoded by *cxl*) encoded within the colicin operon. In contrast, the operon of group B colicins does not encode a lysis protein. Induction of prophages encoded with the genome of a colicinogenic bacterium leads to expression of cognate phage lysis genes (*S*, *R*, *Rz* and *Rz1*). The latter cause lysis and release of various unspecific cytoplasmic components, including group B colicins (encoded by *cxa*).

5.2.5 Impact of prophages on colicin-dependent bacterial fitness

In vitro, competition between ColIb-producing *S*. Tm and colicin-sensitive Ec[MG1655] showed that prophages contribute to the colicin-dependent overgrowth of *S*. Tm over Ec[MG1655] upon supplementation of SOS response inducer mitomycin C (**Figure 4.34**). Remarkably, in the absence of mitomycin C, lysogenic *S*. Tm was slightly overgrowing the colicin-sensitive competitor, though significantly better than the phage deficient strain (**Figure 4.34A,B**). The latter observation could be explained by the spontaneously induced SOS response induction triggering both temperate phages and ColIb expression.

5.2.5.1 Benefits of spontaneous SOS response induction for a colicin expressing lysogen

Spontaneous prophage induction is limited to less than 10^{-5} of the population. It is harmless for the rest of the lysogenic bacteria, due to immunity against superinfection with the phage. This, however, will be deadly for non-lysogenic competitors which will be lysed by the prophage. Thereby, the spontaneous prophage induction benefits the host on a population level (Bossi *et al.*, 2003). Upon nutrient limitation phage induction occurred in up to 0.08% of the actively replicating host population. This was correlated to induction of the SOS response as a result of spontaneously emerging ssDNA due to the arrest of the replication fork (Nanda *et al.*, 2014). Furthermore, release of Shiga-toxin from a tiny fraction (0.005%) of lysogens, as a result of spontaneous Shiga-toxin encoding prophage activation, is proposed to increase bacterial shedding in the environment, i.e. to enhance spreading of the pathogen (Livny & Friedman, 2004).

Spontaneous induction of a small fraction of colicinogenic bacteria is considered an altruistic suicide that supports the rest of the population by killing colicin-sensitive competitors (Cascales *et al.*, 2007). Therefore, it could be argued that spontaneous SOS induction, as a result of endogenous ssDNA, leads to phage-mediated ColIb release by a small number of colicin producers, leading to killing of colicin-sensitive competitors. This effect should be even more pronounced upon iron limitation, due to the increased expression of ColIb (derepression of Fur and LexA) and increased colicin-sensitivity of the competitor. Accordingly, in the absence of prophages, no or too small amounts of spontaneously-induced ColIb would be released in order to confer benefit to the producer. This explains the higher competitive advantage of lysogenic compared to prophage-deficient *S*.Tm.

5.2.5.2 ColIb-producing lysogen upon intestinal inflammation

SOS induction leads to phage-mediated ColIb release by a larger part of the lysogenic population, leading to a distinct competitive fitness advantage of the wild type *S*. Tm, as it was observed *in vitro* (**Figure 4.34**). What would be the expected situation during The lytic infection mode of prophages takes place

mainly in actively growing bacterial population upon nutrient-rich conditions (Court *et al.*, 2007; Mills *et al.*, 2013), such as it is the situation in the inflamed intestine (Stecher *et al.*, 2007a). This could be an additional trigger for prophage activation, apart from the DNA damaging agents (ROS and RNS) released in the inflamed gut. Moreover, beneficial prophage-mediated ColIb release upon iron limitation and SOS response induction *in vivo* would not be a solitary event. Prophage (H-19B) encoded Shiga-toxin 1 is regulated by a Fur repressor (Calderwood & Mekalanos, 1987). Growing in iron-deprived intestine, H-19B lysogenic bacteria will produce Shiga-toxin, but won't be able to release it, unless the prophage is activated upon DNA damage. However, if the toxin gets released it could benefit the lysogenic population due to iron liberated from the erythrocytes, as a result of the Shiga-toxin-elicited intestinal hemorrhage (Brussow *et al.*, 2004).inflammation-inflicted *Eneterobacteriacae* blooms.

5.2.5.3 Which came first, the colicin or the prophage?

Upon infection with a single phage, in about 99% of infected bacteria the phage will undergo a lytic cycle. This number decreases to about 50% in the case of an infection with more than two phages (Court *et al.*, 2007). In contrast, ~100% transfer rates of ColIb-encoding plasmid P2 were observed during inflammation-triggered *Enterobacteriaceae* blooms (Stecher *et al.*, 2012). Therefore, it is likely that colicin plasmids get transferred into a bacterium with formerly established lysogeny, which promotes colicin release. Acquisition of colicin as an additional weapon would benefit an invasive lysogen exploiting prophages as a biological agent (Brown *et al.*, 2009; Gama *et al.*, 2013), i.e. expanding the range of targeted competitors, which could be killed either via phage lysis or bactericidal activity of colicins. In contrast, a non-lysogenic strain paying the cost of colicin production (e.g. metabolic load of protein biosynthesis) would not profit from it, because the toxin remains "locked" in the host bacterium. Of note, bacteria carrying multiple colicins retain only a single lysis protein gene, in order to avoid fitness costs of multiple lysis proteins (Prof. Dr. Margaret A. Riley & Chavan, 2007; Zgur-Bertok, 2012). Therefore, it could be suggested that the majority of group B colicin plasmids have lost their lysis gene, relying completely on the phage lysis proteins or concomitant expression of a group A colicin. Moreover, phage-mediated release is not specific, therefore, lysogens could benefit from uptake of various colicin plasmids. Similar arguments were used in support of concept of Shiga-toxin genes as a recent acquirement of Shiga toxin-producing *E. coli* (Brussow *et al.*, 2004). Furthermore, a multiple prophage lysogen could be a preferable host for a colicin-encoding plasmid. Prophages display diverse induction patterns upon different environmental conditions; and colicins expression could be likewise controlled by other regulators than SOS-associated LexA (Zgur-Bertok, 2012). Thus, phage-mediated host lysis and colicin expression could be co-regulated in various environmental settings, ensuring competitive fitness advantage of the host population.
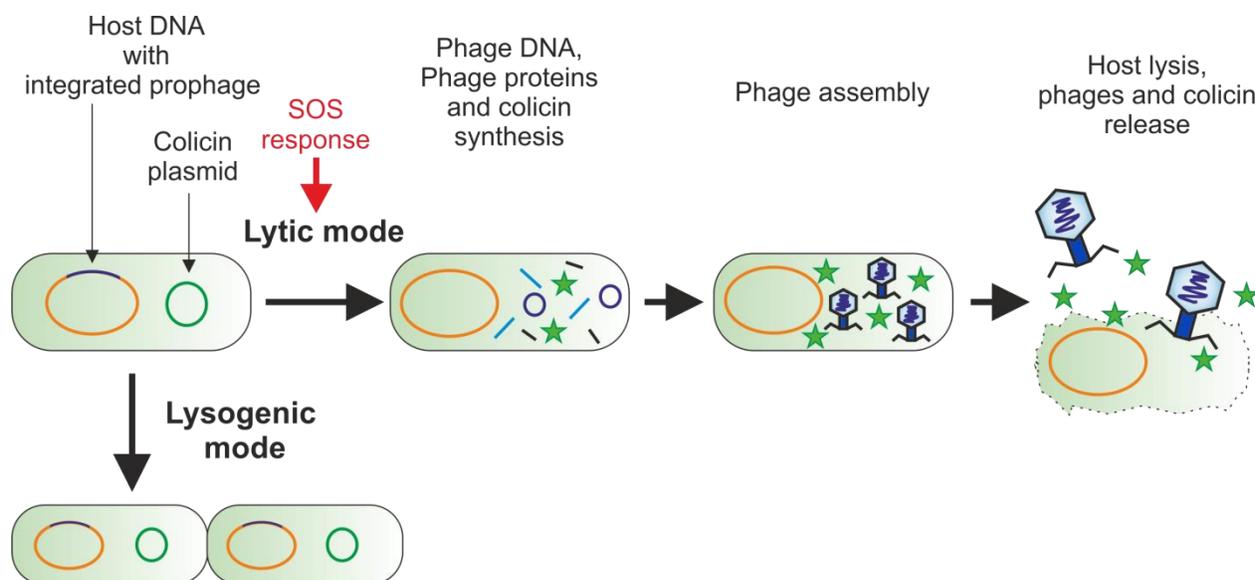
Figure 5.3. Release of group B colicins takes place upon phage-mediated lysis. A bacterial host carrying a colicin plasmid and a prophage inherits both to the next generation of bacteria. Upon activation of the SOS response both, the phage lytic mode (morphogenesis and release of infectious phages via lysis) and colicin expression are induced. Ultimately, this leads to phage-mediated lysis and release of the colicin.

In summary, our results suggest that group B colicins are released as result of phage-mediated lysis (**Figure 5.3**). Furthermore, acquisition of an inducible prophage and a group B colicin plasmid provides a competitive advantage in a colicin-dependent competition. This conclusion is further supported by a recent study, which correlates increase of enterobacterial species in the gut with spread of colicinogeny and decrease in phage sensitivity (Burova *et al.*, 2012). Based on the possibility that superinfection exclusion and immunity by resident temperate phage(s) could be a reason for the decreased phage sensitivity, this study could be a hint for a correlation between lysogeny and colicin production in expanding intestinal *Eneterobacteriacae* populations.

Literature

Alonso, A., Pucciarelli, M. G., Figueroa-Bossi, N. & Garcia-del Portillo, F. (2005). Increased excision of the Salmonella prophage ST64B caused by a deficiency in Dam methylase. *Journal of bacteriology* **187**, 7901-7911.

Angelini, S., Gerez, C., Ollagnier-de Choudens, S., Sanakis, Y., Fontecave, M., Barras, F. & Py, B. (2008). NfuA, a new factor required for maturing Fe/S proteins in Escherichia coli under oxidative stress and iron starvation conditions. *The Journal of biological chemistry* **283**, 14084-14091.

Ayres, J. S., Trinidad, N. J. & Vance, R. E. (2012). Lethal inflammasome activation by a multidrug-resistant pathobiont upon antibiotic disruption of the microbiota. *Nature medicine* **18**, 799-806.

Bailey, T. L. & Gribskov, M. (1998). Combining evidence using p-values: application to sequence homology searches. *Bioinformatics (Oxford, England)* **14**, 48-54.

Barthel, M., Hapfelmeier, S., Quintanilla-Martinez, L., Kremer, M., Rohde, M., Hogardt, M., Pfeffer, K., Russmann, H. & Hardt, W. D. (2003). Pretreatment of mice with streptomycin provides a Salmonella enterica serovar Typhimurium colitis model that allows analysis of both pathogen and host. *Infection and immunity* **71**, 2839-2858.

Baty, D., Lloubes, R., Geli, V., Lazdunski, C. & Howard, S. P. (1987). Extracellular release of colicin A is non-specific. *The EMBO journal* **6**, 2463-2468.

Behnsen, J., Deriu, E., Sassone-Corsi, M. & Raffatellu, M. (2013). Probiotics: properties, examples, and specific applications. *Cold Spring Harbor perspectives in medicine* **3**, a010074.

Bernadac, A., Gavioli, M., Lazzaroni, J. C., Raina, S. & Lloubes, R. (1998). Escherichia coli tol-pal mutants form outer membrane vesicles. *Journal of bacteriology* **180**, 4872-4878.

Bertin, Y., Girardeau, J. P., Chaucheyras-Durand, F., Lyan, B., Pujos-Guillot, E., Harel, J. & Martin, C. (2011). Enterohaemorrhagic Escherichia coli gains a competitive advantage by using ethanolamine as a nitrogen source in the bovine intestinal content. *Environmental microbiology* **13**, 365-377.

Blattner, F. R., Plunkett, G., 3rd, Bloch, C. A. & other authors (1997). The complete genome sequence of Escherichia coli K-12. *Science (New York, NY)* **277**, 1453-1462.

Bossi, L., Fuentes, J. A., Mora, G. & Figueroa-Bossi, N. (2003). Prophage contribution to bacterial population dynamics. *Journal of bacteriology* **185**, 6467-6471.

Bouveret, E., Journet, L., Walburger, A., Cascales, E., Benedetti, H. & Lloubes, R. (2002). Analysis of the Escherichia coli Tol-Pal and TonB systems by periplasmic production of Tol, TonB, colicin, or phage capsid soluble domains. *Biochimie* **84**, 413-421.

Braun, V., Frenz, J., Hantke, K. & Schaller, K. (1980). Penetration of colicin M into cells of Escherichia coli. *Journal of bacteriology* **142**, 162-168.

Braun, V., Patzer, S. I. & Hantke, K. (2002). Ton-dependent colicins and microcins: modular design and evolution. *Biochimie* **84**, 365-380.

Braun, V. & Hantke, K. (2011). Recent insights into iron import by bacteria. *Current opinion in chemical biology* **15**, 328-334.

Brown, J., de Vos, W. M., DiStefano, P. S., Dore, J., Huttenhower, C., Knight, R., Lawley, T. D., Raes, J. & Turnbaugh, P. (2013). Translating the human microbiome. *Nature biotechnology* **31**, 304-308.

Brown, S. P., Fredrik Inglis, R. & Taddei, F. (2009). SYNTHESIS: Evolutionary ecology of microbial wars: within-host competition and (incidental) virulence. *Evolutionary Applications* **2**, 32-39.

Brussow, H. & Hendrix, R. W. (2002). Phage genomics: small is beautiful. *Cell* **108**, 13-16.

Brussow, H., Canchaya, C. & Hardt, W. D. (2004). Phages and the evolution of bacterial pathogens: from genomic rearrangements to lysogenic conversion. *Microbiology and molecular biology reviews : MMBR* **68**, 560-602, table of contents.

Buchanan, S. K., Lukacik, P., Grizot, S., Ghirlando, R., Ali, M. M., Barnard, T. J., Jakes, K. S., Kienker, P. K. & Esser, L. (2007). Structure of colicin I receptor bound to the R-domain of colicin Ia: implications for protein import. *The EMBO journal* **26**, 2594-2604.

Buffie, C. G., Jarchum, I., Equinda, M., Lipuma, L., Gobourne, A., Viale, A., Ubeda, C., Xavier, J. & Pamer, E. G. (2012). Profound alterations of intestinal microbiota following a single dose of clindamycin results in sustained susceptibility to Clostridium difficile-induced colitis. *Infection and immunity* **80**, 62-73.

Burova, L. M., Korneichuk, E. P., Kushkina, A. I. & Tovkach, F. I. (2012). Plasmid profile, colicinogeny and phage sensitivity as indicators of the dynamics of Escherichia coli populations in the human gut. *Mikrobiolohichnyi zhurnal (Kiev, Ukraine : 1993)* **74**, 99-107.

Butala, M., Podlesek, Z. & Zgur-Bertok, D. (2008). The SOS response affects thermoregulation of colicin K synthesis. *FEMS microbiology letters* **283**, 104-111.

Butala, M., Klose, D., Hodnik, V. & other authors (2011). Interconversion between bound and free conformations of LexA orchestrates the bacterial SOS response. *Nucleic acids research* **39**, 6546-6557.

Butala, M., Sonjak, S., Kamensek, S., Hodoscek, M., Browning, D. F., Zgur-Bertok, D. & Busby, S. J. (2012). Double locking of an Escherichia coli promoter by two repressors prevents premature colicin expression and cell lysis. *Molecular microbiology* **86**, 129-139.

Calderwood, S. B. & Mekalanos, J. J. (1987). Iron regulation of Shiga-like toxin expression in Escherichia coli is mediated by the fur locus. *Journal of bacteriology* **169**, 4759-4764.

Campbell, A. (2003). The future of bacteriophage biology. *Nature reviews Genetics* **4**, 471-477.

Canchaya, C., Proux, C., Fournous, G., Bruttin, A. & Brussow, H. (2003). Prophage genomics. *Microbiology and molecular biology reviews : MMBR* **67**, 238-276, table of contents.

Cardelli, J. & Konisky, J. (1974). Isolation and characterization of an Escherichia coli mutant tolerant to colicins Ia and Ib. *Journal of bacteriology* **119**, 379-385.

Carpenter, B. M., Whitmire, J. M. & Merrell, D. S. (2009). This is not your mother's repressor: the complex role of fur in pathogenesis. *Infection and immunity* **77**, 2590-2601.

Cascales, E., Buchanan, S. K., Duche, D., Kleanthous, C., Lloubes, R., Postle, K., Riley, M., Slatin, S. & Cavard, D. (2007). Colicin biology. *Microbiology and molecular biology reviews : MMBR* **71**, 158-229.

Cash, H. L., Whitham, C. V., Behrendt, C. L. & Hooper, L. V. (2006). Symbiotic bacteria direct expression of an intestinal bactericidal lectin. *Science (New York, NY)* **313**, 1126-1130.

Cavard, D. (2004). Role of Cal, the colicin A lysis protein, in two steps of colicin A release and in the interaction with colicin A-porin complexes. *Microbiology (Reading, England)* **150**, 3867-3875.

Chang, D. E., Smalley, D. J., Tucker, D. L. & other authors (2004). Carbon nutrition of Escherichia coli in the mouse intestine. *Proceedings of the National Academy of Sciences of the United States of America* **101**, 7427-7432.

Chao, L. & Levin, B. R. (1981). Structured habitats and the evolution of anticompetitor toxins in bacteria. *Proceedings of the National Academy of Sciences of the United States of America* **78**, 6324-6328.

Chen, Y. R., Yang, T. Y., Lei, G. S., Lin, L. J. & Chak, K. F. (2011). Delineation of the translocation of colicin E7 across the inner membrane of Escherichia coli. *Archives of microbiology* **193**, 419-428.

Chu, B. C., Garcia-Herrero, A., Johanson, T. H., Krewulak, K. D., Lau, C. K., Peacock, R. S., Slavinskaya, Z. & Vogel, H. J. (2010). Siderophore uptake in bacteria and the battle for iron with the host; a bird's eye view. *Biometals : an international journal on the role of metal ions in biology, biochemistry, and medicine* **23**, 601-611.

Chung, H., Pamp, S. J., Hill, J. A. & other authors (2012). Gut immune maturation depends on colonization with a host-specific microbiota. *Cell* **149**, 1578-1593.

Cohen, S., Knoll, B. J., Little, J. W. & Mount, D. W. (1981). Preferential cleavage of phage lambda repressor monomers by recA protease. *Nature* **294**, 182-184.

Court, D. L., Oppenheim, A. B. & Adhya, S. L. (2007). A new look at bacteriophage lambda genetic networks. *Journal of bacteriology* **189**, 298-304.

Craven, J. A., Miniats, O. P. & Barnum, D. A. (1971). Role of colicins in antagonism between strains of Escherichia coli in dual-infected gnotobiotic pigs. *American journal of veterinary research* **32**, 1775-1779.

Darling, A. C., Mau, B., Blattner, F. R. & Perna, N. T. (2004). Mauve: multiple alignment of conserved genomic sequence with rearrangements. *Genome research* **14**, 1394-1403.

Datsenko, K. A. & Wanner, B. L. (2000). One-step inactivation of chromosomal genes in Escherichia coli K-12 using PCR products. *Proceedings of the National Academy of Sciences of the United States of America* **97**, 6640-6645.

de Graaf, F. K. (1973). Effects of cloacin DF13 on the functioning of the cytoplasmic membrane. *Antonie van Leeuwenhoek* **39**, 109-119.

Deriu, E., Liu, J. Z., Pezeshki, M., Edwards, R. A., Ochoa, R. J., Contreras, H., Libby, S. J., Fang, F. C. & Raffatellu, M. (2013). Probiotic bacteria reduce salmonella typhimurium intestinal colonization by competing for iron. *Cell host & microbe* **14**, 26-37.

Desvaux, M. (2012). Contribution of holins to protein trafficking: secretion, leakage or lysis? *Trends in microbiology* **20**, 259-261.

Dethlefsen, L. & Relman, D. A. (2011). Incomplete recovery and individualized responses of the human distal gut microbiota to repeated antibiotic perturbation. *Proceedings of the National Academy of Sciences of the United States of America* **108 Suppl 1**, 4554-4561.

Dewhirst, F. E., Chien, C. C., Paster, B. J., Ericson, R. L., Orcutt, R. P., Schauer, D. B. & Fox, J. G. (1999). Phylogeny of the defined murine microbiota: altered Schaedler flora. *Applied and environmental microbiology* **65**, 3287-3292.

Duquesne, S., Petit, V., Peduzzi, J. & Rebuffat, S. (2007). Structural and functional diversity of microcins, gene-encoded antibacterial peptides from enterobacteria. *Journal of molecular microbiology and biotechnology* **13**, 200-209.

Eckburg, P. B., Bik, E. M., Bernstein, C. N., Purdom, E., Dethlefsen, L., Sargent, M., Gill, S. R., Nelson, K. E. & Relman, D. A. (2005). Diversity of the human intestinal microbial flora. *Science (New York, NY)* **308**, 1635-1638.

Faber, F. & Baumler, A. J. (2014). The impact of intestinal inflammation on the nutritional environment of the gut microbiota. *Immunology letters*.

Fabrega, A. & Vila, J. (2013). Salmonella enterica serovar Typhimurium skills to succeed in the host: virulence and regulation. *Clinical microbiology reviews* **26**, 308-341.

Ferreyra, J. A., Ng, K. M. & Sonnenburg, J. L. (2014). The Enteric Two-Step: nutritional strategies of bacterial pathogens within the gut. *Cellular microbiology*.

Figueroa-Bossi, N. & Bossi, L. (1999). Inducible prophages contribute to Salmonella virulence in mice. *Molecular microbiology* **33**, 167-176.

Figueroa-Bossi, N., Uzzau, S., Maloriol, D. & Bossi, L. (2001). Variable assortment of prophages provides a transferable repertoire of pathogenic determinants in Salmonella. *Molecular microbiology* **39**, 260-271.

Figueroa-Bossi, N. & Bossi, L. (2004). Resuscitation of a defective prophage in Salmonella cocultures. *Journal of bacteriology* **186**, 4038-4041.

Fischbach, M. A., Lin, H., Zhou, L. & other authors (2006). The pathogen-associated iroA gene cluster mediates bacterial evasion of lipocalin 2. *Proceedings of the National Academy of Sciences of the United States of America* **103**, 16502-16507.

Flo, T. H., Smith, K. D., Sato, S., Rodriguez, D. J., Holmes, M. A., Strong, R. K., Akira, S. & Aderem, A. (2004). Lipocalin 2 mediates an innate immune response to bacterial infection by sequestrating iron. *Nature* **432**, 917-921.

Frost, L. S., Leplae, R., Summers, A. O. & Toussaint, A. (2005). Mobile genetic elements: the agents of open source evolution. *Nature reviews Microbiology* **3**, 722-732.

Frye, J. G., Porwollik, S., Blackmer, F., Cheng, P. & McClelland, M. (2005). Host gene expression changes and DNA amplification during temperate phage induction. *Journal of bacteriology* **187**, 1485-1492.

Fukuda, S., Toh, H., Hase, K. & other authors (2011). Bifidobacteria can protect from enteropathogenic infection through production of acetate. *Nature* **469**, 543-547.

Gama, J. A., Reis, A. M., Domingues, I, Mendes-Soares, H., Matos, A. M. & Dionisio, F. (2013). Temperate bacterial viruses as double-edged swords in bacterial warfare. *PloS one* **8**, e59043.

Gantois, I., Ducatelle, R., Pasmans, F., Haesebrouck, F., Hautefort, I., Thompson, A., Hinton, J. C. & Van Immerseel, F. (2006). Butyrate specifically down-regulates salmonella pathogenicity island 1 gene expression. *Applied and environmental microbiology* **72**, 946-949.

Garcia-Russell, N., Elrod, B. & Dominguez, K. (2009). Stress-induced prophage DNA replication in Salmonella enterica serovar Typhimurium. *Infection, genetics and evolution : journal of molecular epidemiology and evolutionary genetics in infectious diseases* **9**, 889-895.

Garrett, W. S., Gallini, C. A., Yatsunenko, T. & other authors (2010). Enterobacteriaceae act in concert with the gut microbiota to induce spontaneous and maternally transmitted colitis. *Cell host & microbe* **8**, 292-300.

Gerding, M. A., Ogata, Y., Pecora, N. D., Niki, H. & de Boer, P. A. (2007). The trans-envelope Tol-Pal complex is part of the cell division machinery and required for proper outer-membrane invagination during cell constriction in E. coli. *Molecular microbiology* **63**, 1008-1025.

Gerlach, R. G., Holzer, S. U., Jackel, D. & Hensel, M. (2007). Rapid engineering of bacterial reporter gene fusions by using Red recombination. *Applied and environmental microbiology* **73**, 4234-4242.

Geuking, M. B., Koller, Y., Rupp, S. & McCoy, K. D. (2014). The interplay between the gut microbiota and the immune system. *Gut microbes* **5**.

Gibson, D. G., Young, L., Chuang, R. Y., Venter, J. C., Hutchison, C. A., 3rd & Smith, H. O. (2009). Enzymatic assembly of DNA molecules up to several hundred kilobases. *Nat Methods* **6**, 343-345.

Gill, S. R. (2006). Metagenomic analysis of the human distal gut microbiome. *Science (New York, NY)* **312**, 1355-1359.

Gillor, O., Vriezen, J. A. & Riley, M. A. (2008). The role of SOS boxes in enteric bacteriocin regulation. *Microbiology (Reading, England)* **154**, 1783-1792.

Gillor, O., Giladi, I. & Riley, M. A. (2009). Persistence of colicinogenic Escherichia coli in the mouse gastrointestinal tract. *BMC microbiology* **9**, 165.

Goetz, D. H., Holmes, M. A., Borregaard, N., Bluhm, M. E., Raymond, K. N. & Strong, R. K. (2002). The neutrophil lipocalin NGAL is a bacteriostatic agent that interferes with siderophore-mediated iron acquisition. *Molecular cell* **10**, 1033-1043.

Gordon, D. M., Riley, M. A. & Pinou, T. (1998). Temporal changes in the frequency of colicinogeny in Escherichia coli from house mice. *Microbiology (Reading, England)* **144 (Pt 8)**, 2233-2240.

Gordon, D. M. & O'Brien, C. L. (2006). Bacteriocin diversity and the frequency of multiple bacteriocin production in Escherichia coli. *Microbiology (Reading, England)* **152**, 3239-3244.

Gordon, M. A., Graham, S. M., Walsh, A. L. & other authors (2008). Epidemics of invasive Salmonella enterica serovar enteritidis and S. enterica Serovar typhimurium infection associated with multidrug resistance among adults and children in Malawi. *Clinical infectious diseases : an official publication of the Infectious Diseases Society of America* **46**, 963-969.

Greig, D. & Travisano, M. (2008). Density-dependent effects on allelopathic interactions in yeast. *Evolution; international journal of organic evolution* **62**, 521-527.

Griggs, D. W., Tharp, B. B. & Konisky, J. (1987). Cloning and promoter identification of the iron-regulated cir gene of Escherichia coli. *Journal of bacteriology* **169**, 5343-5352.

Gunn, J. S., Alpuche-Aranda, C. M., Loomis, W. P., Belden, W. J. & Miller, S. I. (1995). Characterization of the Salmonella typhimurium pagC/pagD chromosomal region. *Journal of bacteriology* **177**, 5040-5047.

Guttman, B., R. Raya, and E. Kutter (2005). Basic phage biology. In *Bacteriophages: Biology and Application*, pp. 29-66.

. Boca Raton, Florida: CRC Press.

Hapfelmeier, S., Ehrbar, K., Stecher, B., Barthel, M., Kremer, M. & Hardt, W. D. (2004). Role of the Salmonella pathogenicity island 1 effector proteins SipA, SopB, SopE, and SopE2 in Salmonella enterica subspecies 1 serovar Typhimurium colitis in streptomycin-pretreated mice. *Infection and immunity* **72**, 795-809.

Hapfelmeier, S., Stecher, B., Barthel, M. & other authors (2005). The Salmonella Pathogenicity Island (SPI)-1 and SPI-2 Type III Secretion Systems Allow Salmonella Serovar Typhimurium to trigger Colitis via MyD88-Dependent and MyD88-Independent Mechanisms. *J Immunol* **174**, 1675-1685.

Harper, R. W., Xu, C., Eiserich, J. P., Chen, Y., Kao, C. Y., Thai, P., Setiadi, H. & Wu, R. (2005). Differential regulation of dual NADPH oxidases/peroxidases, Duox1 and Duox2, by Th1 and Th2 cytokines in respiratory tract epithelium. *FEBS letters* **579**, 4911-4917.

Herrero-Fresno, A., Leekitcharoenphon, P., Hendriksen, R. S., Olsen, J. E. & Aarestrup, F. M. (2014). .Analysis of the contribution of bacteriophage ST64B to in vitro virulence traits of Salmonella enterica serovar Typhimurium. *Journal of medical microbiology* **63**, 331-342.

Hibbing, M. E., Fuqua, C., Parsek, M. R. & Peterson, S. B. (2010). Bacterial competition: surviving and thriving in the microbial jungle. *Nature reviews Microbiology* **8**, 15-25.

Hill, D. A., Hoffmann, C., Abt, M. C., Du, Y., Kobuley, D., Kirn, T. J., Bushman, F. D. & Artis, D. (2010). Metagenomic analyses reveal antibiotic-induced temporal and spatial changes in intestinal microbiota with associated alterations in immune cell homeostasis. *Mucosal immunology* **3**, 148-158.

Hodak, H. & Galan, J. E. (2013). A Salmonella Typhi homologue of bacteriophage muramidases controls typhoid toxin secretion. *EMBO reports* **14**, 95-102.

Hoiseth, S. K. & Stocker, B. A. (1981). Aromatic-dependent *Salmonella typhimurium* are non-virulent and effective as live vaccines. *Nature* **291**, 238-239.

Hooper, L. V. & Macpherson, A. J. (2010). Immune adaptations that maintain homeostasis with the intestinal microbiota. *Nature Rev Immunol* **10**, 159-169.

Ikari, N. S., Kenton, D. M. & Young, V. M. (1969). Interaction in the germfree mouse intestine of colicinogenic and colicin-sensitive microorganisms. *Proceedings of the Society for Experimental Biology and Medicine Society for Experimental Biology and Medicine (New York, NY)* **130**, 1280-1284.

Jakes, K. S. & Finkelstein, A. (2010). The colicin Ia receptor, Cir, is also the translocator for colicin Ia. *Molecular microbiology* **75**, 567-578.

Kaiser, P., Diard, M., Stecher, B. & Hardt, W. D. (2012). The streptomycin mouse model for Salmonella diarrhea: functional analysis of the microbiota, the pathogen's virulence factors, and the host's mucosal immune response. *Immunological reviews* **245**, 56-83.

Kamensek, S., Podlesek, Z., Gillor, O. & Zgur-Bertok, D. (2010). Genes regulated by the Escherichia coli SOS repressor LexA exhibit heterogeneous expression. *BMC microbiology* **10**, 283.

Kelley, W. L. (2006). Lex marks the spot: the virulent side of SOS and a closer look at the LexA regulon. *Molecular microbiology* **62**, 1228-1238.

Kelstrup, J. & Gibbons, R. J. (1969). Inactivation of bacteriocins in the intestinal canal and oral cavity. *Journal of bacteriology* **99**, 888-890.

Kim, M. S., Park, E. J., Roh, S. W. & Bae, J. W. (2011). Diversity and abundance of single-stranded DNA viruses in human feces. *Applied and environmental microbiology* **77**, 8062-8070.

Kirkup, B. C. & Riley, M. A. (2004). Antibiotic-mediated antagonism leads to a bacterial game of rock-paper-scissors in vivo. *Nature* **428**, 412-414.

Kleanthous, C. (2010). Swimming against the tide: progress and challenges in our understanding of colicin translocation. *Nature reviews Microbiology* **8**, 843-848.

Kroger, C., Dillon, S. C., Cameron, A. D. & other authors (2012). The transcriptional landscape and small RNAs of Salmonella enterica serovar Typhimurium. *Proceedings of the National Academy of Sciences of the United States of America* **109**, E1277-1286.

Kroger, C., Colgan, A., Srikumar, S. & other authors (2013). An infection-relevant transcriptomic compendium for Salmonella enterica Serovar Typhimurium. *Cell host & microbe* **14**, 683-695.

Kuwano, Y., Kawahara, T., Yamamoto, H., Teshima-Kondo, S., Tominaga, K., Masuda, K., Kishi, K., Morita, K. & Rokutan, K. (2006). Interferon-gamma activates transcription of NADPH oxidase 1 gene and upregulates production of superoxide anion by human large intestinal epithelial cells. *American journal of physiology Cell physiology* **290**, C433-443.

Laemmli, U. K. (1970). Cleavage of structural proteins during the assembly of the head of bacteriophage T4. *Nature* **227**, 680-685.

Lau, P. C., Hefford, M. A. & Klein, P. (1987). Structural relatedness of lysis proteins from colicinogenic plasmids and icosahedral coliphages. *Molecular biology and evolution* **4**, 544-556.

Lawley, T. D., Clare, S., Walker, A. W. & other authors (2009). Antibiotic treatment of clostridium difficile carrier mice triggers a supershedder state, spore-mediated transmission, and severe disease in immunocompromised hosts. *Infection and immunity* **77**, 3661-3669.

Lazdunski, C. J., Bouveret, E., Rigal, A., Journet, L., Lloubes, R. & Benedetti, H. (1998). Colicin import into Escherichia coli cells. *Journal of bacteriology* **180**, 4993-5002.

Lee, J. W. & Helmann, J. D. (2007). Functional specialization within the Fur family of metalloregulators. *Biometals : an international journal on the role of metal ions in biology, biochemistry, and medicine* **20**, 485-499.

Legrand, D., Elass, E., Carpentier, M. & Mazurier, J. (2005). Lactoferrin: a modulator of immune and inflammatory responses. *Cellular and molecular life sciences : CMLS* **62**, 2549-2559.

Lemire, S., Figueroa-Bossi, N. & Bossi, L. (2011). Bacteriophage crosstalk: coordination of prophage induction by trans-acting antirepressors. *PLoS genetics* **7**, e1002149.

Levitt, M. D., Furne, J., Springfield, J., Suarez, F. & DeMaster, E. (1999). Detoxification of hydrogen sulfide and methanethiol in the cecal mucosa. *The Journal of clinical investigation* **104**, 1107-1114.

Little, J. W. & Mount, D. W. (1982). The SOS regulatory system of Escherichia coli. *Cell* **29**, 11-22.

Little, J. W. (1991). Mechanism of specific LexA cleavage: autodigestion and the role of RecA coprotease. *Biochimie* **73**, 411-421.

Liu, J. Z., Jellbauer, S., Poe, A. J. & other authors (2012). Zinc sequestration by the neutrophil protein calprotectin enhances Salmonella growth in the inflamed gut. *Cell host & microbe* **11**, 227-239.

Livny, J. & Friedman, D. I. (2004). Characterizing spontaneous induction of Stx encoding phages using a selectable reporter system. *Molecular microbiology* **51**, 1691-1704.

Loetscher, Y., Wieser, A., Lengefeld, J., Kaiser, P., Schubert, S., Heikenwalder, M., Hardt, W. D. & Stecher, B. (2012). Salmonella transiently reside in luminal neutrophils in the inflamed gut. *PloS one* **7**, e34812.

Lopez, C. A., Winter, S. E., Rivera-Chavez, F., Xavier, M. N., Poon, V., Nuccio, S. P., Tsolis, R. M. & Baumler, A. J. (2012). Phage-mediated acquisition of a type III secreted effector protein boosts growth of salmonella by nitrate respiration. *mBio* **3**.

Lupp, C., Robertson, M. L., Wickham, M. E., Sekirov, I., Champion, O. L., Gaynor, E. C. & Finlay, B. B. (2007). Host-mediated inflammation disrupts the intestinal microbiota and promotes the overgrowth of Enterobacteriaceae. *Cell host & microbe* **2**, 204.

Lwoff, A., Jacob, F., Ritz, E. & Gage, M. (1952). [Induction of bacteriophage production and of a colicine by peroxides, ethyleneimines and halogenated alkylamines]. *Comptes rendus hebdomadaires des seances de l'Academie des sciences* **234**, 2308-2310.

Majeed, H., Gillor, O., Kerr, B. & Riley, M. A. (2011). Competitive interactions in Escherichia coli populations: the role of bacteriocins. *The ISME journal* **5**, 71-81.

Mankovich, J. A., Lai, P. H., Gokul, N. & Konisky, J. (1984). Organization of the colicin Ib gene. Promoter structure and immunity domain. *The Journal of biological chemistry* **259**, 8764-8768.

Mankovich, J. A., Hsu, C. H. & Konisky, J. (1986). DNA and amino acid sequence analysis of structural and immunity genes of colicins Ia and Ib. *Journal of bacteriology* **168**, 228-236.

McClelland, M., Sanderson, K. E., Spieth, J. & other authors (2001). Complete genome sequence of Salmonella enterica serovar Typhimurium LT2. *Nature* **413**, 852-856.

McCool, J. D., Long, E., Petrosino, J. F., Sandler, H. A., Rosenberg, S. M. & Sandler, S. J. (2004). Measurement of SOS expression in individual Escherichia coli K-12 cells using fluorescence microscopy. *Molecular microbiology* **53**, 1343-1357.

McCormick, B. A., Franklin, D. P., Laux, D. C. & Cohen, P. S. (1989). Type 1 pili are not necessary for colonization of the streptomycin-treated mouse large intestine by type 1-piliated Escherichia coli F-18 and E. coli K-12. *Infection and immunity* **57**, 3022-3029.

McHugh, J. P., Rodriguez-Quinones, F., Abdul-Tehrani, H., Svistunenko, D. A., Poole, R. K., Cooper, C. E. & Andrews, S. C. (2003). Global iron-dependent gene regulation in Escherichia coli. A new mechanism for iron homeostasis. *The Journal of biological chemistry* **278**, 29478-29486.

Miao, E. A. & Miller, S. I. (2000). A conserved amino acid sequence directing intracellular type III secretion by Salmonella typhimurium. *Proceedings of the National Academy of Sciences of the United States of America* **97**, 7539-7544.

Miethke, M. (2013). Molecular strategies of microbial iron assimilation: from high-affinity complexes to cofactor assembly systems. *Metallomics : integrated biometal science* **5**, 15-28.

Mills, S., Shanahan, F., Stanton, C., Hill, C., Coffey, A. & Ross, R. P. (2013). Movers and shakers: influence of bacteriophages in shaping the mammalian gut microbiota. *Gut microbes* **4**, 4-16.

Mirold, S., Rabsch, W., Rohde, M., Stender, S., Tschape, H., Russmann, H., Igwe, E. & Hardt, W. D. (1999). Isolation of a temperate bacteriophage encoding the type III effector protein SopE from an epidemic Salmonella typhimurium strain. *Proceedings of the National Academy of Sciences of the United States of America* **96**, 9845-9850.

Mmolawa, P. T., Schmieger, H. & Heuzenroeder, M. W. (2003). Bacteriophage ST64B, a genetic mosaic of genes from diverse sources isolated from Salmonella enterica serovar typhimurium DT 64. *Journal of bacteriology* **185**, 6481-6485.

Moller, A. K., Leatham, M. P., Conway, T., Nuijten, P. J., de Haan, L. A., Krogfelt, K. A. & Cohen, P. S. (2003). An Escherichia coli MG1655 lipopolysaccharide deep-rough core mutant grows and survives in mouse cecal mucus but fails to colonize the mouse large intestine. *Infection and immunity* **71**, 2142-2152.

Mondot, S., Kang, S., Furet, J. P., Aguirre de Carcer, D., McSweeney, C., Morrison, M., Marteau, P., Dore, J. & Leclerc, M. (2011). Highlighting new phylogenetic specificities of Crohn's disease microbiota. *Inflammatory bowel diseases* **17**, 185-192.

Mrak, P., Podlesek, Z., van Putten, J. P. & Zgur-Bertok, D. (2007). Heterogeneity in expression of the Escherichia coli colicin K activity gene cka is controlled by the SOS system and stochastic factors. *Molecular genetics and genomics : MGG* **277**, 391-401.

Mulec, J., Podlesek, Z., Mrak, P., Kopitar, A., Ihan, A. & Zgur-Bertok, D. (2003). A cka-gfp transcriptional fusion reveals that the colicin K activity gene is induced in only 3 percent of the population. *Journal of bacteriology* **185**, 654-659.

Muller, A. J., Hoffmann, C., Galle, M. & other authors (2009). The S. Typhimurium effector SopE induces caspase-1 activation in stromal cells to initiate gut inflammation. *Cell host & microbe* **6**, 125-136.

N.J. Dimmock, A. J. E. a. K. N. L. (2001). *Introduction to Modern Virology*, Fifth edn: Blackwell publishing.

Nakayama, K., Takashima, K., Ishihara, H. & other authors (2000). The R-type pyocin of Pseudomonas aeruginosa is related to P2 phage, and the F-type is related to lambda phage. *Molecular microbiology* **38**, 213-231.

Nanda, A. M., Heyer, A., Kramer, C., Grunberger, A., Kohlheyer, D. & Frunzke, J. (2014). Analysis of SOS-induced spontaneous prophage induction in Corynebacterium glutamicum at the single-cell level. *Journal of bacteriology* **196**, 180-188.

Nathan, C. (2006). Neutrophils and immunity: challenges and opportunities. *Nature reviews Immunology* **6**, 173-182.

Nedialkova, L. P., Denzler, R., Koeppel, M. B., Diehl, M., Ring, D., Wille, T., Gerlach, R. G. & Stecher, B. (2014). Inflammation fuels colicin Ib-dependent competition of Salmonella serovar Typhimurium and E. coli in enterobacterial blooms. *PLoS pathogens* **10**, e1003844.

Neely, M. N. & Friedman, D. I. (1998). Functional and genetic analysis of regulatory regions of coliphage H-19B: location of shiga-like toxin and lysis genes suggest a role for phage functions in toxin release. *Molecular microbiology* **28**, 1255-1267.

Ng, K. M., Ferreyra, J. A., Higginbottom, S. K. & other authors (2013). Microbiota-liberated host sugars facilitate post-antibiotic expansion of enteric pathogens. *Nature* **502**, 96-99.

Nikaido, H. & Rosenberg, E. Y. (1990). Cir and Fiu proteins in the outer membrane of Escherichia coli catalyze transport of monomeric catechols: study with beta-lactam antibiotics containing catechol and analogous groups. *Journal of bacteriology* **172**, 1361-1367.

Noinaj, N., Guillier, M., Barnard, T. J. & Buchanan, S. K. (2010). TonB-dependent transporters: regulation, structure, and function. *Annual review of microbiology* **64**, 43-60.

O'Brien, A. D., Newland, J. W., Miller, S. F., Holmes, R. K., Smith, H. W. & Formal, S. B. (1984). Shiga-like toxin-converting phages from Escherichia coli strains that cause hemorrhagic colitis or infantile diarrhea. *Science (New York, NY)* **226**, 694-696.

Ohkawa, I., Shiga, S. & Kageyama, M. (1980). Effect of iron concentration in the growth medium on the sensitivity of Pseudomonas aeruginosa to pyocin S2. *Journal of biochemistry* **87**, 323-331.

Orndorff, P. E., Devapali, A., Palestrant, S., Wyse, A., Everett, M. L., Bollinger, R. R. & Parker, W. (2004). Immunoglobulin-mediated agglutination of and biofilm formation by Escherichia coli K-12 require the type 1 pilus fiber. *Infection and immunity* **72**, 1929-1938.

Pelludat, C., Mirold, S. & Hardt, W. D. (2003). The SopEPhi phage integrates into the ssrA gene of Salmonella enterica serovar Typhimurium A36 and is closely related to the Fels-2 prophage. *Journal of bacteriology* **185**, 5182-5191.

Pilsl, H. & Braun, V. (1998). The Ton system can functionally replace the TolB protein in the uptake of mutated colicin U. *FEMS microbiology letters* **164**, 363-367.

Pinou, T. & Riley, M. A. (2001). Nucleotide polymorphism in microcin V plasmids. *Plasmid* **46**, 1-9.

Pitts, A. C., Tuck, L. R., Faulds-Pain, A., Lewis, R. J. & Marles-Wright, J. (2012). Structural insight into the Clostridium difficile ethanolamine utilisation microcompartment. *PloS one* **7**, e48360.

Prof. Dr. Margaret A. Riley & Chavan, D. M. A. (2007). *Bacteriocins*

Ecology and Evolution: Springer Berlin Heidelberg.

Raffatellu, M. (2009). Lipocalin-2 resistance confers an advantage to Salmonella enterica serotype Typhimurium for growth and survival in the inflamed intestine. *Cell host & microbe* **5**, 476-486.

Raffatellu, M., George, M. D., Akiyama, Y. & other authors (2009). Lipocalin-2 resistance confers an advantage to Salmonella enterica serotype Typhimurium for growth and survival in the inflamed intestine. *Cell host & microbe* **5**, 476-486.

Refardt, D. & Rainey, P. B. (2010). Tuning a genetic switch: experimental evolution and natural variation of prophage induction. *Evolution; international journal of organic evolution* **64**, 1086-1097.

Riley, M. A. & Gordon, D. M. (1999). The ecological role of bacteriocins in bacterial competition. *Trends in microbiology* **7**, 129-133.

Riley, M. A. & Wertz, J. E. (2002). Bacteriocins: evolution, ecology, and application. *Annual review of microbiology* **56**, 117-137.

Riley, M. A. (2011). Bacteriocin-Mediated Competitive Interactions of Bacterial Populations and Communities. In *Prokaryotic Antimicrobial Peptides*, pp. 13-26: Springer New York.

Salgado, H., Peralta-Gil, M., Gama-Castro, S. & other authors (2013). RegulonDB v8.0: omics data sets, evolutionary conservation, regulatory phrases, cross-validated gold standards and more. *Nucleic acids research* **41**, D203-213.

Sambrook, J., Fritsch, E. F. & Maniatis, T. (1989). *Molecular Cloning: A Laboratory Manual*: Cold Spring Harbor Laboratory Press.

Schumann, S., Alpert, C., Engst, W., Loh, G. & Blaut, M. (2012). Dextran sodium sulfate-induced inflammation alters the expression of proteins by intestinal Escherichia coli strains in a gnotobiotic mouse model. *Applied and environmental microbiology* **78**, 1513-1522.

Scott, K. P. (2002). The role of conjugative transposons in spreading antibiotic resistance between bacteria that inhabit the gastrointestinal tract. *Cellular and molecular life sciences : CMLS* **59**, 2071-2082.

Segal, A. W. (2005). How neutrophils kill microbes. *Annual review of immunology* **23**, 197-223.

Sekirov, I., Tam, N. M., Jogova, M., Robertson, M. L., Li, Y., Lupp, C. & Finlay, B. B. (2008). Antibiotic-induced perturbations of the intestinal microbiota alter host susceptibility to enteric infection. *Infection and immunity* **76**, 4726-4736.

Shinagawa, H. (1996). SOS response as an adaptive response to DNA damage in prokaryotes. *Exs* **77**, 221-235.

Sommer, F. & Backhed, F. (2013). The gut microbiota--masters of host development and physiology. *Nature reviews Microbiology* **11**, 227-238.

Spees, A. M., Wangdi, T., Lopez, C. A., Kingsbury, D. D., Xavier, M. N., Winter, S. E., Tsolis, R. M. & Baumler, A. J. (2013). Streptomycin-induced inflammation enhances Escherichia coli gut colonization through nitrate respiration. *mBio* **4**.

Stanley, T. L., Ellermeier, C. D. & Slauch, J. M. (2000). Tissue-specific gene expression identifies a gene in the lysogenic phage Gifsy-1 that affects Salmonella enterica serovar typhimurium survival in Peyer's patches. *Journal of bacteriology* **182**, 4406-4413.

Stecher, B., Hapfelmeier, S., Muller, C., Kremer, M., Stallmach, T. & Hardt, W. D. (2004). Flagella and chemotaxis are required for efficient induction of Salmonella enterica serovar Typhimurium colitis in streptomycin-pretreated mice. *Infection and immunity* **72**, 4138-4150.

Stecher, B., Robbiani, R., Walker, A. W. & other authors (2007a). Salmonella enterica serovar typhimurium exploits inflammation to compete with the intestinal microbiota. *PLoS biology* **5**, 2177-2189.

Stecher, B., Robbiani, R., Walker, A. W. & other authors (2007b). Salmonella enterica Serovar Typhimurium Exploits Inflammation to Compete with the Intestinal Microbiota. *PLoS Biol* **5**, e244.

Stecher, B., Chaffron, S., Kappeli, R. & other authors (2010). Like will to like: abundances of closely related species can predict susceptibility to intestinal colonization by pathogenic and commensal bacteria. *PLoS pathogens* **6**, e1000711.

Stecher, B. & Hardt, W. D. (2011). Mechanisms controlling pathogen colonization of the gut. *Current opinion in microbiology* **14**, 82-91.

Stecher, B., Denzler, R., Maier, L. & other authors (2012). Gut inflammation can boost horizontal gene transfer between pathogenic and commensal Enterobacteriaceae. *Proceedings of the National Academy of Sciences of the United States of America* **109**, 1269-1274.

Stecher, B., Berry, D. & Loy, A. (2013a). Colonization resistance and microbial ecophysiology: using gnotobiotic mouse models and single-cell technology to explore the intestinal jungle. *FEMS microbiology reviews* **37**, 793-829.

Stecher, B., Maier, L. & Hardt, W. D. (2013b). 'Blooming' in the gut: how dysbiosis might contribute to pathogen evolution. *Nature reviews Microbiology* **11**, 277-284.

Stelter, C., Kappeli, R., Konig, C., Krah, A., Hardt, W. D., Stecher, B. & Bumann, D. (2011). Salmonella-induced mucosal lectin RegIIIbeta kills competing gut microbiota. *PloS one* **6**, e20749.

Taylor, C. M., Osman, D. & Cavet, J. S. (2009). Differential expression from two iron-responsive promoters in Salmonella enterica serovar Typhimurium reveals the presence of iron in macrophage-phagosomes. *Microbial pathogenesis* **46**, 114-118.

Thiennimitr, P., Winter, S. E., Winter, M. G. & other authors (2011). Intestinal inflammation allows Salmonella to use ethanolamine to compete with the microbiota. *Proceedings of the National Academy of Sciences of the United States of America* **108**, 17480-17485.

Turnbaugh, P. J., Backhed, F., Fulton, L. & Gordon, J. I. (2008). Diet-induced obesity is linked to marked but reversible alterations in the mouse distal gut microbiome. *Cell host & microbe* **3**, 213-223.

Turnbaugh, P. J. (2009). A core gut microbiome in obese and lean twins. *Nature* **457**, 480-484.

Vaishnava, S., Behrendt, C. L., Ismail, A. S., Eckmann, L. & Hooper, L. V. (2008). Paneth cells directly sense gut commensals and maintain homeostasis at the intestinal host-microbial interface. *Proc Natl Acad Sci USA* **105**, 20858-20863.

Wadolkowski, E. A., Laux, D. C. & Cohen, P. S. (1988). Colonization of the streptomycin-treated mouse large intestine by a human fecal Escherichia coli strain: role of growth in mucus. *Infection and immunity* **56**, 1030-1035.

Wagner, P. L., Neely, M. N., Zhang, X., Acheson, D. W., Waldor, M. K. & Friedman, D. I. (2001). Role for a phage promoter in Shiga toxin 2 expression from a pathogenic Escherichia coli strain. *Journal of bacteriology* **183**, 2081-2085.

Walker, A. W., Sanderson, J. D., Churcher, C. & other authors (2011). High-throughput clone library analysis of the mucosa-associated microbiota reveals dysbiosis and differences between inflamed and non-inflamed regions of the intestine in inflammatory bowel disease. *BMC microbiology* **11**, 7.

Wang, I. N., Smith, D. L. & Young, R. (2000). Holins: the protein clocks of bacteriophage infections. *Annual review of microbiology* **54**, 799-825.

Wang, R. F. & Kushner, S. R. (1991). Construction of versatile low-copy-number vectors for cloning, sequencing and gene expression in Escherichia coli. *Gene* **100**, 195-199.

Wang, X., Kim, Y., Ma, Q., Hong, S. H., Pokusaeva, K., Sturino, J. M. & Wood, T. K. (2010). Cryptic prophages help bacteria cope with adverse environments. *Nature communications* **1**, 147.

Weaver, C. A., Kagan, B. L., Finkelstein, A. & Konisky, J. (1981). Mode of action of colicin ib: formation of ion-permeable membrane channels. *Biochimica et biophysica acta* **645**, 137-142.

Winter, S. E., Thiennimitr, P., Winter, M. G. & other authors (2010). Gut inflammation provides a respiratory electron acceptor for Salmonella. *Nature* **467**, 426-429.

Winter, S. E., Lopez, C. A. & Baumler, A. J. (2013a). The dynamics of gut-associated microbial communities during inflammation. *EMBO reports* **14**, 319-327.

Winter, S. E., Winter, M. G., Xavier, M. N. & other authors (2013b). Host-derived nitrate boosts growth of E. coli in the inflamed gut. *Science (New York, NY)* **339**, 708-711.

Wloch-Salamon, D. M., Gerla, D., Hoekstra, R. F. & de Visser, J. A. (2008). Effect of dispersal and nutrient availability on the competitive ability of toxin-producing yeast. *Proceedings Biological sciences / The Royal Society* **275**, 535-541.

Wlodarska, M., Willing, B., Keeney, K. M., Menendez, A., Bergstrom, K. S., Gill, N., Russell, S. L., Vallance, B. A. & Finlay, B. B. (2011). Antibiotic treatment alters the colonic mucus layer and predisposes the host to exacerbated Citrobacter rodentium-induced colitis. *Infection and immunity* **79**, 1536-1545.

Young, I., Wang, I. & Roof, W. D. (2000). Phages will out: strategies of host cell lysis. *Trends in microbiology* **8**, 120-128.

Young, R. (2013). Phage lysis: do we have the hole story yet? *Current opinion in microbiology* **16**, 790-797.

Young, R. (2014). Phage lysis: three steps, three choices, one outcome. *Journal of microbiology (Seoul, Korea)* **52**, 243-258.

Zgur-Bertok, D. (2012). Regulating colicin synthesis to cope with stress and lethality of colicin production. *Biochemical Society transactions* **40**, 1507-1511.

Zumbrun, S. D., Melton-Celsa, A. R., Smith, M. A., Gilbreath, J. J., Merrell, D. S. & O'Brien, A. D. (2013). Dietary choice affects Shiga toxin-producing Escherichia coli (STEC) O157:H7 colonization and disease. *Proceedings of the National Academy of Sciences of the United States of America* **110**, E2126-2133.

Acknowledgments

Curriculum Vitae

Personal information

Name	Lubov Petkova Nedialkova
Date of birth:	27.03.1985
Place of birth:	Zelenchukskaia, Russia

Education

10/2010 - present   PhD student in the research group of Prof. Dr. Bärbel Stecher at the Max von Pettenkofer Institute, Faculty of Medicine, Ludwig-Maximilians University Munich, Germany

08/2008 – 05/2010   M. Sc. Applied Biotechnology
Uppsala University, Uppsala, Sweden

10/2004 – 07/2008   B. Sc. Molecular Biology
Sofia University "St. Kliment Ohridski", Sofia, Bulgaria

09/1998 - 07/2004   High-school education
National high school of Natural Sciences and Mathematics "Academician Lyubomir Chakalov", Sofia, Bulgaria

Publications

Nedialkova, L. P.*, Denzler*, R., Koeppel, M. B., Diehl, M., Ring, D., Wille, T., Gerlach, R. G. & Stecher, B. (2014). Inflammation fuels colicin Ib-dependent competition of *Salmonella* serovar Typhimurium and *E. coli* in enterobacterial blooms. PLoS Pathogens 10, e1003844

* = Authors contributed equally to this work

Conferences

Nedialkova, L. P., Denzler, R., Koeppel, M. B., Diehl, M., Ring, T., Gerlach, R. G. & Stecher, B. "Inflamation triggers colicin Ib-dependent competition of *Salmonella serovar* Typhimurium and colicin-sensitive *E. coli* in enterobacterial blooms", *6th Seeon Conference Microbiota, Probiota and Host*, Kloster Seeon, Germany (2013), poster presentation

Nedialkova, L. P., Denzler, R., Diehl, M., Koeppel, M. B. & Stecher, B. "The role of the host response in colicin-dependent *E. coli-Salmonella* competition in the gut", *64. Jahrestagung der Deutschen Gesellschaft für Hygiene und Mikrobiologie (DGHM)*, Hamburg, Germany (2012), oral presentation

Nedialkova, L. P., Denzler, R., Diehl, M. & Stecher, B. "The role of the host response in colicin-dependent *E. coli-Salmonella* competition in the gut", *How bugs kill bugs*: *progress and challenges in bacteriocin research*, University of Nottingham, United Kingdom (2012), poster presentation

Nedialkova, L. P., Denzler, R., Diehl, M. & Stecher, B. "The role of the host response in colicin-dependent *E. coli-Salmonella* competition in the gut", *5th Seeon Conference Microbiota, Probiota and Host*, Kloster Seeon, Germany (2012), oral presentation

Denzler, R., Nedialkova, L. P., Lötscher, Y. & Stecher, B. "The role of the host response in colicin-dependent *E. coli-Salmonella* competition in the gut", *4th Seeon Conference Microbiota, Probiota and Host*, Kloster Seeon, Germany (2011), poster presentation